Robustness of a Timber Core with a Braced System

Under Lateral Wind Load on a 10-Storey Building During Fire Conditions

Ivo Postma

Delft University of Technology

TU Delft

To be realised Urban Woods project Delft
Location: 52.02041945512458, 4.365855383388567
Cover source: theurbanwoods.com

Robustness of a Timber Core with a Braced System

Under Lateral Wind Load on a 10-Storey Building During Fire Conditions

by

Student Name	Student Number
Ivo Postma	4963849

Graduation committee:	
Chair from 20/06/2024, TU Delft:	Prof. dr. ir. J.W.G. van de Kuilen
Chair until 20/06/2024, TU Delft:	Dr. ir. G.J.P Ravenshorst
Supervisor, TU Delft:	Ir. M. Felicita
Supervisor, TU Delft:	Dr. ir. P.C.J Hoogenboom
Supervisor, Arcadis:	Ing. D. van Loon
Project Duration:	August, 2023 - October, 2024
Faculty:	Faculty of Civil Engineering and Geosciences, Delft

Preface

This report is part of my graduation thesis for completing the Master's degree in Building Engineering at Delft University of Technology. My interest in timber as a construction material comes from its relatively recent adoption in the field, which introduces new and unexplored topics. Throughout my thesis, it was encouraging to hear from structural engineers that other timber projects were being developed, highlighting the material's growing relevance. The potential environmental benefits of timber compared to traditional construction materials have also deepened my interest. I hope this thesis contributes to a better understanding of timber and its appropriate use in future projects.

At Arcadis, the engineering firm, there was a shared interest in this topic. At the time, Arcadis was working on the Urban Woods project, a timber structure with a glulam braced system and a timber core, located just 500 meters from where I live. Together with Dietmar van Loon from Arcadis, Geert Ravenshorst and Maria Felicita, we developed a subject focused on investigating the additional benefits of a timber core. As the thesis progressed, the topic and research questions evolved into their current form. In addition to Dietmar van Loon, Maria Felicita, and Geert Ravenshorst, Pierre Hoogenboom joined the committee, bringing his expertise in Finite Element Method. Jan-Willem Verkuilen later joined the committee, replacing Geert Ravenshorst in the final phase.

Throughout this thesis, I expanded my knowledge of timber as a construction material, as well as my understanding of robustness and fire safety. I am grateful to my colleagues at Arcadis for their warm welcome and support. Special thanks go to Dietmar van Loon, whose insights and guidance were invaluable. I also wish to express my gratitude to Maria Felicita for providing relevant papers and thoughtful feedback. Lastly, I would like to thank Pierre Hoogenboom for his guidance on FEM programs and his help in improving my writing, as well as Jan-Willem Verkuilen for stepping in as chair.

Ivo Postma
Delft, Oktober 2024

Abstract

Timber as a construction material for high-rise buildings is gradually entering the construction industry. Timber is considered a sustainable option, because it is a natural material that absorbs CO_2 rather than producing it. However, using timber as a building material also introduces new challenges, one of which is the problem with lateral stability, due to the relatively low stiffness of the elements and their connections.

This research investigates the value of a timber core in a building that has bracings in the façade. The study examines this value in both normal conditions and the accidental limit state in case of a fire situation. The key question being addressed is:

Can a timber core sustain lateral load as a secondary load path, in case of failure of the stability bracing?

First, a literature review is conducted to understand the material and relevant safety mechanisms. A parametric program is used to explore the core's parameters, alongside a linear elastic 3D FEM (Finite Element Method) program that utilises members and surfaces to analyze the building structure. The considered building is a 10-story rectangular structure (28.8 x 21.6 meters) with glulam beams, glulam columns, and CLT floors. The building was designed on an infinite stiff foundation by using a timber core and timber bracings in the façade. The core consists of cross-laminated timber (CLT) panels, connected with slotted steel plates and dowels. The bracings are glue laminated timber and are connected with two slotted in steel plates and dowels. The CLT panel connections and the bracing connections were calculated by hand and implemented in the FEM model. Which was validated by hand calculations. Additionally, wind load, variable load and permanent load were applied on the model.

This model was used to answer the following question.

What percentage of the lateral force can the core take?

The model with a timber core in the Urban Woods shows an 18% reduction in global deflection compared to the model without a timber core in the ultimate limit state. The deflection of both models where to be within the prescribed limit. Additionally to the deflection reduction, the forces in the bracing are reduced by 33% in the model with a timber core. The core parameters that influence these reductions are the connections between the core panels and the cut-outs in the timber core. A core parameter study has been carried out to answer the following question:

How do the core parameters influence the global deflection?

For the connections, increased stiffness enhances the contribution of the core to reducing global deflection, with reductions ranging from 0% to 22%. Using longer panels results in fewer connections, which makes up for 7% of the global deflection reduction at any given stiffness of the CLT connections. Regarding the cut-outs, a larger cut-out size results in a lower contribution to deflection reduction. The reduction in global deflection for different cut-out sizes ranged from 5% to 27%. As the number of floors increases, the value of a timber core diminishes.

In the accidental limit state of fire, strong wind and failure of a facade bracing element, the timber core will serve as a sufficient alternative load path. However due to the wind force reduction in the ALS the remaining bracing is also capable of withstanding the lateral wind force. When two elements are removed than the core will be necessary. The unity checks for the CLT elements and connections did suffice.

Contents

1 Introduction

Timber is gradually making its way into the construction of high-rise buildings. Its growing popularity is largely due to its environmental advantages over traditional building materials like steel and concrete. The manufacturing of these conventional materials plays a significant role in making the building sector one of the largest polluters in the world. The Global Status Report for Buildings and Construction 2022 states that operational CO_2 emissions and energy use reached an all-time high in 2021. This surge can be partly attributed to the increased demand for housing, particularly in the wake of the COVID-19 pandemic, with the African continent also experiencing substantial growth. Buildings, which include operational use and the manufacturing of building materials, will represent around 37 percent of the world's CO_2 emissions in 2021. The emission from materials was about 3.6 Gt CO_2 [49].

Timber stands out as a remarkable natural building material that, through the process of photosynthesis, adeptly captures and stores CO_2 from the atmosphere. This unique quality positions timber as an exceptionally favorable choice for the construction industry, offering an ideal solution from the perspective of carbon dioxide emissions.

The Netherlands is suffering from a housing shortage. By March 2022, it was estimated that the shortage would be about 273.000 houses. In response, the minister of public housing and spatial planning has announced an ambitious plan to construct 100,000 homes per year between 2024 and 2030. This initiative will necessitate large-scale development, focusing on areas with the most pressing housing demands. These areas are predominantly found in the Dutch cities, often in close proximity to train stations [45]. Given the robust demand for housing in these sought-after locations, the necessity for high-rise buildings has become increasingly apparent.

As environmental concerns continue to gain prominence, an increasing number of clients are expressing a preference for timber as the primary material for their buildings. The ability to easily obtain longitudinal elements, combined with its high strength and low density, makes timber an excellent choice for construction. In the last decade, more and more high-rise timber buildings have been realized. Advancements in timber engineering and construction techniques have allowed these structures to reach new heights. As of August 2023, the tallest timber building to date, Mjøstårnet, has reached 81 meters in height [1]. In the Netherlands, there is a growing trend with timber high-rise buildings being designed. Important examples include the Urban Woods, Cube House, SAWA, and HAUT 1.1.

(a) Urban Woods (32 meter) [66]

(b) Cube House (55 meter)[10]

(c) SAWA (50 meter)[68]

(d) HAUT (73 meter)[20]

Figure 1.1: Dutch timber projects

The use of timber as a building material introduces new design challenges. So the weight of timber is much less than that of conventional building materials such as steel and concrete. This leads to problems with the stability of the building. From the dutch examples given 1.1, is the Urban-Woods the only project that has opted for a full timber construction. The timber core in the Urban Woods is combined with bracings in the façade as the main stability system. Most of the timber constructions today have opted for a concrete core, which gives much more stiffness to the system. There is little research on the effect of a timber core in a braced system. How do the timber core parameters impact the stiffness of timber buildings? Timber is a brittle material in tension and a combustible material. The strategies to increase the robustness of a building are given in the NEN-EN 1991-1-7. However these strategies are based on concrete and steel as a building material with strategies for timber still being in the draft stage. Here a knowledge gap is experienced. Despite these challenges, integrating a timber core into a braced system could enhance structural robustness by introducing a secondary load path. The question that will be answered is therefore:

Can a timber core sustain lateral load as a secondary load path, in case of failure of the stability bracing?

2

Research framework

2.1. Research objective

This research aims to investigate the structural behaviour of a CLT core with a Glulam bracings system, with the removal of one of the bracings elements in the normative direction. This is done to see if a timber core can maintain the stiffness in the accidental limit state during an abnormal event.

2.2. Research questions

The main research question for this thesis is as follows:

Can a timber core sustain lateral load as a secondary load path, in case of failure of the stability bracing?

To answer this question different aspects needs to be researched. The stiffness of the CLT core and the Glulam bracings needs to be investigated. Because the core does not consist of one solid piece, some of the stiffness is lost in the connections. To figure out how the core behaves a literature study needs to be applied. In which the stiffness of the connections are considered and the behaviour of the panels. Same as for the wind bracing which will be investigated. For the secondary load path, will be assumed that the first load path will slowly diminish by a fire situation. Therefore timber in the fire situation will also be taken a look into.

The insights from the literature study on connections in timber constructions and fire behavior will be adapted and incorporated into a Finite Element Method (FEM) model. With the Finite Element Method the following sub questions can be answered.

What percentage of the lateral force can the core take?
How do the core parameters influence the global deflection?

2.3. Research strategy

The design of the building will be like the design of the Urban Woods, which is a project that is going to be realised. With the same two stability systems, floor plan, number of columns, CLT panels, level height and the kind of floors. To test the value of the timber core, two variants of the building will be compared. One variant without a timber core, this variant is like the Urban Woods with a bracing but instead of a core the beams and floors are extended to overlap the core space. The other variant is the one with a timber core 2.1. The forces that are applied are permanent, variable and wind load. Analysing the global deflection and the internal forces in the bracings for both cases will give a answer on how the timber core contributes to the stiffness.

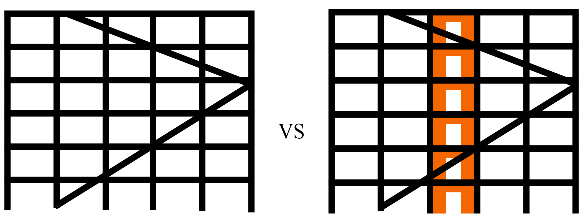

Figure 2.1: schematic drawing of the comparison

To analyse the additional robustness a timber core gives to the system, the construction is tested in the accidental limit state with the reduced cross sections due to fire, followed by the removing of bracing elements. The forces in the core and in the bracings will be analysed.

Part I

Literature

3

The Urban Woods

To better understand the purpose and construction of urban woods, this chapter provides a brief description. With these insights, the model for further investigation can be realised.

3.1. Concept and sustainability

The Urban Woods is a concept of the Urban Climate Architects. The project is as of 2024 being build in Delft. The aim of the concept is to accomplish more than just housing. Sustainability is a topic they value in the concept of the Urban Woods. In the construction of the building the aim is to be sustainable. With using timber as a construction material, the amount of CO_2 and NO_x is low, compared with the more common building materials. A timber bracing system was chosen in the façade to clearly demonstrate that the building's stability is achieved through a timber structure. And therefore emphasise the sustainability of the project [66].

3.2. Construction

The construction of the Urban Woods consist of Glulam beams and columns with CLT floor elements and walls. The building is a rectangular of 24 m x 34 m and is 10 stories high (32 meter).The building has also a cellar that is 1 storey deep.

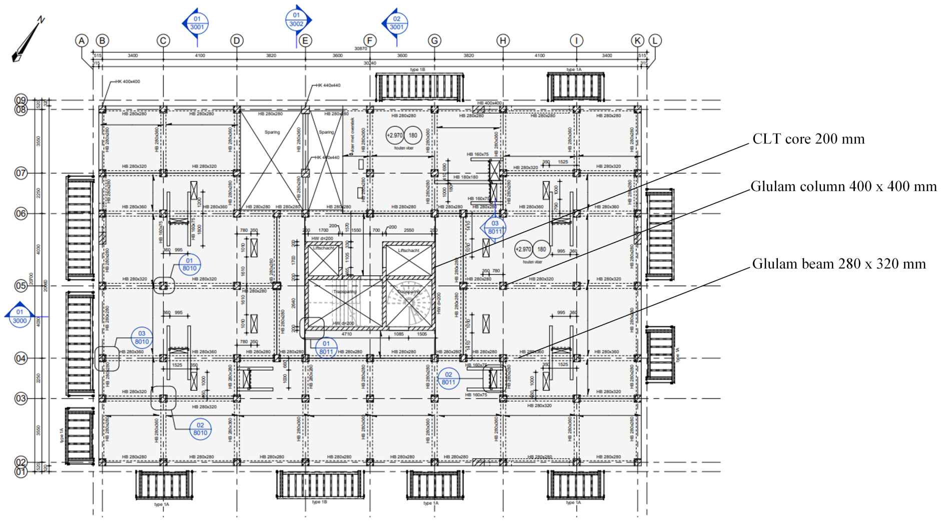

Figure 3.1: Plot of the Urban-Woods

The vertical loads are carried parallel to the grain in the Glulam columns. With the beams being imposed on the columns 3.2. The beams are 320 mm high with a floor of 180 mm. The beams and the floor are put in place by screws connected with a metal plate to the column.

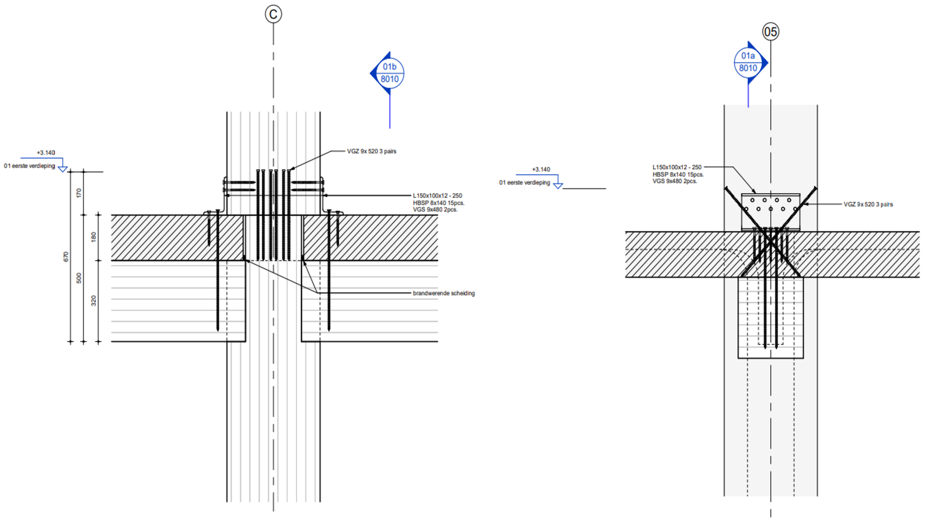

Figure 3.2: Column to beam, Arcadis

Horizontal stability is achieved through the use of the core and wind bracings in the façade. This design was chosen to create an open floor plan, allowing each apartment to be tailored to its desired size. The diagonal bracings on the sides form a single continuous line with a change in direction at midpoint.

The construction has a fire resistance of 120 minutes which will be accomplished by over sizing of the elements so that it is sufficient in the ULS fire combination calculated using NEN1995-1-2 and ETA-14/0349. The connections are protected by fire strips. In chapter 6 different connections will be examined, like the slotted in steel plates. The strength, stiffness and the fire resistance will be discussed.

As for robustness, the only aspect mentioned is the requirement for the floor to be supported by more than two columns. In case of a column loss, the other columns could carry the load (see figure 3.3[4].

The building has also balconies which give the building extra loads to carry at the façade. The maximal F_z from the balconies is 60 kN [28].

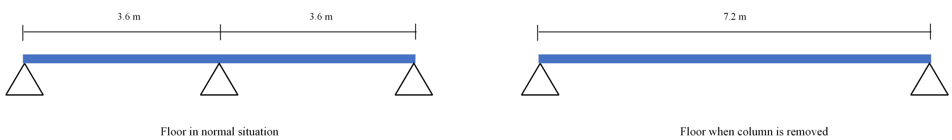

Figure 3.3: Column removal example

3.3. Conclusion

In this chapter, it becomes clear why timber was chosen as the construction material for the Urban Woods project. The idea to realize the Urban Woods results from the demand of sustainable housings. Also the construction of the Urban woods is clarified in this chapter. The use of the glue laminated bracing in the façade, in combination with a CLT core, will be further examined.

4 Materials

This chapter takes a deeper dive into the materials used in timber buildings. To get a better understanding of the properties like design value, how the grain direction affects strength. Also what the properties are of the different timber products will be discussed. With emphasis on CLT and glulam, who are going to be used for the model.

4.1. Timber

Timber is a bio-based material. The properties vary because of the irregularities in different trees like growth disturbances and the way the boards are taken out of the tree (see figure 4.1). Also, there are different kinds of timber materials on the market. For the structural engineer, it is not possible to account for the difference in material. That is why the timber is being sorted into classes so that the structural engineer can assume that the material is homogeneous.

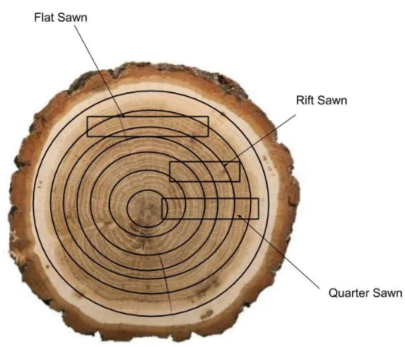

Figure 4.1: Different types of sawing [13]

Timber is an isotropic material. Parallel to the grain, the timber is strong in tension as well as in compression. But perpendicularly, the material is weak in tension and relatively strong in compression. The difference between parallel and perpendicular can be up to 15 to 30 times greater in the case of tension strength. Timber has a brittle tensile failure mechanism parallel aswell as perpendicular to the grain. This together with the low strength in the perpendicular direction makes timber less desirable for construction. The behaviour of timber in compression and tension for the different directions are given in diagram 4.2

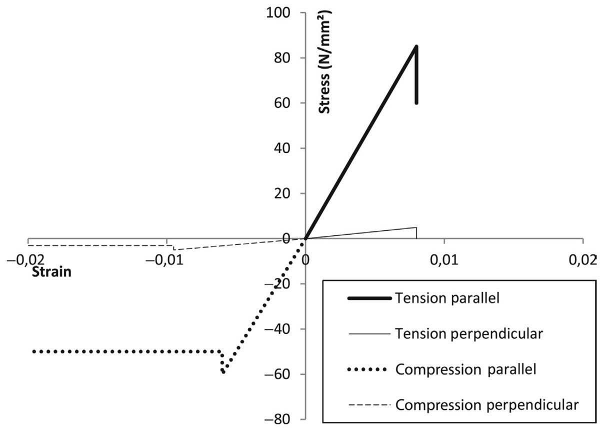

Figure 4.2: Tension and compression perpendicular and parallel to the grain [22]

Modeling for timber constructions can be challenging due to the complex behavior. To describe these complex behavior subroutines will be in place. Features such as orthotropic elastic behavior, plastic anisotropic hardening and isotropic ductile damage can be used to describe the complex structural behavior of timber [22].

Like other construction materials, timber can be placed in strength classes. These classes range from C14 up to C50 for poplar and coniferous timber, and D18 to D70 for deciduous timber. The number of the class corresponds to the bending strength. The real strength of the material may be much higher than the classes prescribes because of the uncertainties the irregular timber has.

Timber in the construction industry is treated to fully meet the needs of the situation. Glue laminated timbers for example are mostly beams that consist of long boards that are glued together with polyurethane adhesives or melamine. Timber can also be used as a plate material. Plywood is constructed from layers of veneer glued together in a crosswise manner. The veneers are obtained by 'peeling' tree trunks. Crosswise gluing results in high-dimensional stability. Laminated veneer lumber (LVL) is like plywood, constructed from layers of veneer glued together. With LVL, the material is pressed together, which makes the material stronger. Cross-laminated Timber (CLT) is like plywood but with boards of timber. The boards are glued crosswise to give strength in both directions. Other timber products are oriented strand board (OSB), chipboard, and medium density fiberboard (MDF) [14].

From the Euro code, the calculation value of the resistance is calculated as follows:

$$R_d = \kappa_{mod} \frac{R_k}{\gamma_M} \tag{4.1}$$

With:

κ_{mod} is a modification factor that takes into account the influence of the loading period and the moisture content.

R_k is the characteristic value of the strength

γ_M is the partial factor for a material property

The k_{mod} changes per load duration and the service classes and are specified in table 4.1

Load-duration class	κ_{mod} service class 1-2	κ_{mod} service class 3
Permanent	0.60	0.50
Long-term	0.70	0.55
Medium-term	0.80	0.65
Short-term	0.90	0.70
Instantaneous	1.10	0.90

Table 4.1: κ_{mod} for different service classes and loading[55]

Timber as a organic material will react to a increased moisture content. With a higher moisture content, the stiffness and the strenght decreases, creep deformation increases, the thermal conductivity increases and the wood becomes more prone to fungal infection [55].

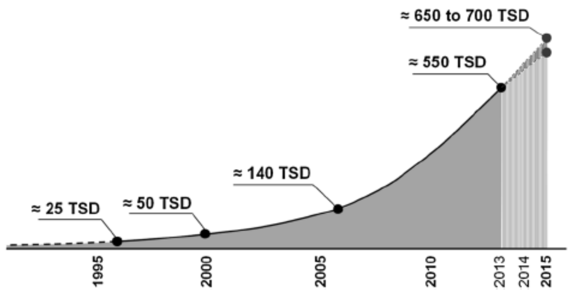

Figure 4.3: Worldwide production of CLT until 2013 and forecast 2015 [63]

4.2. Glued Laminated Timber (GLT)

Glue laminated timber consists of boards glued together that are connected to each other with finger joints. The boards are graded following NEN-EN 14080 from T8 up to T30. The finger joints will have a higher bending strength than the board itself. Multiple glulams glued against each other are called block-glued glulams [35]. If the same strength class for all the boards is used, the buildup is homogeneous. If for instance, the inside boards are weaker, then we talk about a combination. The thickness of the boards is, most of the time, between 22 mm and 45 mm. Strength classes are given to glulam whose most typical range is from GL24h up to GL36c.

4.2.1. Strength calculation

For homogeneous glued laminated timber apply the following from NEN-EN 14080 [35] The bending strength of glulam $f_{m,g,k}$ is calculated as follows:

$$f_{m,g,k} = -2,2 + 2,5 f_{t,0,l,k}^{2,5} + 1,5(f_{m,j,k}/1,4 - f_{t,0,l,k} + 6)^{0.65} \tag{4.2}$$

With:

$f_{t,0,l,k}$ is the tensile strength of the outer lamination's
$f_{m,j,k}$ is the bending strength of the finger joints

The characteristic tensile strength parallel to the grain $f_{t,0,g,k}$ shall be taken as 80% of the bending strength $f_{m,g,k}$. And the tensile strength perpendicular to the grain $f_{t,0,g,k}$ shall be taken as 0,5 N/mm^2. The compression strength parallel to the grain $f_{c,0,g,k}$ can be taken as 100% of the bending strength $f_{m,g,k}$. For the compression strength perpendicular to the grain, 2.5 N/mm^2 can be assumed. The characteristic shear strength $f_{v,g,k}$ can be assumed to be 3.5 N/mm^2. The rolling shear strength $f_{r,g,k}$ can be taken as 1,2 N/mm^2.

4.3. CLT

The use of cross-laminated timber (CLT) for structural purposes is increasing in popularity (figure 4.3).A significant rise in production is to be expected within the next decade [63]. The number of layers varies with the lowest amount of 3 and increases with steps of 2 so that the outer layers are aligned in the same direction [16]. The softwoods that are used could be spruce, fine, fir, pine, larch or Douglas [70]. Currently, mainly spurce from Norway is used in the production of CLT [63]. CLT allows it to be used as a wall or floor element able to bear loads in and out-of-plane. Also, the shrinkage and swelling are less for CLT than for sawn timber. The boards used for the CLT have a thickness of 12-45 mm. Like glulam, the boards are connected by finger joints. The length of the finger joints is between 15-20 mm. A larger length of finger joint (LFJs) can be used, but it reduces resistance in cases of bending out-of-plane. The finger joints could be placed flat so that the fingers will not be visible on the surface. The adhesive that penetrates into the wood increases the elastic modulus and the shear modulus at the finger interface [65].

It is possible to have a combination layup. The longitudinal layers have a different board class type than the transverse layers. The most common strength class for homogeneous CLT is C24. And for a combination, it is strength class C24 in longitudinal direction and C16/C18 in transverse direction [63].

The adhesive used and the amount depend on the material and the bonding pressure. The pressure can be applied using a hydraulic press, which can apply pressure of 1 N/mm or higher. Or with a vacuum press, which

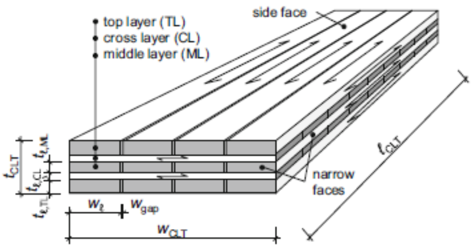

Figure 4.4: Technical drawing of a CLT element [63]

can deliver a pressure of up to 0.1 N/mm. Another way is by screws and staples/nails with a pressure of 0.2 N/mm.

4.3.1. Properties

The properties of a CLT panel could be determined based on the properties of the layers in combination with the bearing models or by tests on the CLT elements. For tension and compression, only the area A_{net} of the layers parallel to the grain is taken into consideration. For net-shear strength, only the layers in the weak direction are taken into consideration.

For the in-plane shear stresses, three different failure mechanisms have been identified. The first mechanism is net shear, which is shearing perpendicular to the grain. The second mechanism is torsion, and the third is gross-shear, which is parallel to the grain. Mechanisms 2 and 3 are reasonably known; however, mechanism 1 (shearing perpendicular to the grain) is up for debate. The most important factors for the shear stress are the thickness of the layers, the annual ring orientation, and the width of the gap between the boards w_{gap} (see 4.4)[58]. A minimum width for the boards is proposed as $w_l \geq 4t_l$ because of the rolling shear stresses in layers in CLT loaded out of plane (see figure 4.4). Otherwise, the tension perpendicular to the grain together with the rolling shear lead to a decrease in resistance [63]. Rolling shear failures are mostly spotted along the annual rings of the wood. The sawing of the board has thus also major influence on the rolling shear failure mechanism [15]. Due to the effect of the sawing of the boards, in Europe CLT products have an increasing amount of boards taken from the center of the tree rather than the sides. These products give higher resistance against shear modules [63].

The shear stiffness of the CLT panel can be computed using the formula 4.3:

$$S_{CLT} = \kappa \sum (G_{lay,i}, w_{lay,i}, t_{lay,i}) \tag{4.3}$$

With:

$G_{lay,i}$ is the shear modulus
$w_{lay,i}$ is the width of the i layer
$t_{lay,i}$ is the thickness of the i layer
κ is the shear correction coefficient

Since the the CLT elements are load bearing in two directions, the assumption can be made that the panels behave like diaphragms. A study done by Ashtari [3], the behaviour of a CLT element is described as a semi-rigid diaphragm. The following parameters are affecting the in-plane behaviour and the distribution of the lateral load: response of the CLT panel-to-panel connections, the in-plane shear modulus, the stiffness of shear walls perpendicular to the floor, the stiffness of the CLT floor and the floor diaphragm configuration.

4.3.2. Regulation

CLT is taken into the Eurocode as EN 16351. First as a draft in 2011 [36] and currently on the 2021 update [37]. The Eurocode focuses on characteristic strength, bonding strength, resistance and reaction to fire, dimensional stability and durability. The ISO also adopted a version for CLT in ISO-16696-1. The ISO shows the requirements for the CLT panels like adhesive requirements and layup requirements.

4.3.3. Fire resistance

There are two methods the Euro code prescribes when it comes to reaction to fire. The first method is a minimum requirement for the mean density (380 kg/m^3), overall thickness (40 mm) and minimum class. If the requirements are not met, the other method is applied, which is based on testing the product according to the standards referred to in EN 13501-1.

In EN 16351 the resistance on fire of a CLT may be determined by a designer on the basis of EN 1995-1-2 and the right timber characteristics like species, densities and the charring rate. The behavior of timber will be further discussed in Chapter 8.

4.4. Conclusion

Timber is gaining popularity as a building material, offering various strengths and challenges due to its anisotropic nature. While it exhibits strong tensile properties parallel to the grain, its brittleness and weakness perpendicular to the grain can limit its applications. Products like CLT and glulam enhance timber's utility by providing strength in multiple directions and making it more reliable for structural purposes. However, timber's combustibility and sensitivity to moisture present significant considerations in construction, especially concerning fire resistance and durability. Due to its brittleness and combustibility, robustness is an important topic to address. As a result, proper classification, treatment, and understanding of timber's behavior are essential for effective use in modern construction.

5
Current state of timber high rise

This chapter provides an overview of the current state of timber high-rises. Which can answer the question: what are the challenges in high rise timber in case of stability design, and how are these challenges solved in the past? This question will be answered with different cases that use different stability designs. First, the early developments in timber high-rises are discussed, beginning with the TF2000 project. This is followed by an analysis of two major high-rise timber buildings, the Treet and the Mjøstårnet, with a focus on their connections, robustness, and stabilization methods.

5.1. Last decade

The first modern multi-storey timber building in central Europe was built in the 1990s, much later than in North America [53]. The building built in Europe was 3 stories high. The regulations on timber as a construction material in Europe were first eased in Sweden and Austria. In 1994, timber buildings were allowed to have 6 to 8 stories in Sweden. This started the pioneering of Sweden in the timber construction industry. The Nordic Wood Program was formed, which ran a joint venture between different institutes, universities, companies and trade associations [53]. In the program, a lot of timber buildings were built. In 1995, the first five-storey building was built in Växjö Sweden [29]. More and more timber buildings were built. In 2007, the mid-rise timber building E3 was realised. The E3 is seven stories tall and was constructed in Berlin. A couple years later, in 2012 the Forté was constructed in Melbourne. Forté is 10 stories tall and has a height of 32 meters [54]. With the private desire for sustainable buildings, taller buildings were created [53]. The first timber building that reached 50 meters was the Treet building in Norway in 2015. And in 2018 Norway had again the largest timber building with the Mjorstarnet reaching 81 meters.

The search for timber buildings increasing in height is still going on. With projects like the Super Tall Timber Project, new insights are gained. This project is a collaboration of international architects and engineers and aims to provide the necessary understanding to make super-tall timber buildings possible [30]. In comparison to other steel and concrete buildings, the timber buildings are far from tall and may not even be considered high-rise. Hence, some discussion has come up to define timber buildings as being tall at lower heights. However this would underestimate the potential of the material. Also, it is difficult to characterise a timber building because of the use of hybrid structural elements [52].

5.2. TF2000 project

Due to innovations in timber design, the regulations for timber construction were outdated at the end of the last decade. In 1995, the Timber Frame 2000 Project (TF2000) was started. This project was a joint collaboration and was set up by the Office of the Deputy Prime Minister (ODPM), Department of Environment, Transport, and the Regions (DETR), the UK timber frame industry, BRE and the TTL. The project was a 6-storey timber construction on which varies tests were carried out 5.1. On structural stability and robustness, fire safety, differential movement and achieving performance. These tests resulted in various insights, leading to the adaptation of regulations [51].

5.2.1. Structural stability and robustness

During the project, the following things concerning stability and robustness were examined:

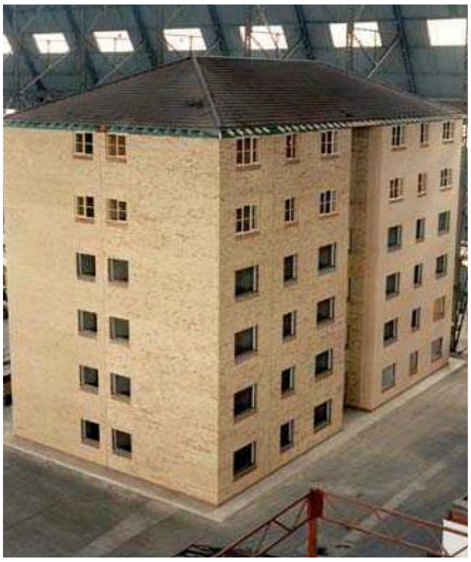

Figure 5.1: TF2000 building [51]

- Strength and stiffness design
- Robustness design based on good practice
- Robustness design based on case-specific calculations

Strength and stiffness design

The findings on stiffness were significantly higher than the building code prescribed. Different layouts were tested for the stiffness design, with the cellular layout being the best suited for a multi-storey building. Because the internal load-bearing walls could take up the horizontal forces. With the addition of plasterboard lining to the walls, the lateral stiffness increased by a factor of 3.3. And with masonry cladding, the stiffness increased by a factor of 17.7.

Disproportionate collapse test

Robustness tests were done by removing two walls that carried internal and external load 5.2. This resulted in the walls above the removed panels acting as a deep beam, which carried the loads to the sides of the panels. The floor panels that were supported by the removed wall were deflected by 24 mm for the inner wall. At the place where the outer wall was removed, the deflection of the floor panels was 4 mm. The project proposed the use of rim beams positioned between the vertical panels, providing support for the walls and the floor above in the event that one of the lower walls needed to be removed. Another alternative is to use continuous floor frame systems above multiple load-bearing walls [51].

Figure 5.2: Removal outer wall TF2000 [51]

The results from the TF2000 project were certainly useful, to understand how the stiffness design calculations act in real life. However, the results can be difficult to apply to other timber structural typologies because of the differences in behaviour of the members [61].

5.3. Treet

Treet started his construction in April 2014 and was finished in 2015 [26]. At that moment, Treet was one of the tallest timber buildings to date. The building was made out of load-carrying glulam trusses. Two levels of the building were made out of concrete, which acts as a base. On top of those levels, prefabricated timber modules were placed.

What is special about the Treet building is that while it is also one of the largest timber buildings, the load-bearing structure also mainly consists of timber. While other buildings like the King in Australia or the E3 in Berlin have hybrid structures, the Treet building has only concrete slabs that are used as a one of the major contribution to the structure [54]. What is also special about the Treet is how the building is made out of modules that are stacked upon each other. The first four levels are stacked on the ground. The fifth level is supported by the glulam truss and does not carry loads to the first four modules. Storeys 6–9 are stacked upon each other on the first concrete slab, followed by storey 10 supported by the glulam truss, and storeys 11–14 are stacked upon each other on another concrete slab. The modules that were prefabricated consisted of four different types (see figure 5.3).

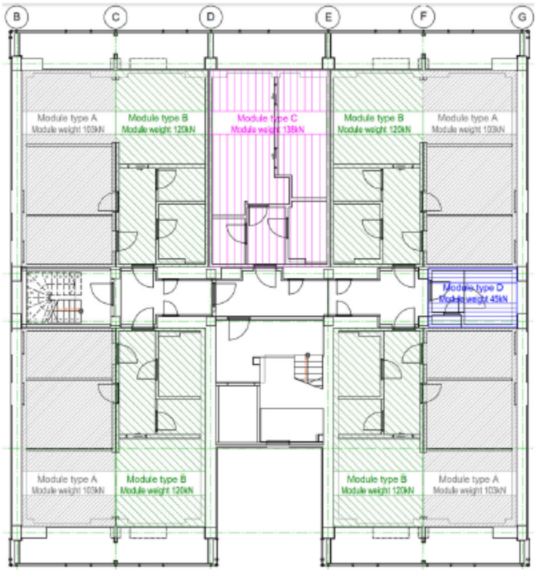

Figure 5.3: Layout modules Treet building [26]

5.3.1. Connections

The glulam bracing and the beams and columns in the façade are connected by slotted-in steel plates with steel grade S355 and dowels with type A4-80, which is an acid-proof stainless steel grade. This type of connection is also used in timber bridges. Three steel plates with a thickness of 8 mm and multiple 12 mm dowels are used. The number of dowels depends on the force the connection needs to carry. Gaps between the columns were introduced to handle the tolerances. These gaps were filled with acrylic mortar after installation. The connection with steel plates and dowels is supposed to be an easy connection. The building modules and the glulam trusses had a clearance of 34 mm. This is necessary to avoid the differential horizontal movement between modules and trusses that leads to damage.

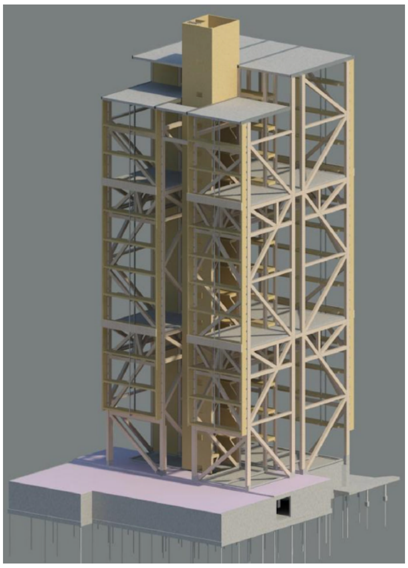

Figure 5.4: Treet [26]

5.3.2. Stabilisation

The elevator shaft and the inner walls are made out of CLT. However, the CLT does not contribute to the stability of the building. Most of the stiffness of the building comes from the glulam trusses that are placed in the façade.

5.3.3. Robustness

The paper by Malo et al (2016) states that the structure has a robust design. Every failing member results in an alternative load path. The truss members are verified in the accidental limit state combination [26].

5.3.4. Durability and fire resistance

For durability, the structural timber is covered by glass or metal sheeting. This will make the construction less susceptible to the outside weather. The glulam has strength classes of GL30c and GL30h. The CLT C24 has the closest resemblance to the kind of CLT used. All the timber is from a Norwegian source.

The main load-bearing structure is supposed to resist 90 minutes of exposure to fire without collapse and 60 minutes for the secondary load-bearing systems. Some of the systems incorporated for fire protection are:

- fire stops between storeys on the façade
- fire-resistant layer in escape routes (teknosafe 2407/2467)
- sprinkling system
- elevated pressure in escape stair shafts
- effective residual cross section after 90 minutes.

5.3.5. Assembly

The four different types of modules are prefabricated and put into place at the building site using a tower crane. Because of the light weight of the modules, large sections are relatively easily put into place. Also, large sections, depending on the transportation limits of the glulam frame are pre-manufactured and put into place at the building site. After the foundation and the garage are built, the first four levels of modules are placed. Followed by the construction of the glulam frame for the fifth storey and the concrete slab. This repeats until the building is finished.

5.3.6. Innovations and takeaways

As timber is a lightweight material, the accelerations due to wind loads are problematic when increasing the height of timber buildings [12]. It is therefore important for timber buildings to get an understanding of the natural frequency and the damping possibilities of the structure.

Since the use of modules in a timber project was a first in the industry, the modules where tested for their dynamic behaviour. A model analysis (MA) and a system identification (SID) where carried out on a module.

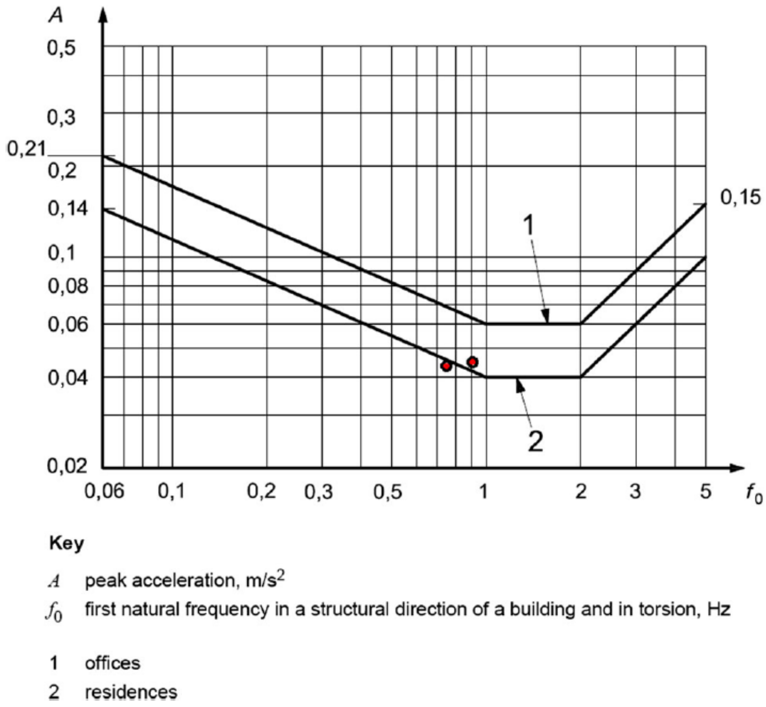

Figure 5.5: Treet accelerations top floor [26]

With the use of a hammer, an excitation was put onto the module, from which the response of the module was measured with sensors or accelerometers, depending on the kind of analysis. The effects of stacking the modules have been analysed using a FEM program. From this, it showed that the modules that were stacked had higher natural frequencies than the ones that were bound to the glulam frame (storey 5 and 10). The acceleration was calculated, and the results were slightly higher than the recommended value at the top of the building. In figure 5.5 the natural frequency of the top floor is put against the peak acceleration. The value is slightly above the ISO 10137 curve.

5.4. Mjøstårnet

As of today, the Mjøstårnet is one of the tallest timber buildings. The building stands at an impressive height of 81 meters and comprises 14 stories. The stability structure is fully made out of timber. With the foundation made out of concrete, the first 9 floors were CLT followed by 7 floors made out of concrete. Groundwork started in April of 2017, and the building was completed in March of 2019. The building made use of local resources. Norway spruce is mainly used as the building material for the structural timber parts, estimated at roughly 14 000 trees [11] .

Like the Treet building, the stability system of the Mjøstårnet is fully made out of timber. Large glulam trusses in the façade handle the horizontal forces and give stiffness to the building. The CLT walls of the elevators do not contribute to the lateral stability. These are installed as a secondary load bearing for the elevators and the stairs. Other walls do not contribute to the construction and are only there for separating purposes.

Unlike the Treet building, the Mjøstårnet does not make use of building modules. This will provide a more open floor plan for mixed functions. The concrete floors at the top are for acoustic purposes. On the top floors are the apartments, which require more sound isolation. The floors made out of timber at the first 9 stories are Moelven's Trä8 floor elements made out of glulam and rockwool. These are good enough for 90 minutes of fire resistance and fulfill the acoustic requirements [1].

5.4.1. Connections

The connections used are like the Treet slotted in steel plates with dowels. The timber is on the inside of the façade to protect it from outside forces. The connections at the bottom need to resist a tension force of 5500 kN because the horizontal forces will outweigh the vertical down force of their own weight [1].

5.4.2. Stabilisation

The stabilisation is done by the glulam trusses in the façade. Like the Treet building the wind loading is the dominant factor. With the findings on the Treet building, the damping factor was calculated. From this, the acceleration at the top level could be determined. At the top level, the acceleration is slightly above the ISO-curve just like the Treet building 5.5.

5.4.3. Robustness

The concrete floors on the upper levels serve a dual purpose: aside from enhancing acoustic performance, they also play a vital role in mitigating wind-induced vibrations. Furthermore, the columns have been over designed to ensure their capability to support heavy loads, even in the event of a fire. In the construction of connections, a ductile behavior approach has been implemented. Additionally, the entire structure has been engineered to withstand potential impacts from falling concrete floors [46].

The Mjøstårnet was assembled 4 stories at a time with prefabricated glulam beams. This leads to fewer vertical discontinuities, which leads to fewer weak spots. The fewer vertical discontinuities also come with fewer zones where large displacements can happen and energy can dissipate. The columns were designed as key elements and therefore protected from outside forces [61].

5.4.4. Assembly

During the construction, the structural elements are exposed to the outside. From experience, this was not problematic as long as the shell was on the structure and the members exposed to the weather conditions could air out. A moisture control plan was carried out, which measures the moisture of specific parts of the structure [1].

5.4.5. Innovations and takeaways

Being the highest timber building to date shows the possibilities a timber building can have even without the use of concrete segments for the construction. The slotted-in steel plates connections with glulam beams from the Treet building have again proven to be useful, even in bigger connections.

5.5. Improvements Eurocode

In all the years the timber construction material is researched, the Eurocode adapts the findings into the code. The part of the structural Euro-codes that includes the design of timber structures is EN 1995 which is divided into different parts. EN 1995-1-1 includes the general timber design with common rules and rules for buildings [41]. EN 1995-1-2 covers the structural fire design [42]. There is a special part EN 1995-2 for timber bridge design [43].

5.5.1. Robustness

The EN 1995-2 which focused on timber bridge design, discussed the topic of robustness with the following:

- A reference to EN 1990:2023 for general robustness.
- A table with the minimum dimensions of structural timber members.
- Mentioning that lightning can cause significant damage to timber

In Annex E of EN 1990-2021, additional guidance for enhancing the robustness of buildings and bridges is given. This does not apply exclusively to timber and, in some way, is not applicable to the material. Due to the material's limited ductility.

In Annex A of the draft version of EN 1995-1, guidance is provided for increasing the robustness of timber structures, particularly in response to local failures. The annex outlines strategies such as creating alternative load paths to redistribute forces and segmenting the structure to isolate damage. It also covers the analysis required for scenarios involving the removal of structural elements and the use of fuse elements designed to fail under specific conditions to prevent progressive collapse.

5.6. Conclusion

Through the examination of projects such as the Treet, HoHo Wien, and Mjøstårnet, it is evident that timber, once constrained by regulatory and technical limitations, has evolved into a viable material for tall structures. The case studies reveal how hybrid designs, modular construction, and advanced connection techniques have addressed issues of robustness, fire resistance, and wind-induced vibrations, pushing the boundaries of timber architecture.

As the field continues to progress, ongoing research and development, such as the Super Tall Timber Project, will be crucial in overcoming the remaining challenges and further solidifying timber's role in sustainable high-rise construction. The integration of these advancements into standards like the Eurocode will also play a pivotal role in guiding future timber high-rise developments.

6 Connections

In this chapter the connections are discussed. To answer the questions: what are the possible connection types and how do the stiffness and the strength of the connections be calculated. These connection types will be used for the modeling of the core and the bracing in the case study.

Timber is brittle in tension both along and parallel to the grain, making rupture of the material a significant risk. To prevent this, connections in timber structures should be designed to be ductile, allowing for deformation and before the timber material reaches its brittle failure point.

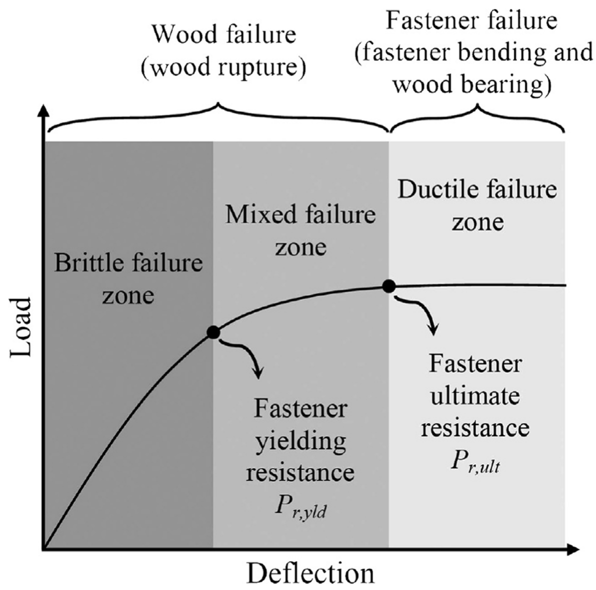

Figure 6.1: Failure types in a connection [22]

6.1. Timber connections

Most of the connections make use of steel elements, because of its high load bearing capacity and stiffness. However there are examples of full timber connections. The Tamedia building in Zurich is an example of a medium high-rise timber building that makes use of full timber connections in the load bearing frame. No mechanical parts or adhesive are used in the connection. The beams and columns are connected via prefabricated beechwood pins figure 6.2. The difficulty of timber connections is the fire resistance and the lack of redundancy. Because the connections make use of singular beechwood pins, the pins can be made big so more timber can be added. This excess timber can char up in case of a fire, so that the inside is protected and can hold the structure [21].

Figure 6.2: Tamedia office building [21]

6.2. CLT connections

CLT can be used as a load-bearing wall or floor. A timber core made with CLT elements is able to transfer vertical and horizontal load to the foundation. The connections need to be strong but also stiff for the least amount of deflection or acceleration. Different kinds of connections are possible. These connections are the following: (1) wall-to-wall / floor-to-floor connection, (2) wall-to-floor connection and (3) a wall-to-foundation connection. The connections from wall-to-wall are impotent for determining the stiffness of a timber core. The core is going to consist of CLT wall segments connected together. A common way of connecting these CLT panels is by using self-tapping screws. Hold-downs could be used to transfer tensile force from the CLT panels to the foundation (see figure 6.3. Angle brackets for transferring shear forces from the CLT-walls to the foundation or to the floors [70].

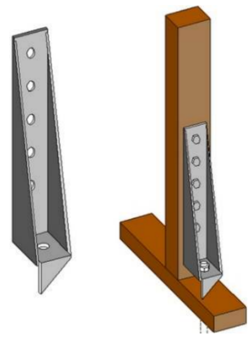

Figure 6.3: Traditional hold-downs for timber buildings [69]

Figure 6.4: TTV Angle brackets [18]

6.2.1. Self tapping screws

Self-tapping screws can have a significant load-carrying capacity when they are axially loaded. These screws are commonly employed in modern engineered timber structures for various applications, including the connection of linear components such as solid timber or glued laminated timber (glulam), as well as in flat components like cross-laminated timber [56].Self-tapping screws can be used to connect two walls in plane or two walls perpendicular[70]. The screws are mostly applied under an angle of 90- or 45 degrees. The withdrawal capacity of self-tapping screws depends on the characteristic density of the timber material. A test has shown that not only the density of the timber is a parameter but also the amount of layers which the fastener goes trough [56]. Table 6.1 shows the strength and the stiffness of the self tapping screws. The screw diameter, penetration depth, edge distance and spacing between the screws were selected based on commonly used values. These parameters would alter the strength and stiffness's.

Angle	Loading	F_{max} [kN]	K_{ser} [kN/mm]
90	Axial	20,8	17,5
90	Lateral	10,3	0,5
45	Axial	33,6	16,6
45	Lateral	30,0	19,9

Table 6.1: Strength and stiffness self tapping screws [57]

Stiffness self tapping screws

In a paper of Brown et al [8], different screwed connections in a CLT wall system where examined. It concluded that mixed angle screws where the most effective. By using screws installed with mixed angles both stiff and ductile performance can be achieved. For the stiffness of self tapping screws that are latterly loaded, the K_{ser} can be taken from the rigidities K_{ax} in the direction of the screws and with the use of virtual work. For a set up like figure 6.5 , the K_{ser} in the direction parallel to the shear plane can be calculated as follows [55]:

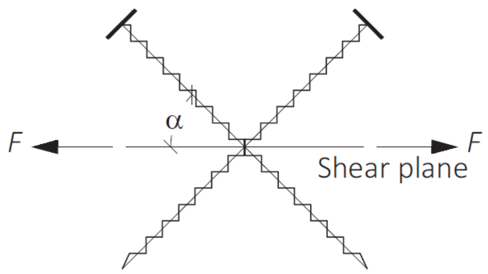

Figure 6.5: Cross-wise arranged screws at angle α [55]

$$K_{ser} = K_{ax} \cdot cos^2\alpha \tag{6.1}$$

Table 6.1 shows the stiffness for the self tapping screws in different setup's.

Self taping screws will be used in the model for the vertical CLT connections (see 6.6.

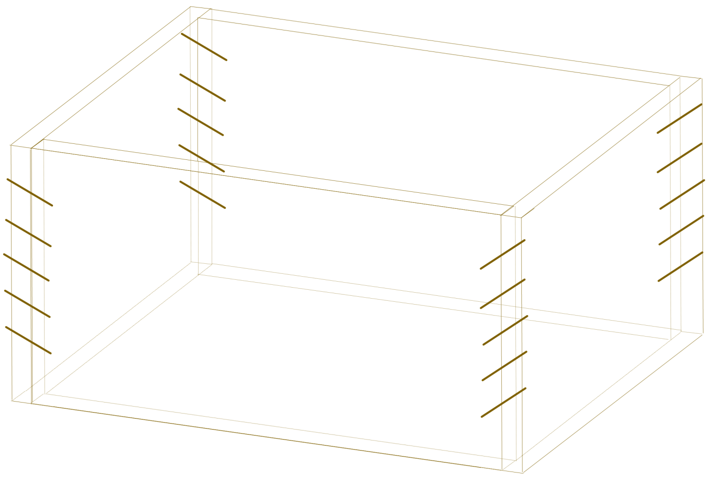

Figure 6.6: Self tapping screws in core model

6.3. Steel fasteners

6.3.1. Dowel type fasteners

Dowel-type fasteners can experience bending, tensile, embedment, and shear stresses within the connection. The category includes: nails, staples, bolts, screws, dowels and threaded rods[55].

For the dowel type fasteners the embedded strength is being determined by an apparatus test [44]. The euro code prescribes how a connection with a dowel type should be calculated. The connections in the model that is going to be used in the case study, the bracing and the horizontal core connections are connected by slotted in steel plates with dowels 6.7.

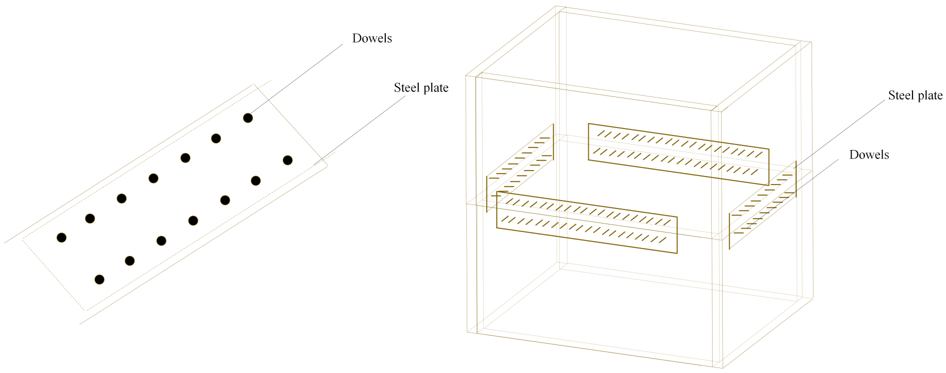

Figure 6.7: Bracing connection (left) and horizontal line connection (right) model.

For a steel on timber connection the failure mechanism are illustrated as in figure 6.8. The failure mechanism depend on the thickness of the steel plate (thin or thick) and how the timber and the dowels behave. Whether the crush strength of the timber is met or the moment capacity of the dowels. The crush strength along the direction of the grain can be calculated using the following equation:

$$f_{h,0,k} = 0.082(1 - 0.01d)\rho_k \tag{6.2}$$

With:

d is the diameter of the dowel in mm
ρ_k is the characteristic value of the mass in kg/m^3

If the direction of the grain is at a angle a reduction is applied. The reduction depends on the kind of timber that is being used (hardwood, softwood or LVL) and the dimension of the diameter.

$$fh, \alpha, k = \frac{f_{h;0;k}}{k_{90} sin^2\alpha + cos^2\alpha} \tag{6.3}$$

With:

α is the angle with the grain
k_{90} is the constant depending on the diameter and the kind of timber.

The moment capacity of the dowels can be determined with the following equation:

$$M_{y,k} = 0.3 \cdot f_{u,k} \cdot d^{2.6} \tag{6.4}$$

With:

d is the diameter of the dowel in mm
$f_{u,k}$ is the characteristic tension strength in N/mm^2

All failure mechanism should be checked with different formulas to find the normative failure mechanism [14]. The formula on the specific failure case can be determined via equilibrium of the forces (see appendix B.4). If a screw thread is applied a extra effect(rope effect) takes place which gives extra capacity to the connection.

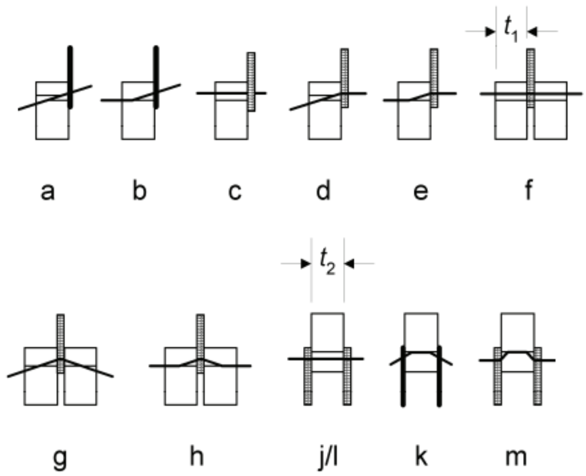

Figure 6.8: Types of failure mechanism dowels [55]

To ensure robustness a minimum of two dowels are required in the connection.

Multiple dowels

For most connections that exhibit big forces multiple dowels are necessary to transfer the forces. Joints with multiple dowels are prone to exhibit brittle failure modes. These failure modes are illustrated in figure 6.9. The corresponding failure modes are as follows: (i) row shear failure, (ii) block shear failure, (iii) embedment and plastic hinge failure, (iv) splitting failure and (v) net tension failure.

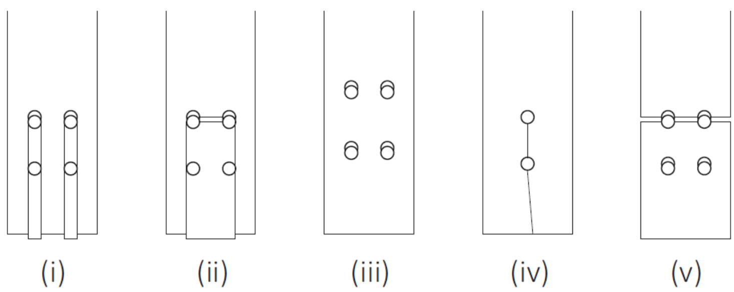

Figure 6.9: Failure modes multiple dowels [55]

In the case of multiple fasteners, the effective amount of fasteners n_{eff} is lower because the risk of brittle failure is higher which gives a lower load bearing capacity to n amount of screws [41].

$$n_{eff} = n^{0.9} \cdot \sqrt[4]{\frac{a_1}{13d}} \tag{6.5}$$

With:

a_1 is the distance between the dowels in the direction of the grain.
d is the diameter of the fastener.
n is the amount of fasteners in a row.

The correlation between the single dowel strength and the spacing parameters with the multiple dowels strength was elaborated by Jorrisen[25] using the pearson correlation coefficient. The correlation with the parameters and the $F_{multiple}$ was as follows: number of fasteners parallel to the grain (n = 0.91), number of fasteners perpendicular to the grain (m = 0.88), ratio of the thickness of the timber to the diameter of the whole ($\frac{t_m}{d} = 0.33$), ratio of the distance between the dowels in the direction of the grain to the diameter ($\frac{a_1}{d} = 0.58$), and the strength of a single dowel ($F_{single} = 0.84$). The equation that followed from these correlations was:

$$F_{multiple} = 0.37 \cdot n^{0.90} \cdot (\frac{a_1}{d})^{0.30} \cdot (\frac{t_m}{d})^{0.20} \cdot F_{single} \tag{6.6}$$

The correlation with the number of rows (m) was taken out of the equation but can influence the $F_{multiple}$. Compared to the Euro code, the equation generated by Jorrisen is more conservative for thin pieces of timber and more conservative for thick pieces of timber.

Stiffness

From multiple tests the stiffness equation K_{ser} for a pre-drilled bolted- and dowelled joints per shear plane, in a timber-to-timber connection:

$$K_{ser} = \frac{d \cdot \rho_m^{1.5}}{23} \tag{6.7}$$

With:

d is the diameter of the fastener $[mm]$.
ρ_m is the density of the timber member $[kg/m^3]$.

For a timber to steel connection the value can be multiplied by 2 [55]. This is because the steel plates elastic deformation is much lower compared to the timber. Nails and staples have a slightly other equation see Appendix B.7. The equation can be used for fasteners up to 30 mm following the Eurocode. This however, is quite conservative since tests on bigger fasteners show bigger stiffnesses. Therefore, Ehlbeck and Werner [67] use a stiffness constant for bigger dowel types of:

$$K_{ser} = (1.2 \cdot d - 1.6) \cdot \rho_m \tag{6.8}$$

To compute the stiffness of multiple dowels in a connection, the stiffness can be multiplied by the shear planes and than by the amount of dowels. In a study done by Malo et al [64], the influence of multiple dowels to the stiffness has been examined. A clear trend is being examined of a decreasing stiffness with a increasing number of dowels in the direction of the grain. With different results including big scale connections, the following equation is extracted.

$$K_{ser,mod} = k_{ser} \cdot m \cdot n_{spd} \cdot n_0(q_{0,1} + q_{0,2}e^{\frac{1-n_0}{r_0}}) \cdot n_{90} \cdot (q_{90,1} + q_{90,2}e^{\frac{1-n_{90}}{r_{90}}}) \tag{6.9}$$

In the same paper by Malo et al [64], the average relative stiffness was tested of multiple 12 mm dowels perpendicular to grain and parallel to the grain. From tests it was shown that the stiffness per dowel depends on the amount of dowels and the grain direction. The average relative stiffness is visualised in figure 6.10.

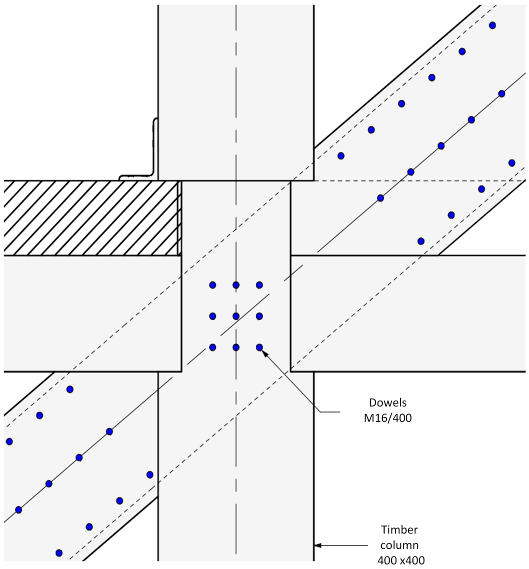

Figure 6.11: Slotted-in steel plate connection Urban Woods [62]

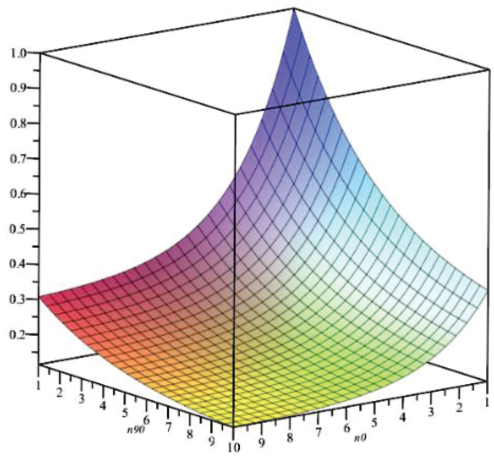

Figure 6.10: Average relative stiffness dependent on dowels in the two directions [64]

The axial slip modulus per panel for fasteners is calculated as follows:

$$K_{ax} = 25 \cdot d \cdot l_{ef} \tag{6.10}$$

With:

l_{ef} is the length of the dowel or screw.

Combining the two panels for the connection, the following equation can be used:

$$k_m = \frac{1}{\frac{1}{k_{ax,1}} \frac{1}{k_{ax,2}}} \tag{6.11}$$

The screw configuration under an angle is:

$$K_A = k_{ser} \cdot sin^2(\phi) + k_m \cdot cos^2(\phi) \tag{6.12}$$

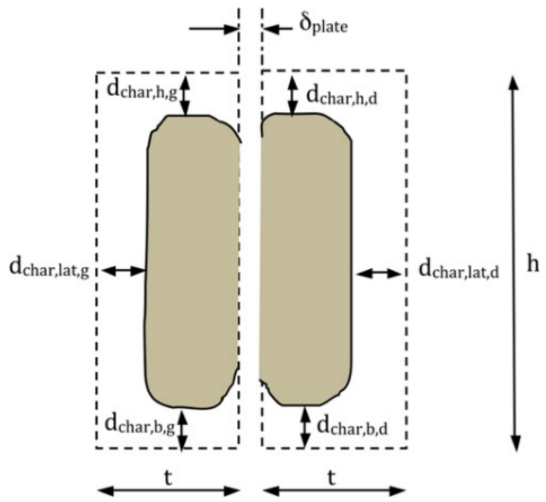

Figure 6.12: Residual cross section after charring [7]

6.3.2. Surface type fasteners

This group also includes metal fasteners, which can be used in timber construction. With surface-type fasteners, most of the force is transmitted through the surface of the timber member. In this group are connections like split rings, toothed-plate connectors, and punched metal plate fasteners [55].

6.3.3. Corrosion

The steel connections should be designed so that no water can come in to prevent corrosion. A cover over the timber construction is sometimes applied to shield the structure from water and the sun. In cases of exposure, a coating could be applied or stainless steel could be used [55].

6.4. Initial slip

Due to the hole clearance in the slotted-in steel plate connections and the imperfections in the drilling, initial slip can occur. Initial slip in the connection causes extra deflection in the structure [32]. The inclusion of initial slips in the connections was not included in the design of the Treet building. However, a sensitivity analysis was carried out to investigate the influence of slip on the connections. Due to the low number of connections where slip could occur, the Treet building was not very sensitive to the deflection following the initial slip [26].

6.5. Fire resistance connection

The metal in the connection that is used as a fastener has a high thermal conductivity, which transmits heat into the member and decreases the strength and stiffness around the connector. Continuous heating will result in the connection being more prone to embedment failure. For timber heated to 150 °C, the embedment strength will be reduced up to 60% [5]. This will result in the connection rapidly declining in strength for unprotected connections. The charring occurs at a higher rate at the connections due to:

- When steel is exposed to fire, the steel will transfer the heat into the timber. Even when not directly exposed, the steel will still attract heat in the connection.
- gaps that are between the connecting elements where heat can penetrate.

In research done by M. Audebert et al [7], a charring rate of 0.88 mm/min was measured at the a connection with one steel plate. The biggest charring rate occurred at the upper and lower sides of the cross section 6.12. For bolts, there is more heat transfer because the bolt head and the nut increase the surface area to which the fire is exposed. According to the Eurocode, a connection factor of 1.5 is used for timber-to-timber connections [42].

For unprotected nails, screws, bolts, and fasteners corresponding to EN 912, the fire resistance duration $t_{d,fi}$ is 15 minutes, and for Dowels, 20 minutes, with a minimum thickness of the timber side member of 50 mm. The characteristic value of shear in the connection during a fire can be calculated with:

$$F_{v,Rk,fi} = \eta F_{v,RK} \tag{6.13}$$

With:

$$\eta = e^{kt_{d,fi}} \tag{6.14}$$

With:

k is a parameter given by the EC 1995-1-2 table 6.3
$t_{d,fi}$ is the calculation value of the fire resistance of a unprotected connection.

The calculation of $t_{d,fi}$ is as follows:

$$t_{d,fi} = -\frac{1}{k} ln \frac{\eta_{fi}\eta_0 k_{mod}\gamma_{M,fi}}{\gamma_M k_{fi}} \tag{6.15}$$

With:

η_{fi} is the reduction factor for the calculation value from the EC
η_0 is the ratio between the design strength and the design load at room temperature.
k_{mod} is the modification factor
γ_M is the partial factor of the connection
k_{fi} is a parameter given by the EC 1995-1-2 table 2.1 (1.05)
$\gamma_{M,fi}$ is the partial safety factor for timber in the fire situation(1.0).

The fire resistance duration can be increased by increasing the end- and edge distance by factor α_{fi}:

$$\alpha_{fi} = \beta_n \cdot k_{flux} \cdot (t_{req} - t_{d,fi}) \tag{6.16}$$

With:

α_{fi} is the end/edge distance increase factor
β_n is the effective charging rate
k_{flux} is the heat flow coefficient (generally = 1.5)
t_{req} is the required fire resistance duration
$t_{d,fi}$ is the fire resistance according to EN 1995-1-1

A higher fire resistance duration for the connections could also be achieved with protected joints. Joints are protected if the external steel plate is equipped with cladding material made of wood or wood-like material. The thickness of the cladding needs to be at least α_{fi}.

6.6. Conclusion

In the construction of timber high-rises, the design of connections plays a critical role. This is in the case of strength calculation, but also when the height of the building increases, the stiffness of the connections play a role in the overall stability. In this chapter, the types of connections to be used in the model are provided.

7 Stability

In this chapter the stability systems that are relevant to the case study are going to be discussed. First the core, followed by the bracing in the façade.

7.1. Designing for height

When increasing the height of a building, other failure mechanisms come into play. The growing tower in figure 7.1 shows that first shear failure is the major factor for lateral force with a height ratio if 1:4. When increasing the height ratio to 1:8, bending failure gains the upper hand, followed by deformation at 1:20 and natural frequency at 1:30.

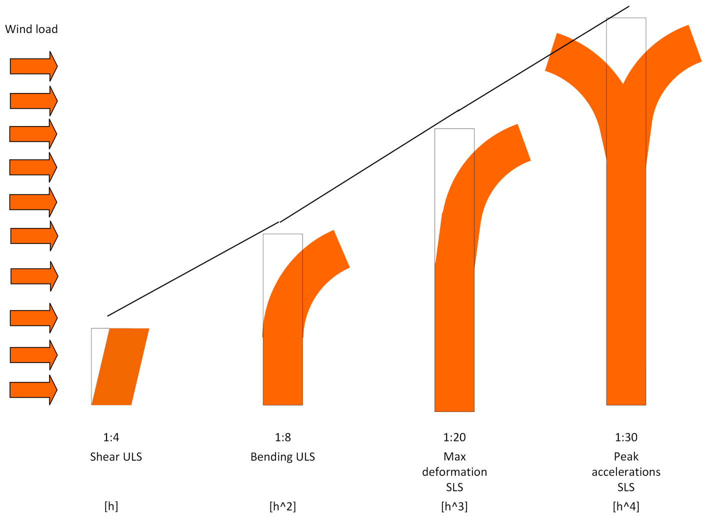

Figure 7.1: The growing tower[34]

For timber high rise buildings like the Mjøstårnet and the Treet, the acceleration is the major bottleneck (see figure 5.5). The height ratio is lower than that of the growing tower. However due to the low weight and flexibility of the timber material, the natural frequency is earlier achieved and results in high accelerations. These accelerations are mostly problematic for the serviceability limit state (SLS) especially at the top level of the building. Users may perceive these accelerations, resulting in an unpleasant experience. For about 50 percent of individuals, the limit of acceleration perception is approximately 0.049 m/s². Accelerations beyond this threshold, reaching 0.098 m/s², could even lead to feelings of nausea [12]. The Dutch NEN standard for maximum acceleration is slightly more relaxed compared to the ISO 10137. This relaxation is based on the consideration that some individuals are more sensitive to motion and may experience nausea even at lower levels of acceleration. The standard is set based on the percentage of the population that can tolerate building movements, particularly during events like storms with a return period of one year. This threshold is somewhat arbitrary, as it accounts for the majority who can tolerate the movement, rather than those who are always sensitive to it.

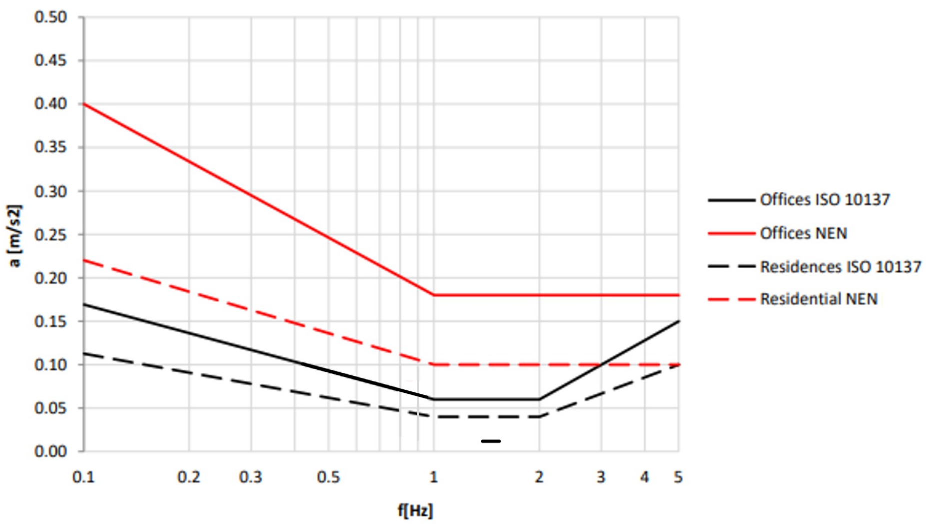

Figure 7.2: Acceleration curves ISO 10137 and NEN

Similarly, the Treet building 5.3, despite having a higher acceleration value than what is recommended by ISO 10137, is still considered acceptable. This suggests that there is a level of flexibility in applying these standards, based on practical considerations and acceptable levels of discomfort for most occupants.

To calculate the standard deviation of the characteristic along wind acceleration, the NEN-EN 1991-1-4 is used (see Appendix B.1) [2]. The along wind acceleration depends on the natural frequency of the building. In the withdrawn NEN 6702 a determination of the natural frequently is given by the following equation:

$$f_e = \sqrt{\frac{a}{\delta}} \tag{7.1}$$

With:

a is a numerical value depending on the static system (0.384 with the mass equally divided)
δ is the biggest deflection of the system

With the aid of FEM software, it is possible to determine the natural frequencies of a structure.

7.1.1. Damping

From the examples of timber buildings in chapter 4, the damping of a timber building is of importance for the stability of the structure. For the Treet building multiple test were carried out to investigate the natural frequency and the damping factor [26]. The total equivalent viscous damping can be approximated by the damping in the materials and the damping of the whole structure:

$$\zeta = \zeta_{struct} + \zeta_{mat} \tag{7.2}$$

In case of the Treet building, material damping of ζ_{mat} = 0.005-0.010 was found for the glulam members [26]. The structural damping was in the range of 0.010-0.020, and is mainly due to the energy dissipation in the connections and interaction between surfaces. The Eurocode prescribes a structural damping factor for concrete and steel buildings but not for timber buildings. NEN-EN 1995-2 does have a structural damping coefficient for timber bridges ranging from ζ_{struc} = 0.005 to 0.02.

7.2. Structural systems

To reach height in steel and concrete, better stability system needs to be in place. There can be opted for a outrigger system, in which a stiff head is placed on top of the core with columns on the side of the structure which could be in tension. Another option is the tube in tube structure. This structure consist of an outer frame tube structure along with an inside core. The outer and inner tubes act together to resist the horizontal and the vertical loads.

With material of the outer tube put out of the center, the moment of inertia is much greater following Steiner's theorem.

$$I = I_{cm} + m \cdot d^2 \tag{7.3}$$

With:

I_{cm} is the moment of inertia of the body mass.
m is the body mass.
d is the distance from the body mass to the center.

(a) Example outrigger system, China world tower (Beijing)[31]

(b) Example tube in tube system, World trade center (NYC)

(c) Example bracing system, John Hancock center (Chicago)

Figure 7.3: Examples structural systems

With the higher moment of inertia the global stiffness could be much higher with an outer tube. Diagonals give extra stiffness to the outer tube, because of the superior truss working. Figure 7.4 from the 1970's shows different types of structural systems with the height they could achieve [31].

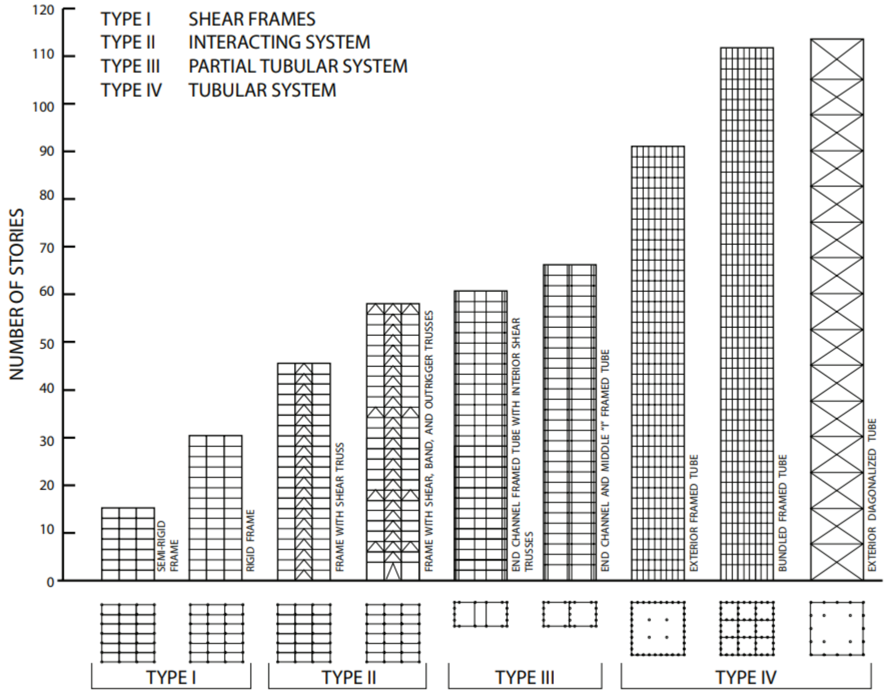

Figure 7.4: Structural systems with their reachable heights [31]

7.3. Timber structural systems

For timber the same idea for structural stability can be adapted. However, because of the lack of stiffness and low weight of the material, more emphasis relies on the structural systems. Various innovative approaches have emerged. Some designs incorporate a concrete core (HAUT), solving the lack of stiffness of a timber core by implementing a concrete core. Another approach is to use a concrete core with a timber bracing system (Cube House), where the timber bracing acts as the outer tube. Additionally, there are designs like the Urban Woods that rely entirely on timber, with a timber core and timber bracing systems. Most of the stability is provided by the bracings in the façade of the building.

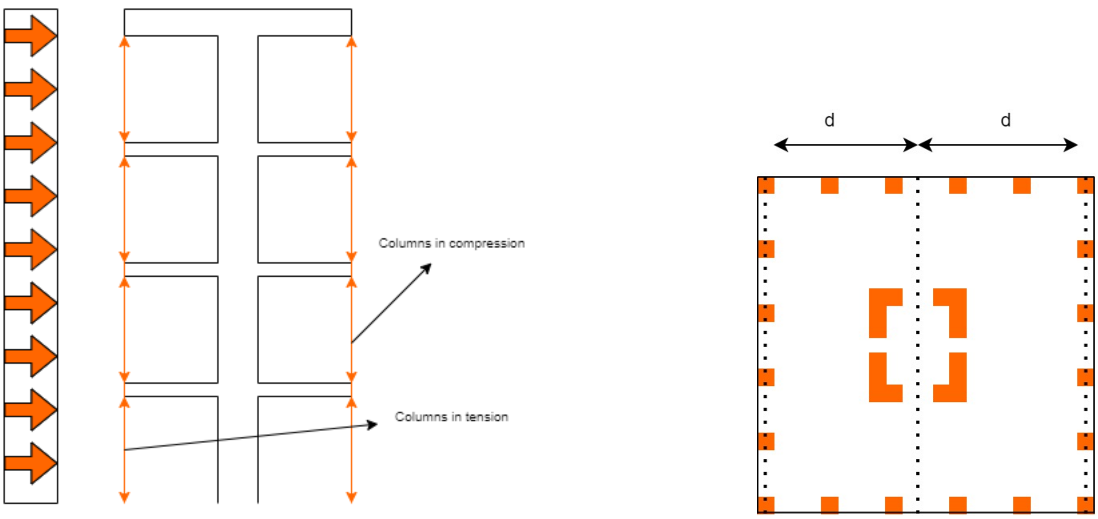

(a) Schematic representation of an outrigger system (side view)

(b) Tube-in-tube system (top view)

Figure 7.5: Comparison of two systems

Numerous studies have delved into the effectiveness of different stability systems. The outrigger system was in different case studies tested by Janssens [23]. Depending on the amount of outriggers, the lateral acceleration was reduced by 25%. A study constructed by Felicita [17] looked at the different stability systems. Among them, the Glulam diagrid system was the most efficient system compared to the CLT core and the Glulam frame systems. Efficiency was evaluated based on the maximal slenderness in relation to the amount of timber used to achieve the unity check in SLS. A optimal stability system is crucial for a low density material like timber. The form of the implementation can be seen in timber projects like the Mjøstårnet and the Treet building [26]. These buildings do not use the exact same principle the diagrid system of the paper of Felicita uses. The Mjøstårnet and the Urban Woods incorporates beams at every façade crossing from one side to the other. The Treet makes use of multiple diagonals figure 7.6.

To enhance the concept of a timber glulam diagrid, Jacob Versteeg Conlledo [9] introduced a circular floor plan combined with a timber glulam diagrid structure. The adoption of a circular building layout was a strategic choice aimed at minimizing the impact of wind loads on the structure. Since the force coefficient used to calculate the along wind force is less for a circular shaped building than for a square.

(a) Mjøstårnet **(b)** Treet **(c)** Urban Woods

Figure 7.6: Examples structural systems

7.3.1. Angle of stability system

The angle of the bracing system in the façade has influence on the stability of the system. The following figure 7.7 shows the deflection with the bracing like the one in the Urban Woods, with having different angles for the bracings. The preliminary test is carried out by a constructed FEM model of the Urban Woods. For this test a 30 meter high timber construction was used with a square surface and the following stiffnesses.

Vertical line hinges core kN/cm^2	horizontal line hinges core kN/cm^2	Bracing member hinge kN/cm^2
u_x/u_y = 0	u_x = 0	u_x = 2000000

Table 7.1: FEM model

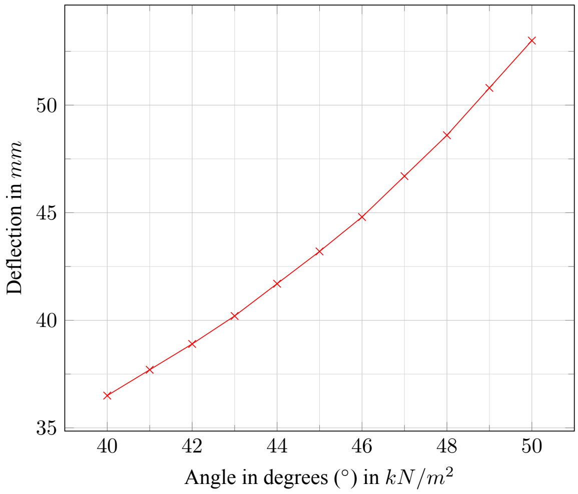

Figure 7.7: Relationship between angle bracing (°) and deflection in bracing connections.

7.3.2. Stiffness of stability system

The performance of the bracing system depends on the stiffness of the material and the connections. The members of the bracing will only experience axial forces. For the spring stiffness, u_x is the governing stiffness. Figure 7.8 shows the decrease in deflection resulting from an increase in connection stiffness for a 10-story (30-meter) building. This preliminary test was carried out on the Urban Woods model. The comparison is made with the core line hinges from the Urban Woods, without any cutouts. For a 30-meter building, the maximum global deflection in the SLS is 30 mm.

Another way to decrease the global deflection is by increasing the cross section of the bracings, which gives more material and thus stiffness to the construction 7.9. This test was carried out on the same model as 7.7.

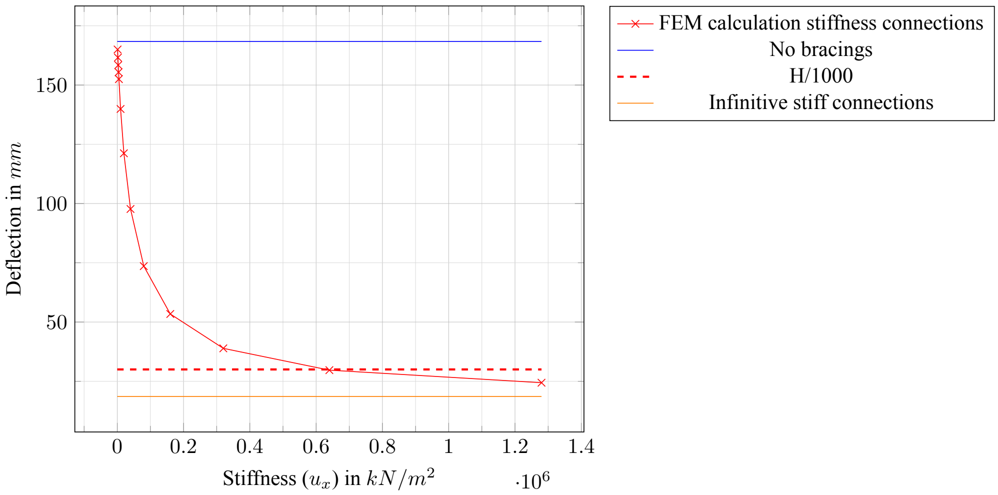

Figure 7.8: Relationship between stiffness (u_x) and deflection in bracing connections.

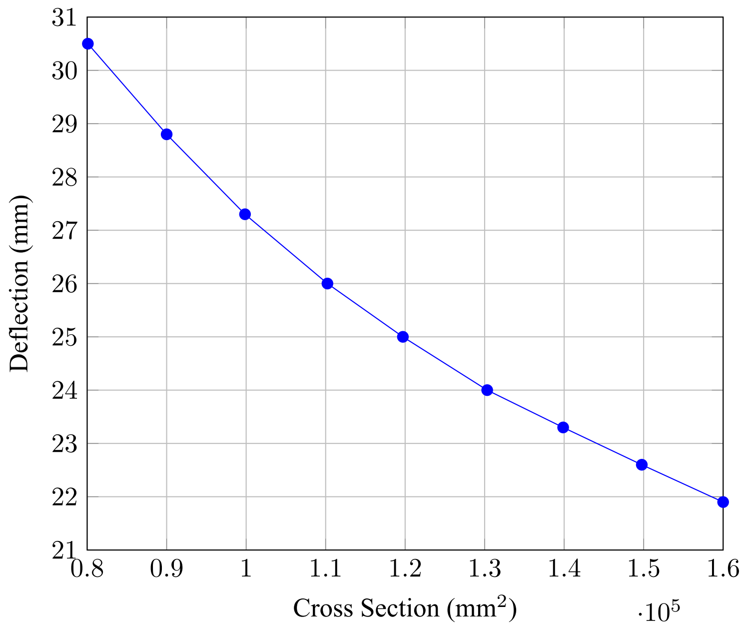

Figure 7.9: Deflection vs. Cross Section Area

7.4. Timber core stability

Like buildings with a concrete core, the global distribution of the lateral forces will be the same for low rise buildings with a timber core. With a stiff core, it is not necessary to have stiff column to beam connections [34]. The core can be seen as a column with a rotational spring at the base. The core consist of multiple thick walls connected together. The walls are used as stabilizing element. The lateral force is taken by the façade and goes trough the floor to the core. The core walls that are aligned in the direction of the force will take up the force and redirect the force resulting in vertical stresses (see figure 7.10). The deflection and the acceleration of the wind

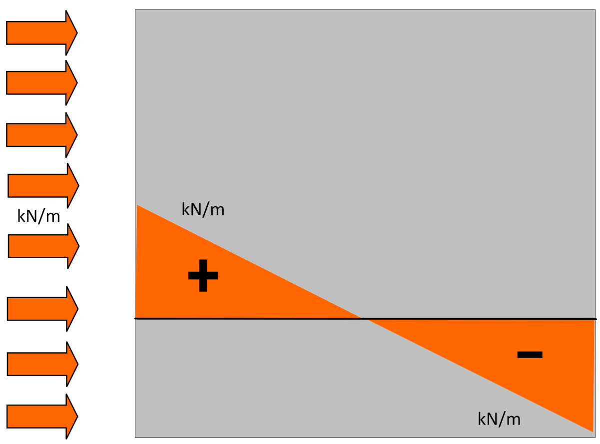

Figure 7.10: Vertical stress due to wind load

load on the core depends on the stiffness of the used walls and the stiffness of the connection. For a timber core it is difficult to make the members and the connections stiff [70]. Elements like doors, windows and ducts make the core less stiff see figure 7.11. The stiffness of the lintels decide how the two different wall panels that are divided by the cut-out behave. The position of the opening has relative small impact on the the cooperation of the two different wall panels.

A example on how the lintels cooperate on the cores moment of inertia: A core with no cut-out has a width of 7,2 meters. The moment of inertia with a panel thickness of 0.2 meters will be:

$$I_y = \frac{t_{wall} \cdot L_{wall}}{12} = 6,22m^3 \tag{7.4}$$

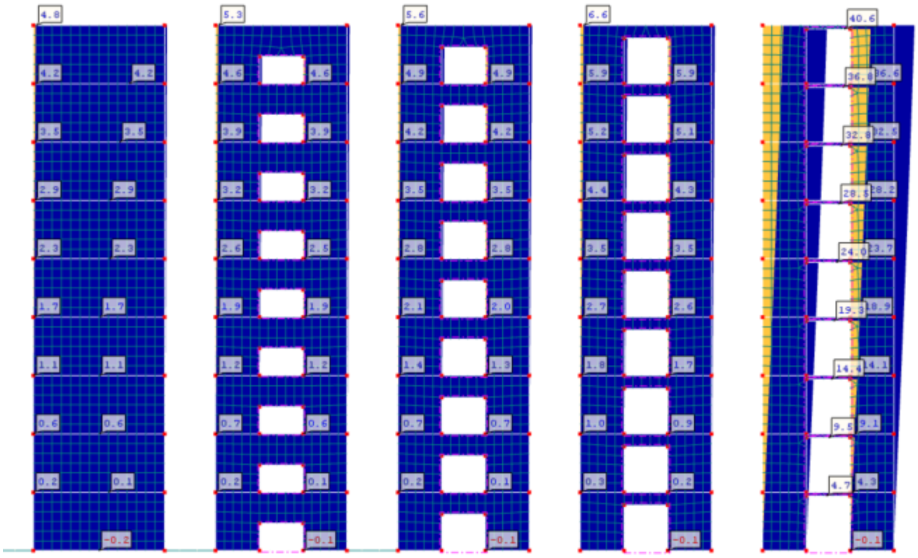

Figure 7.11: Example of deflection depending on the holes in the wall panels.

If the lintels are small, they do not contribute to the cooperation of the two different wall panels. The moment of the individual wall panel will be when the cut-out is 2 wide:

$$I_y = \frac{0,2 \cdot 2,6^3}{12} = 0,3m^3 \tag{7.5}$$

For a example of a core of 30 meters, a E of 1100 kN/cm^2 and a $q_{horizontal}$ of 12 kN/m the deflection is calculated as follows:

$$\frac{1}{8} \cdot \frac{q_{hor} \cdot H_{wall}^4}{E * I_y} \tag{7.6}$$

Results in a deflection of 17,8 mm in the no cut-out panel and deflection of 184,1 mm when the two panels do not interact.

When openings are in place in the core CLT panels, the lintels need to be able to transfer the bending moment and the shear force. The moment and shear force in the lintels above the openings can be determined as follows [60]:

$$\Delta V_{Ed} = \frac{\Delta\sigma_{min} + \Delta\sigma_{max}}{2} \cdot (e_{max} - e_{min}) \cdot t_{wall} \tag{7.7}$$

$$\Delta M_{Ed} = \Delta V_{Ed} \cdot (0.5 \cdot L_{beam} + a_i) \tag{7.8}$$

With:

$\Delta\sigma_{min}$ is the minimum stress from the bending moment depending on the width of the opening.
$\Delta\sigma_{max}$ is the maximum stress from the bending moment depending on the width of the wall .
e_{min} is half of the width of the opening.
e_{max} is half of the width of the wall.
t_{wall} is the thickness of the wall
a_i is extra distance where the force applies, depending on the lintel length (L_{beam}) and height of the lintel (H_{beam})

The vertical stress for the two panels of 2,6 meter due to the cut-out can be compared by the moment of resistance.

$$W = \frac{1}{6} \cdot t_{wall} \cdot L_{wall}^2 \tag{7.9}$$

The moment of resistance for the panel without the cut-out is 3.83 times bigger.

$$7,2^2/(2 \cdot 2,6^2) = 3,83 \tag{7.10}$$

The lintels in the CLT do not have much capacity since it is the same material as the whole panel. No additional strength has been given to the lintels. For the model, no additional strength will be given to the lintels, only the CLT panels with a cut-out.

7.5. Stiffness

In comparison to a concrete core, the CLT elements needs to be tied together. Stiffness of the whole core-system gets lost in the connections see 6.2. For the most commonly used strength class (C24) for CLT the $E_{0,mean}$ is $11kN/mm^2$ parallel to the grain. For the highest graded strength class (D70) the $E_{0,mean}$ is 20 kN/mm^2. For the highest concrete strength class C50/60 the modulus of elasticity E_{cm} is 37 kN/mm. The crosswise layering of CLT gives that the $E_{0,mean}$ does not fully get used since the $E_{90,mean}$ is much lower.

7.6. Lateral deformability components

The per storey deformation has a couple of different components that are contributing, with a panel parallel to the lateral load (see 7.12). The global rotation is the rotation of the whole system. The global deformation of the global rotation is linear increasing. The global rotation could be decreased with better connections between the foundation and the core. Another deformability component is rocking in which the panels get slightly separated. An greater connection stiffness between the panels in the y direction could improve the amount of deformation due to rocking. The deformation caused by sliding can be enhanced through increased connection stiffness in the x-direction. Finally the in-plane wall deformation does also affect the global deflection. Parameters that influence this effect are the material, the dimensions of the panels and the modulus of elasticity. The sum of the four components is the total deflection due to a lateral load [59].

$$\delta_{i,tot} = \delta_{i,g} + \delta_{i,r} + \delta_{i,s} + \delta_{i,w} \tag{7.11}$$

With:

$\delta_{i,g}$ is the deflection due to the global deformation
$\delta_{i,r}$ is the deflection due to rocking
$\delta_{i,s}$ is the deflection due to sliding
$\delta_{i,w}$ is the deflection due to in-plane wall deformation

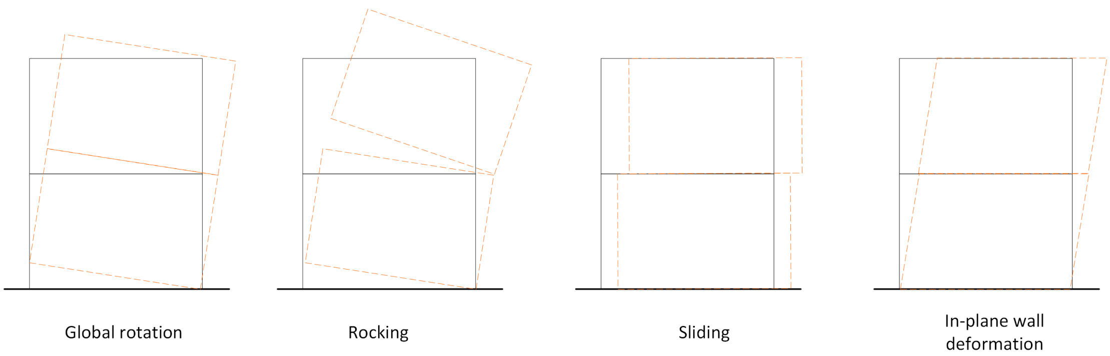

Figure 7.12: Lateral deformability components

7.7. Pre-stressed CLT core

To give more strength and stiffness to a timber core, studies have experimented with post tensioning CLT. Brown and al [8] experimented with a C-shaped CLT core where post tensioning was applied. The tensioning in combination with the screwed connections showed significant strength and stiffness while also maintaining ductility and drift capacity. In the thesis paper of Znabei [70], the post-tensioning reduces uplift and sliding. However, the estimation of long-term force loss could be challenging with the moisture content of the timber fluctuating during its lifetime.

7.8. Diaphragm action floors

For the core to be activated, the floors need to transfer the lateral wind load to the core (figure 7.13). In situ concrete floors are capable of transferring the lateral load through the floor. The forces transfer to the floor like a high beam. Even for hollow-core slabs, the load could transfer through the floor because the joints between the slabs can transfer shear force. For timber construction that relies on the use of a core for stability, the floor needs to be able to transfer the load. For the Urban woods the force is carried through the CLT panels, which creates a tension force at the façade. This tension force is taken by metal that is incorporated in the façade. In chapter 4, it was shown that the CLT could act as a semi-rigid diaphragm. Depending on the panel-to-panel connection and the stiffness of the CLT. Also the amount of panels is affecting the diaphragm action. With more connected CLT floors, the in-plane stiffness decreases. This will have impact on wider floor configurations. The flexibility of the CLT depends on the relative stiffness of the shear wall in the core and the CLT of the floor [3].

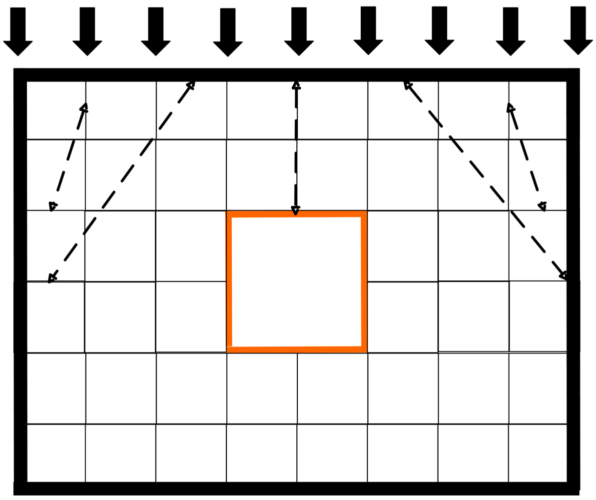

Figure 7.13: Distribution lateral force

7.9. Conclusion

In this chapter it becomes clear how the heigth of the building influences the stability. It examines stability systems in timber high-rise buildings, addressing challenges like shear, bending, and natural frequency. Timber's light weight and flexibility can cause serviceability issues, requiring innovative solutions like concrete cores and advanced bracing. Stiffness of the stability is critical, with timber needing more emphasis on the stability design due to its lower stiffness. Shear action in floors is crucial for distributing lateral forces to maintain stability. For this thesis, it is assumed that diaphragm action occurred.

8
Fire situation

This chapter will be answering how the timber will behaves in a fire situation and what for protective measures are in place. To get a better understanding of how a fire will affect the building. It is based on the NEN-EN 1995-1-2 and will be adapted into the FEM model.

8.1. Fire behaviour

Fire could occur because of many reasons which could be accidental or deliberate. Since timber is a combustible material, it imposes a significant risk for timber constructions. Numerous studies have been done one the behaviour of timber in a fire situation [50]. The intensity of a fire is a complex function consisting of several parameters like the chemical structure, technical properties of the timber, age of the timber constructions and the intensity of the external heat flow. To deal with this behaviour as a structural engineer the EC has provided guidelines to ensure that timber structures are designed with adequate fire resistance.

8.2. Fire protection

Before dimensioning of the cross sections, the fire resistance of a building needs to be determined, which depends on the consequence class. The resistance is measured in minutes the structure needs to survive before failing. The REI is a method to quantify three different fire resistant capacities. With the R of resistance of the load bearing elements, E of exposure and I of insolation. If the R value fails in the test than automaticly E and I fail. This thesis focuses on the structural capacity (R) of the construction. To protect a building against fire, the structural engineer has the following options:

- Over sizing of structural elements.
- Covering the timber with fire protected sheeting.
- Apply sprinklers to the building 5.3.
- Compartmentalization, to stop fire from spreading
- Combination of the above.

8.3. Calculations for the fire situation

8.3.1. Design value

The design values of the mechanical properties (strength and stiffness) in the fire situation should be calculated from the normal situation as follows [42].

$$X_{d,fi} = k_\theta \cdot k_{fi} \cdot X_k / \gamma_{M,fi} \tag{8.1}$$

With:

$X_{d,fi}$ is the design value for strength or stiffness for a fire temperature design.
k_θ is the temperature dependent reduction factor.
k_{fi} is the modification factor.

X_k is the characteristic value of a strength or stiffness according to normal temperature timber design.
$\gamma_{M,fi}$ is the partial factor for the relevant mechanical property for the fire situation.

8.3.2. Load case

The capacity of the structural elements will be tested in the accidental limit state (ALS). This is a reduced state that only applied for accidental circumstances. The accidental limit states are as follows:

$$1 \cdot (Deadload + Permanent - load) + 0.2 \cdot Wind - load_x + 0.3 \cdot Variable - load \tag{8.2}$$

$$1 \cdot (Deadload + Permanent - load) + 0.2 \cdot Wind - load_y + 0.3 \cdot Variable - load \tag{8.3}$$

$$1 \cdot (Deadload + Permanent - load) + 1 \cdot Variable - load \tag{8.4}$$

8.3.3. Charring

To protect the building against fire, the structural engineer can opt to oversize the structural elements. The fire-resistant behavior of thick timber elements is characterized by the effective charring depth, which corresponds to a specific charring rate:

$$d_{char} = \beta \cdot t \tag{8.5}$$

$$d_{ef} = d_{char,0} + k_0 d_0 \tag{8.6}$$

The charring rate β from CLT is not specifically given in the Euro code. Frangi et al [24], tested cross laminated panels in comparison to homogeneous timber panels and came to the conclusion that the adhesive that is being used has an effect on the behaviour of the panels in fire tests. Charred layers falling off leading to an increase in charring rate in comparison to the homogeneous panels. The charring rate is not however like that off thin panels, but more in the range of 0,9 mm/min. In the Eurocode the effective cross section for different CLT floor and wall layups are generalised after 30, 60 and 90 minutes. The glulam columns and bracings have a charring rate of 0,9. For the glulam columns and bracings, the charring will occur at a two dimensional space. The effective depth of the cross section is in the Eurocode prescribed with the following formula:

$$h_{ef} = h - k_{side} \cdot d_{ef} \tag{8.7}$$

With:

h is the depth of the initial cross section.
k_{side} is the number of respective opposite sides exposed to fire.

From the Eurocode, shear in the fire situation can be neglected if the shear in the normal situation is not governing.

8.3.4. Bracings

From the Eurocode 1995-1-2[42], the fire resistance of the bracing shall be verified where relevant. If the bracing fails, the stability shall be verified as for an unbraced member. The bracing shall not fail if the residual cross section is at least 60% of the required cross section at normal temperature design. The residual cross section will be calculated using equation 8.7. The mechanical strength and stiffness can be calculated as in equation 8.1, with k_θ = 1,0 and k_{fi} = 1,15. Since the bracing members are not protected the notional charring rates for glue laminated members where the bond line integrity is maintained should be calculated as in phase 1.

$$\beta_n = k_n \cdot \beta_0 \tag{8.8}$$

With:

k_n is the conversion factor (1,23 for rectangular structural timber members)

For glue-laminated timber elements where the bond line integrity of face bonds is not maintained, the charring will occur at different rates for the different directions of the element 8.1.

$$\beta_n = 1,3 \cdot k_n \cdot \beta_0 \qquad \text{Charring direction A} \tag{8.9}$$

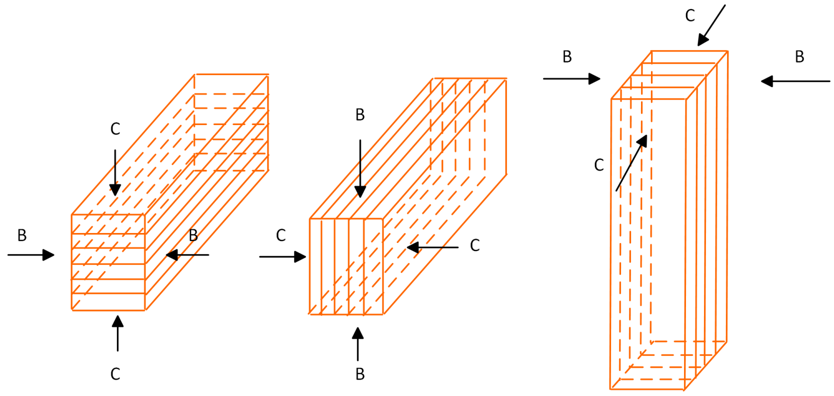

Figure 8.1: Charring rate directions, horizontal and vertical members

$$\beta_n = 1,1 \cdot k_n \cdot \beta_0 \qquad \text{Charring direction C} \tag{8.10}$$

$$\beta_n = k_n \cdot \beta_0 \qquad \text{Charring direction B and D} \tag{8.11}$$

For a timber glulam beam in tension, the strength over time is plotted in the graph 8.2.

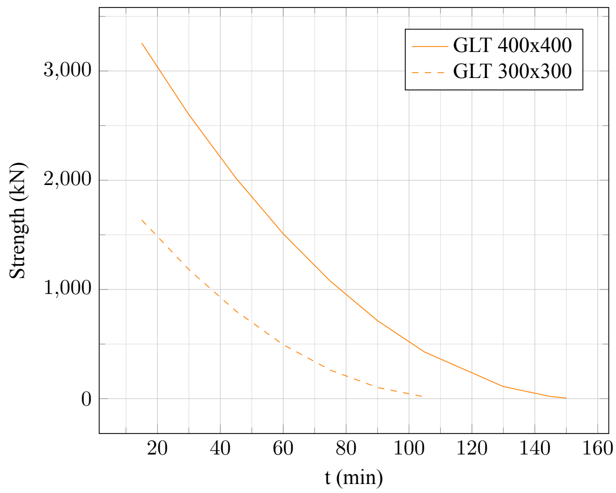

Figure 8.2: Strength over time (C direction)

8.3.5. CLT

For a non protected CLT member the charring rate should be calculated for phase 1 as follows.

$$\beta_n = k_g \cdot \beta_0 \tag{8.12}$$

With:

k_g is the conversion factor (1,0 for gaps $\leq$ 2 mm, 1,2 for gaps $\geq$ 2 mm and $\leq$ 5 mm)

8.3.6. Connection

For the timber-to-timber or timber-to-steel connection without protection, the following minimum bearing capacity for the fire situation needs to hold in the Eurocode 8.13.

$$\eta_{fi} = \frac{E_{d,fi}}{R_k} \leq 0.3 \tag{8.13}$$

With:

η_{fi} is the ratio between the design effect of actions for the fire situation and the characteristic load-bearing capacity.

$E_{d,fi}$ is the design effect of actions.

R_k is the characteristic load-bearing capacity at normal temperature.

In the draft version of Eurocode 1995-1-2 from 2023, the reduction method for the connections of slotted in steel plates has a exponential development.

$$t_{fi} = \alpha_1 \cdot t_{1,fi} - 1\frac{1}{\alpha_2} \cdot \ln(\eta_{fi} \cdot 100) + \alpha_3 \tag{8.14}$$

With:

t_{fi} is the fire resistance time (min)

α_i are coefficients dependent on the connection and the fastener.

$t_{1,fi}$ is the thickness of the timber from the outside to the steel plate.

From chapter 6, the end- and edge distances of the timber need to increase by a factor α_{fi}, if the fire resistance time is not met.

$$\alpha_{fi} = \beta_n \cdot k_{flux} \cdot (t_{req} - t_{d,fi}) \tag{6.16 revisited}$$

In the case of a protected connection, the protection elements should give the connection increased fire resistance. The fire protection system is graded based on the time it takes before charring behind the fire protection system starts and the time it takes before the fire protection system fails.

8.4. Fire scenario model

The fire scenario for the model is based on the Urban Woods project. In the Urban Woods, each apartment is a fire compartment, separated by fire-resistant boards (Promatect). In the fire scenario for the Urban Woods construction, it is assumed that the entire building has a reduced cross-section for conservatism and to limit the analysis to a single fire scenario. The same assumption is applied to the model in the removal scenarios for this thesis.

8.5. Conclusion

The timber will be affected by exposure to fire, so the elements need to be designed to ensure that the construction can hold the load in the accidental limit state. For the model, reduced cross sections will be applied to all elements, forming the basis for the removal scenarios.

9 Robustness

For building within consequence class 3, the structural engineer is required to conduct a robustness analysis. According to NEN-EN 1990, the construction must be designed to ensure that exceptional external forces do not cause a disproportionate collapse. Examples of such exceptional forces include explosions, vehicle impacts, and human errors. Also in consequence class 2, the structural engineer has to be aware of the potential risks. In the NEN-EN 1991-1-7, robustness strategies are described, but these strategies are based on constructions of steel and concrete, and not (yet) on timber. In the draft version of the NEN-EN 1995-1-1, the robustness strategies of a timber building are given [39].

9.1. Disproportionate collapse

A disproportionate collapse is a collapse that is disproportionate to the cause. The most famous example is the collapse of the Ronan Point tower in 1968. There is also an example of a timber structure that suddenly collapsed with fatal implications. The roof of the ice rink arena in Bad Reichenhall Germany collapsed after severe snowfall. The roof was a timber structure in which the box girders eventually failed. Multiple factors contributed to this failure. One significant issue was the use of glue not suitable for moist environments. Additionally, errors in the static calculations were not rechecked, further contributing to the failure. There are different measures to prevent a progressive collapse. These measures could be structural as well as non structural. Structural measures may include strengthening elements, enhancing ductility, and connecting building components. Non-structural measures include, for example, prohibiting certain types of traffic and implementing additional quality controls.

9.2. Robustness strategies

9.2.1. Fuse element

By use of a fuse element, the upper design value of the resistance needs to be lower than the design effect of the action that the fuse element will carry in case of a collapse.

$$R_{sup,d} \leq E_{fuse,d} \tag{9.1}$$

A example is a beam column connection that will fail and rotate in case of a column removal (see figure 9.1).

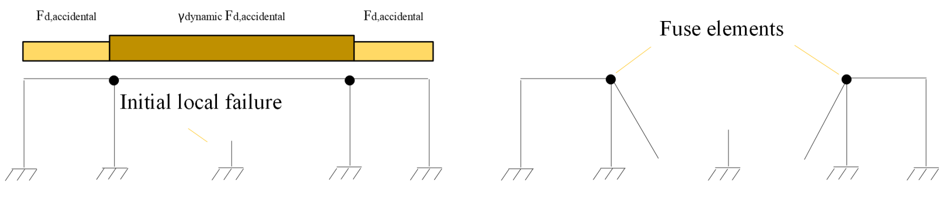

Figure 9.1: Example of a fuse element connection [39]

9.2.2. Ductility

Timber is a brittle material 4.2, which is not a desired property for a building. Ductility of the structure can be implemented in the connections. Ductile failure of the connection should occur prior to the brittle failure of the timber. For a connection with a slotted in steel plate, ductility can be achieved by yielding of the fasteners or the steel plate.

9.2.3. Alternative load path

Another option is to ensure a alternative load path. In case of a element failure, the force is then distributed to another part of the building, which is able to carry the extra load. A rim beam is a example of a alternative load path, which is a continuous beam which is located above internal or peripheral walls. The rim beam is supposed to bridge the gap after the removal of a load carrying wall [6].

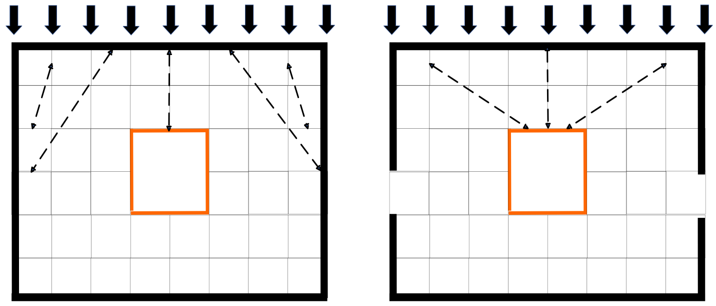

Figure 9.2: Secondary load path stability Urban Woods

For this thesis, the core will be tested to function as an alternative load path in the event of failure of one or more bracing elements during a fire (see Figure 9.2). Before the removal, the horizontal wind load transfers from the façade to the floor beams, where it is modeled as a member line load. The horizontal load is then transferred through the bracings and partially through the CLT core to the foundation. When one or more bracings are removed, a greater portion of the horizontal load must transfer through the CLT core, as the bracings are no longer present. For the alternative load path to function, the connections in the floors must be able to transfer the load, as well as the connections with the remaining bracing and the floor.

In this study the second load path is considered with the removal of the bracing in the façade. When a sudden removal of a element is present a Dynamic amplification factor (DAF) is applied [47]. This factor expresses the ratio between the peak dynamic response and the final response in equilibrium state 9.2.

$$\gamma = \frac{\Delta_p}{\Delta_{fin}} \tag{9.2}$$

There are two approaches to designing for the removal of structural elements: dynamic analysis and quasi-static analysis. In a dynamic analysis, the failure is instantaneous, leading to dynamic effects and the impact of falling debris. For this scenario, a dynamic amplification factor (k_{dyn}) is applied. In contrast, the quasi-static analysis assumes a short-term load duration, where a dynamic amplification factor (k_{dyn}) is not applicable. This method is used in scenarios where there is a gradual loss of an element, such as during a fire or due to excessive settlement of a foundation.

9.3. Building failure

Possible causes of building failures could be distinguished into different categories. Frühwald came up with 9 categories [19].

- Wood material performance
- Manufacturing errors in factory
- Poor manufacturing principles
- On-site alterations
- Poor principles during erection
- Poor design/lack of design with respect to mechanical loading
- Poor design/lack of design with respect to environmental actions

- Overload in relation to building regulations.
- Other/unknown reasons (e.g. lack of maintenance).

A significant portion of structural failures can be attributed to multiple categories. The majority of these failures are primarily due to human error, accounting for 50% to 80% of cases. Specifically, designers are often responsible for these errors, which frequently arise from inadequate strength design or challenges related to environmental actions. Additionally, a considerable number of failures (5% to 25%) are linked to personnel working on site, where poor practices during erection and on-site alterations contribute to the issues. Furthermore, 11% of the failures are attributed to substandard materials or production methods[19].

Part II

Model tests

10
Case Study

This chapter will provide a overview of the program of requirements. The design draws inspiration from the Urban Woods, but significant simplifications have been made to adapt it for parametric design.

10.1. Program of requirements

Since the building is based on a existing building. The program of requirements are based upon the Urban Woods. However, the building has been simplified to make it more practical for parametric design. So is the grid size fixed in all directions, and the core is simplified to a square which contain square holes which represent the openings in the core. The layout of the supporting structure has also been simplified (see figure 10.1).

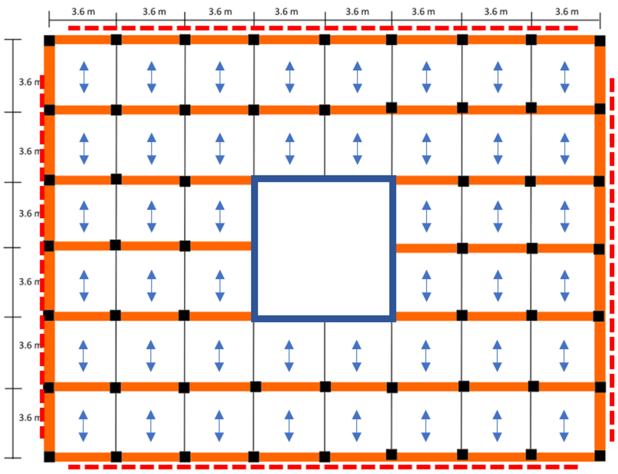

Symbol	Item	Dimensions	Material
	Columns	400x400	GL24
	Beams	280x320	GL24
	Core walls	200	C24
	Bracings	400x400	GL24
	Floor	200	C24

Figure 10.1: Floor plan, case study

10.2. Designing the core connections

The core is connected to the foundation with the use of hold downs. The amount of hold down dowels will depend on the moment capacity that the core will take. To model the stiffness of the connections, a line hinge will be applied. The coordinate system of the line hinge in R-FEM is displayed in figure 10.2.

The boundary conditions for the line hinge for the connection with the wall and the foundation is displayed in table 10.2. The stiffness of the spring in the u_x and u_y directions depends on the amount of dowels the connection needs, which depends on the governing failure mechanism. The stiffness will then be calculated as described in 6.3.1. Figure 10.3, gives an overview of the line connections of the core

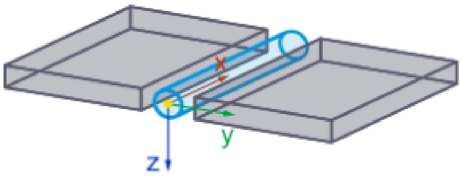

Figure 10.2: Coordinate system line hinge R-FEM

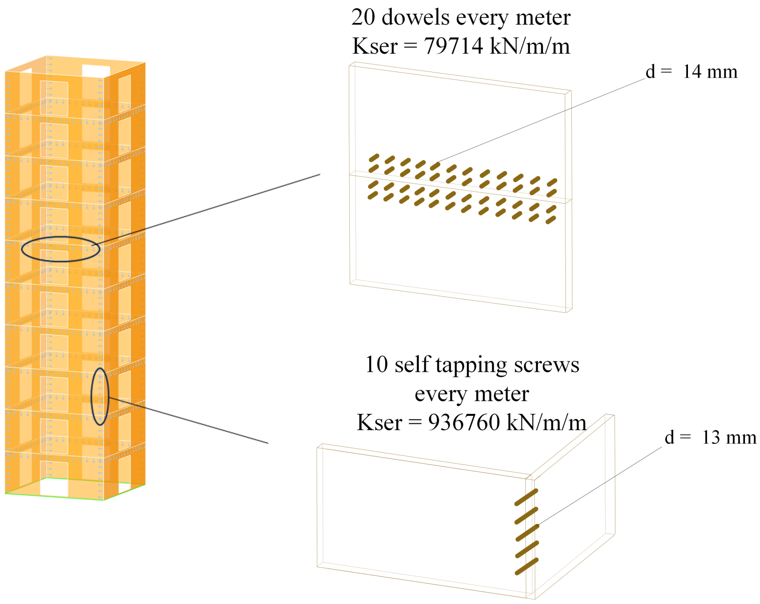

Figure 10.3: Horizontal and vertical line hinge in core

The horizontal wall-to-wall connection has like the wall-to-foundation connection the same boundary conditions. With u_x and u_y a having spring stiffness and u_z and ϕ_x being rigid.

u_x	u_y	u_z	ϕ_x
spring	spring	free	free

Table 10.1: Boundary conditions horizontal joint

In the corners of the core the connections are being realised by self-tapping screws. The hinge connection of the corner is ridgid in the u_y and the u_z directions of the coordinate system 10.2. The u_z, because the in plane shear walls have a much higher stiffness than the out of plane shear walls. And the u_y because it is expected that the walls remain in contact with each other. In the u_x direction, the spring stiffness of a self taping screw connection can be calculated using the load slip modulus and the axial slip modulus combined.

u_x	u_y	u_z	ϕ_x
spring	rigid	rigid	free

Table 10.2: Boundary conditions vertical corner joint

Between the panels in the core, line hinges are introduced. Like discussed in chapter 10.3 the horizontal line hinge will have a stiffness in the u_x and the u_y, and the vertical connection only in the u_x.

10.2.1. Calculation stiffness

The stiffness in the horizontal line hinge depends on the amount of dowels per meter. For the calculation for the line hinges is like the calculation of the lateral stiffness of a slotted in steel plates with only one shear plane.

$$K_{ser}, K_{lat} = \frac{d \cdot \rho_m^{1.5}}{23 \cdot a} \cdot 2 \quad \text{(6.7 revisited)}$$

With:

a is the distance between the fasteners in a row.

Opting for a slotted-in steel plate rather than a steel plate on the side of the CLT, gives 2 shear planes on which the dowel can interact and thus 2 times more stiffness. In table 10.3, the relation between the parameters and the stiffness is given.

δ parameter	δ Stiffness
δ diameter dowel (mm)	$\frac{\delta d}{d} \cdot K$
δ column dowels per m (pcs)	$\frac{\delta nc}{nc} \cdot K$
δ rows dowels per m (pcs)	$\frac{\delta nr}{nr} \cdot K$
δ timber density (kg/m^3)	$\frac{(\delta\rho+\rho)^{1.5} \cdot K}{\rho^{1.5}} - K$
δ shear planes	$\frac{\delta_{nsp}}{nsp} \cdot K$

Table 10.3: Relation between parameter and stiffness

For the stiffness of the vertical line hinges with self taping screws, the axial stiffness is used. This because the lateral force is expressed on the corners of the core, resulting that the fasteners in the corner get pulled out of the connection. The axial stiffness is much lower than the stiffness of the slotted in steel plates used for the horizontal connection. The calculation of the axial stiffness of one component will be as follows:

$$K_{ax} = 25 \cdot d \cdot l_{ef} \quad \text{(6.10 revisited)}$$

With:

l_{ef} is the length of the tread minus the length of zero embedment and withdrawal capacity of the CLT x_1 [33].

$$x_1 = \frac{f_{h,\phi} \cdot d_{ef} \cdot \tan\phi \cdot f_{rs}}{2} \quad (10.1)$$

To combine the two timber components for the axial stiffness, the equation is as follows:

$$K_m = \frac{1}{\frac{1}{K_{ax,1}} + \frac{1}{K_{ax,2}}} \quad \text{(6.11 revisited)}$$

If self taping screws are under a angle θ, the lateral stiffness of the screw are also taken into account 6.7 revisited.

$$K_A = k_{lat} \cdot sin^2(\phi) + k_m \cdot cos^2(\phi) \quad \text{(6.12 revisited)}$$

10.2.2. Strength CLT connection

For the accidental limit state the strength of the connection needs to be examined. From chapter 6 the moment capacity was calculated as follows:

$$M_{y,k} = 0.3 \cdot f_{u,k} \cdot d^{2.6} \quad \text{(6.4 revisited)}$$

The axial strength of a self taping screw in the vertical connection can be calculated as follows [41]:

$$F_{ax,k,Rk} = \frac{n_{eff} \cdot fax,k \cdot l_{ef} \cdot k_d}{1.2 \cos^2\alpha \cdot \sin^2\alpha} \quad (10.2)$$

$$f_{ax,k} = 0.52 \cdot d^{-0.5} \cdot l_{ef}^{-0.1} \cdot \rho_k^{0.8} \quad (10.3)$$

With:

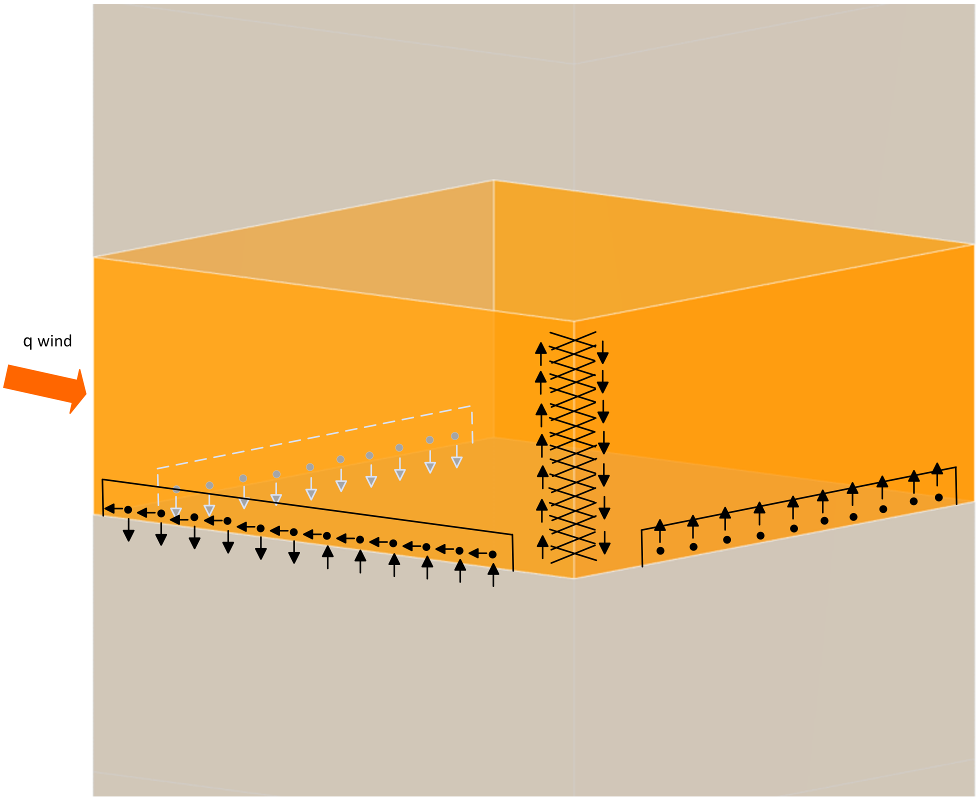

Figure 10.4: Overview line hinges CLT core

n_{eff} is the effective number of screws ($n^{0.9}$).
k_d is min(d/8;1)
α is the angle between the grain direction and the screw.
ρ_k is the density of the timber.
l_{ef} is the penetration depth of the screw thread.
d is the diameter of the screw thread.

The tensional strength in the screws should also be checked with the following equation.

$$F_{t,Rk} = n_{eff} \cdot f_{tens,k} \tag{10.4}$$

With:

$f_{tens,k}$ is the characteristic tension force of the screw.
n_{eff} is the effective number of screws ($n^{0.9}$).

The shear strength of the self taping screws depends on the failure mechanisms. The angle of the screw has effect on the embedment strength 6.2 and 6.3. The placement of the screws are 20 times the diameter of the screw.

$$fh, \alpha, k = \frac{0.082(1 - 0.01d)\rho_k}{k_{90} sin^2\alpha + cos^2\alpha} \tag{10.5}$$

10.3. Designing the brace connections

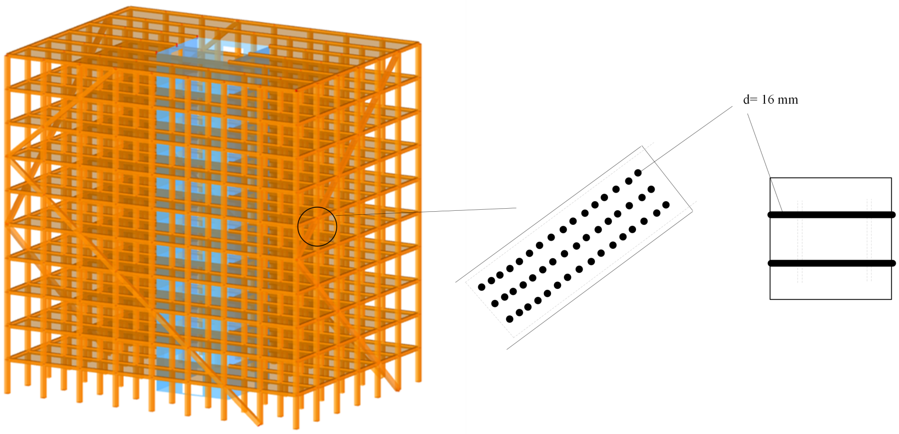

Figure 10.5: Bracing member hinge

The connections in the braced system will be modeled by a member hinge. The connection of the bracing with the column in the Urban Woods is a steel-in-plate connection. The rod is connected with 48 bolts with a diameter of 16 mm in 3 rows 10.5. The strength of the connection can be calculated using the formulas corresponding to the different failure mechanisms of a bolted connection (B.4). For the normative failure mode 7, the load capacity per bolt is:

$$(-\frac{1}{2}t_1 + \frac{1}{2}\sqrt{t_1^2 + \frac{2M_y}{d \cdot f_{h,0}}} + \sqrt{\frac{M_y}{d \cdot f_{h,0}}}) \cdot d \cdot f_{h,0} = 12.19kN \tag{10.6}$$

The effective number of bolts in a row is:

$$n_{eff} = n^{0.9} \cdot \sqrt[4]{\frac{a_1}{13d}} = 8.88 \tag{10.7}$$

The block shear failure will be:

$$F_{bs,Rk} = max \begin{cases} 1,5A_{net,t}f_{t,0,k} \\ 0,7A_{net,v}f_{v,k} \end{cases} = 2352000kN \tag{10.8}$$

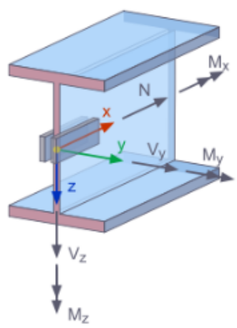

Figure 10.6: Coordinate system member hinge R-FEM

The connection stiffness of the bracing is a significant parameter concerning the overall stability of the structure. The stiffness is being obtained with:

$$K_{ser} = \frac{d \cdot \rho_m^{1.5}}{23} \cdot (2)^* \tag{6.7 revisited}$$

The equation is times 2 because the connection is steel to timber. With two slotted in steel plates, four shear planes are present. For the connection with the dowel arrangement of 3x16 as seen in figure 10.5, the stiffness in direction u_x is 2299308,83 N/mm. Due to the increasing number of dowels in the connection, the connection strength increases and the stiffness of the building increases.The increasing stiffness leads to a reduced deflection.

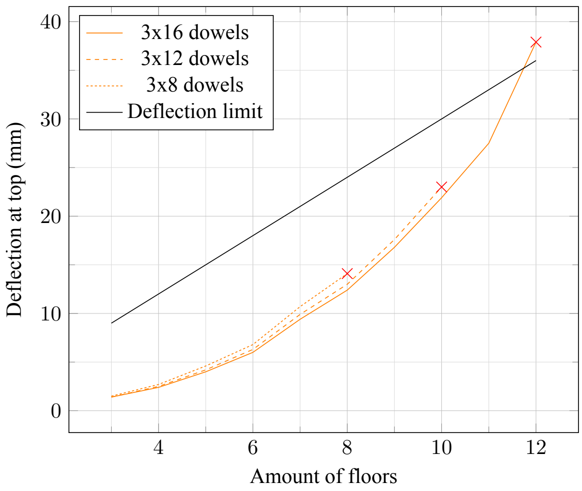

Figure 10.7: Lateral deflection bracing until failure connection.

10.4. Loads

For the loads that are applicable for the case study, the main calculation of the Urban Woods is consulted. The loads used in the model are permanent load, variable load and wind load.

10.4.1. Permanent load

The permanent load that is applied on the building is given in table 10.4.

	Load	
CLT floor	3,65	kN/m^2
CLT roof	3,40	kN/m^2

Table 10.4: Permanent load [28]

10.4.2. Variable load

The variable loads that are applied on the model are given in table 10.5.

	Load	
Floor load	2,55	kN/m^2
Roof load	1	kN/m^2

Table 10.5: Variable load [28]

10.4.3. Wind-Loads

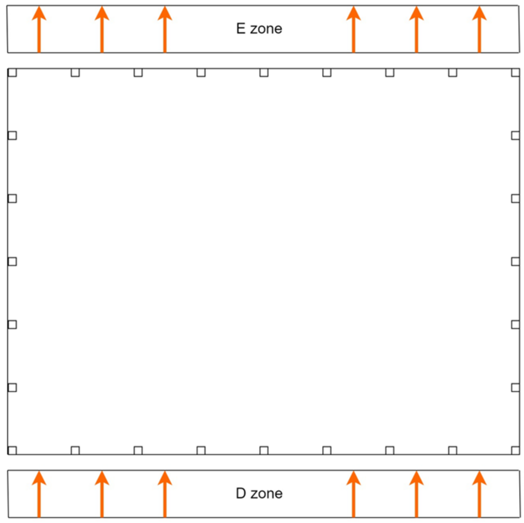

Figure 10.8: Wind loads on the building

As the height of the building increases, the impact of the wind load steadily increases, see 7.1. The wind loads that should be applied on the model is carefully described in the Eurocode. Different zones are prescribed for different wind loads 10.8.

The case study on which the model is based has the following parameters: Wind area 2 and a building height of 30 meter. At this height the wind pressure is: 1.03 kN/m^2 and the height of the floors is 3 meter which makes the line load on the beams:

$$Zone_D = 0.8 \cdot 1.03 \cdot 3 = 2.472 kN/m \tag{10.9}$$

$$Zone_E = 0.5 \cdot 1.03 \cdot 3 = 1.545 kN/m \tag{10.10}$$

10.5. Load combinations

From the Eurocode 1990 the following load combinations are extruded[38].

$$1,35 \cdot G_{k,j,sup}/0,9 \cdot G_{k,j,inf} + \sum 1,5 \cdot \psi_{0,1} Q_{k,i} \tag{10.11}$$

$$1,2 \cdot G_{k,j,sup}/0,9 \cdot G_{k,j,inf} + 1,5 \cdot Q_{k,1} \sum 1,5 \cdot \psi_{0,1} Q_{k,i} \tag{10.12}$$

For the accidental limit state the Eurocode prescribes.

$$G_{k,j,sup}/G_{k,j,inf} + \psi_{1,1} Q_{k,1} \sum \psi_{2,i} Q_{k,i} \tag{10.13}$$

Appendix B.11 gives a overview of the load combinations that are applicable for the case study.

10.6. Serviceability criteria

The serviceability criteria in timber high-rise buildings, as discussed in Chapters 5 and 7.1, remain an important problem. The maximum lateral deflection and the wind-induced vibration are probably the main failure mechanisms in SLS. In the model the acceleration curve of the NEN will be used.

10.7. Design assumptions

For the FEM model, some assumptions are made to make the results more clear.

10.7.1. Foundation

In the design of the Urban Woods, the basement is made out of concrete like the foundation. The basement has his own stiffness and is also contributing to the global deflection. From chapter 7.12, the global rotation is affected by the connection of the building with the foundation. In the model contrary to reality, the foundation is assumed to be stiff. For this assumption the global drift maximum needs to be altered.

$$\delta_{\text{global drift}} = \frac{h_{\text{total height}}}{500} \tag{10.14}$$

To be on the safe side it is assumed that the foundation takes up to 50 percent of the global deflection. The new maximum lateral global deflection of the building then becomes twice as big.

$$\delta_{\text{global drift}} = \frac{h_{\text{total height}}}{1000} \tag{10.15}$$

This assumption is also applied in the design of Urban Woods. Eventually, the deformation due to building deflection and the deformation caused by foundation stiffness are combined 10.9.

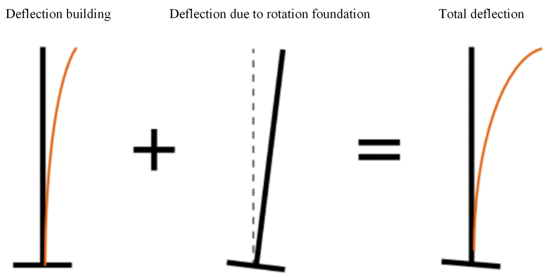

Figure 10.9: Build-up delfection

10.7.2. Material

For the design of the building, orthographic behavior of the material is expected. For glulam all the panels are in the same direction, which gives the beam strength along the grain but is weak in the perpendicular direction. For CLT, the panel is slightly stronger in one direction because of the odd amount of panels. The CLT used in the urban woods for the core is: CLT 200 with 5 layers. The layers are 40 mm thick each. The columns and bracings are equipped with a GL24h with a dimension of 400 by 400 mm. And the floors are spurce CLT of 180 mm ($5 \cdot 36$ mm).

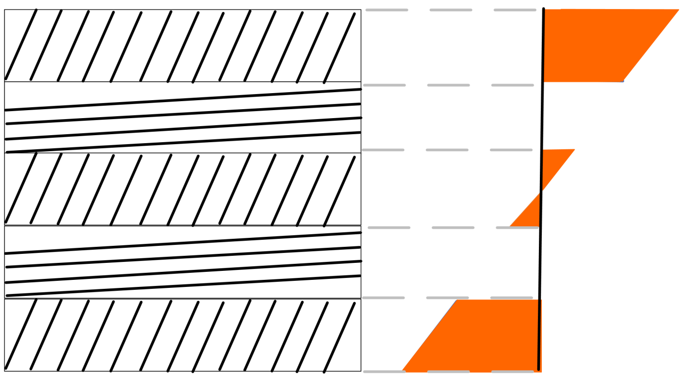

Figure 10.10: Moment capacity 5 layers CLT panel source: Ivo

The bending stiffness of the plane with different-oriented layers will have two directions of elasticity modulus.

$$E_x = \frac{\sum_{i=1,3..}^{n} E_0 A_i + \sum_{i=2,4..}^{n} E_{90} A_j}{A_{tot}} \tag{10.16}$$

$$E_y = \frac{\sum_{i=1,3..}^{n} E_{90} A_i + \sum_{i=2,4..}^{n} E_0 A_j}{A_{tot}} \tag{10.17}$$

Also two different shear modulus:

$$G_{yz} = k_y \frac{\sum_{i=1,3..}^{n} G_0 t_i + \sum_{i=2,4..}^{n} G_{90} t_j}{t_{tot}} \tag{10.18}$$

$$G_{xz} = k_x \frac{\sum_{i=1,3..}^{n} G_{90} t_i + \sum_{i=2,4..}^{n} G_0 t_j}{t_{tot}} \tag{10.19}$$

For CLT the stiffness matrix stated by Mindlin-Reissner is as follows[27]:

$$\begin{Bmatrix} m_x \\ m_y \\ m_{xy} \\ v_{x,z} \\ v_{y,z} \\ n_x \\ n_y \\ n_{xy} \end{Bmatrix} = \begin{bmatrix} K_x & 0 & 0 & 0 & 0 & 0 & 0 & 0 \\ 0 & K_y & 0 & 0 & 0 & 0 & 0 & 0 \\ 0 & 0 & K_{xy} & 0 & 0 & 0 & 0 & 0 \\ 0 & 0 & 0 & S_x & 0 & 0 & 0 & 0 \\ 0 & 0 & 0 & 0 & S_y & 0 & 0 & 0 \\ 0 & 0 & 0 & 0 & 0 & D_x & 0 & 0 \\ 0 & 0 & 0 & 0 & 0 & 0 & D_y & 0 \\ 0 & 0 & 0 & 0 & 0 & 0 & 0 & D_{xy} \end{bmatrix} \cdot \begin{Bmatrix} \kappa_y \\ \kappa_x \\ \kappa_{xy} \\ \gamma_{xz} \\ \gamma_{yz} \\ \varepsilon_x \\ \varepsilon_y \\ \gamma_{xy} \end{Bmatrix} \tag{10.20}$$

The full determination by Mindlin-Reissner is layed out in the Appendix B.8.

The FEM program includes a laminate add-on module, which can calculate the stiffness parameters of the CLT and the glulam. The results from the program will be checked with the stiffness matrix calculation.

10.8. Design strategy

In Figure 10.11, an overview of the workflow is presented. The green tiles indicate steps carried out using Rhino/Grasshopper, while the yellow tiles represent steps executed in RFEM. The workflow is divided into three stages:

- **Normal Stage (ULS and SLS)**: In the first stage, the added value of the timber core to a braced system is assessed using parameters as described.
- **Sensitivity Analysis (ULS and SLS)**: In the second stage, a sensitivity analysis is conducted by altering the core design parameters to evaluate how these changes affect the added value of a timber core in a building stabilized with bracings.
- **Fire Scenario (ALS)**: In the third stage, the cross-sections are reduced to simulate a fire scenario. Elements are removed, and the structure is re-analyzed under these conditions.

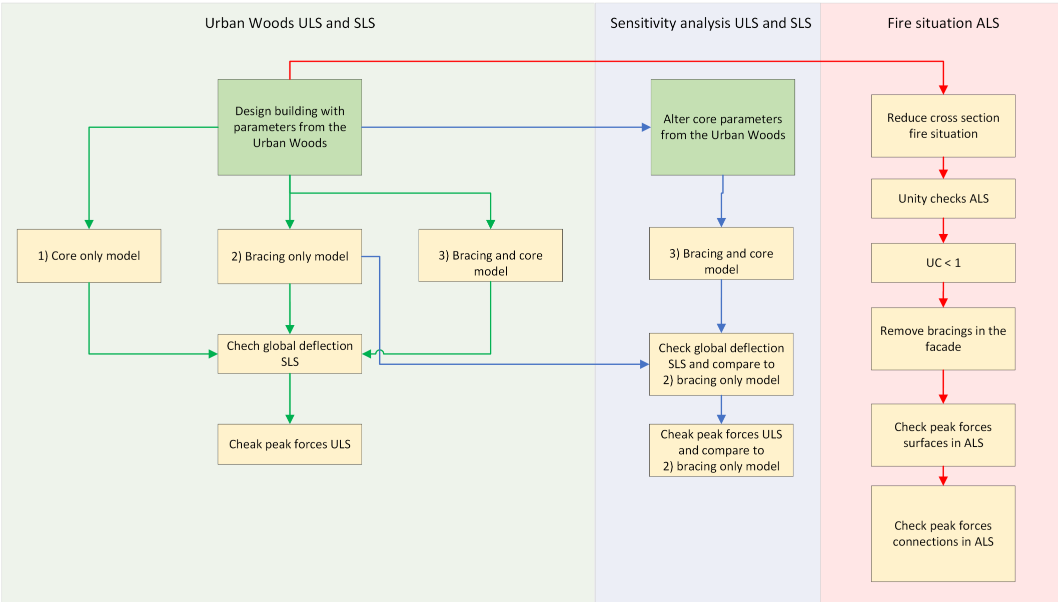

Figure 10.11: Workflow design strategy

Model parameters

With the model in Grasshopper changes in the design are easily implemented. The following parameters are adjustable.

- Grid size
- Amount of columns in the x and y direction
- Height storey
- Amount of storeys
- Size core
- cut-out in core
- Bracing on or off
- Material properties
- Stiffness core, bracing and column connections

Measuring stability

Measuring the added value can be achieved by comparing the deflection (SLS) of the building with and without a timber core, while keeping all other parameters constant 10.12. In the scenario without a timber core, continuous columns, beams, and floors will replace the core at its original location.

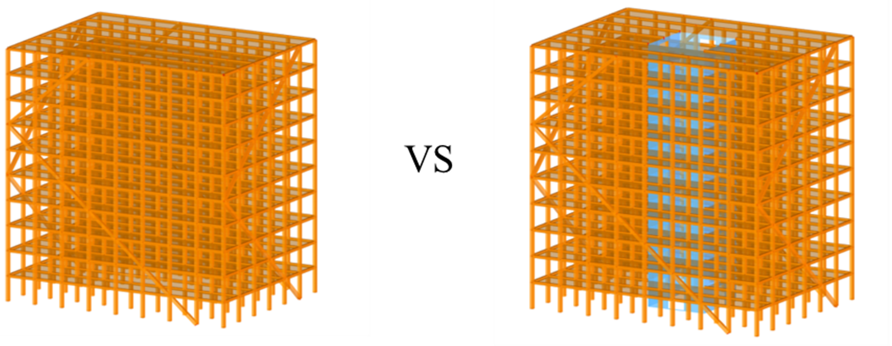

Figure 10.12: Building without a core (left) and building with a core (right)

Another approach is by comparing the two different axial stresses in the bracings (ULS). The core would take up some horizontal force so that the bracing stresses get reduced.

For the sensitivity analysis, deflection (SLS) will be used to evaluate different parameters, as this thesis primarily focuses on stability, and deflection is a critical failure mechanism in timber buildings.

The sensitivity analysis will focus on the core parameters and building parameters:

- Core hinges
- Core cut-outs
- Plot size of the building
- Amount of floors

In the fire scenario (ALS), a bracing element will be removed to determine if the building is robust enough to handle the additional load. The location of the removed element will be chosen based on which element is the most critical. After analyzing the forces in the building, another element on the opposite side will be removed. These scenarios will be compared to a scenario without a timber core to assess whether the core adds value in terms of robustness. An overview can be seen in figure 13.1.

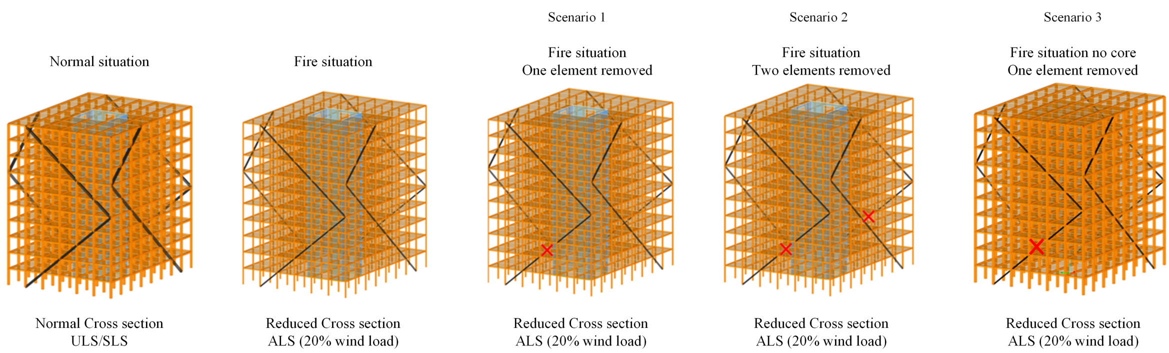

Figure 10.13: Removal scenarios with their cross section and limit state

The two removal scenarios will be taken to the extreme by also analysing a whole bracing façade removal.

10.9. Conclusion

In this chapter it becomes clear how the case study is going to be realised. The connection strength and stiffness are based upon calculations from the Eurocode. For the core dimensions the layout has been simplified. The workflow is divided into three components, the analysis of the timber core in the main structure, a sensitivity analysis on a timber core and the removal scenarios in the fire situation.

11
Results

In this chapter, the results of the different stability system will first be analysed followed by the removal scenario's for the secondary load path study.

11.1. Results stability systems

For a 10 floors high building like the urban woods the deflection will be analysed for 3 different stability scenario's (see figure 11.1).

(1) Stability by timber core
(2) Stability by timber bracing
(3) Stability by timber bracing and core

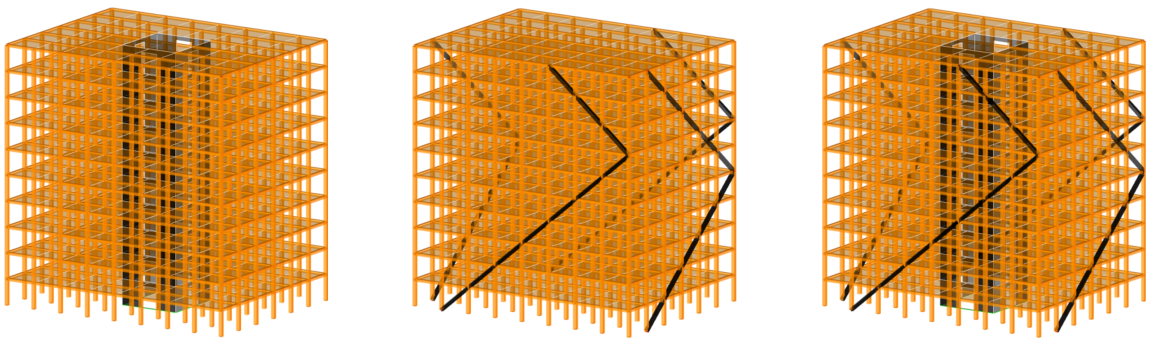

Figure 11.1: 3 different stability systems, stability by core, stability by timber bracing and stability by timber bracing and core

The core-only model and the bracing-only model illustrate the differences in stability systems. The added value of a timber core can be determined by comparing the bracing-only model with the combined stability system model.

For the stability by bracing, the core will be removed and replaced by regular columns, beams and floors. For the other cases the stiffness of the cores are calculated as in chapter 10.

FEM model	Horizontal line hinges kN/m/m	Vertical line hinges kN/m/m
Core only/Core and bracing	u_x/u_y = 79713.57	u_x = 936760.29

Table 11.1: Stiffness core

The cases which include the bracings (2 and 3), will have the following stiffness in the bracing members:

FEM model	Member hinges kN/m
Bracing only/Core and bracing	u_x = 2299308.83

Table 11.2: Stiffness bracing

A complete overview of all the parameters used, are in table 11.3.

Parameters	Value	Unit
Grid size	3.6	m
Grid x direction	8	grids
Grid y direction	6	grids
Height storey	3	m
Amount of storeys	10	storeys
Core x and y direction	2	grids
Core cut horizontal	2	m
Core cut vertical	2,5	m

Table 11.3: Parameters used, 10 storeys high.

For the full calculation of the stiffnesses in the hinges see Appendix D.4 and D.4.2. The internal forces in the floor panels are present in the normal situation (ULS). In figure 11.2, the internal forces in the x and y direction are displayed. In the y direction, the lateral forces can be seen going to the corners of the core and to the connection with the bracing. The connection with the bracing must therefore be designed to withstand these loads. This is also necessary for the removal scenarios (ALS), as the floor needs to transfer the horizontal load to the core.

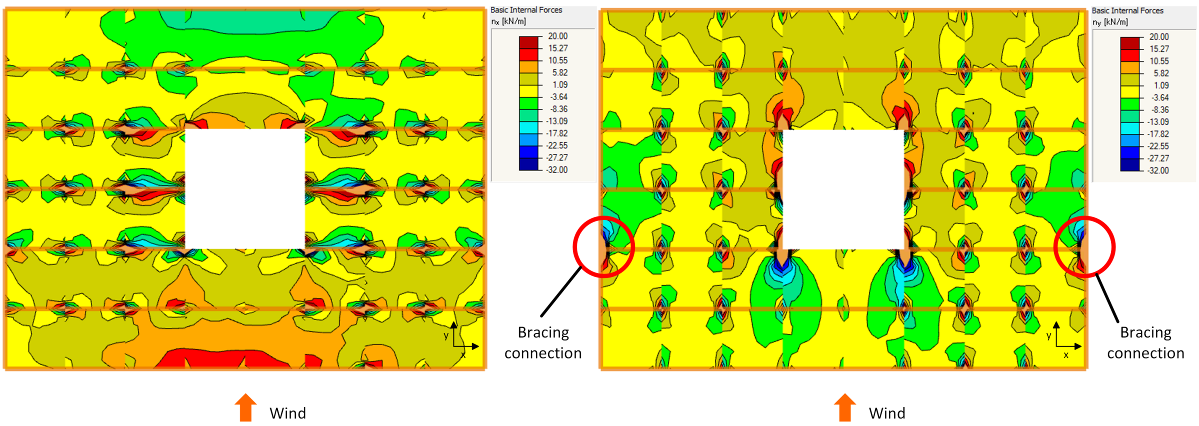

Figure 11.2: Internal forces n_x and n_y (ULS)

For the three different stability options the following maximum deflection are calculated in RFEM (table 11.4). The normative wind direction is in the y direction. In appendix D.1, the other wind directions with their respective deflections are given.

Load case	Timber core stability (1)	Bracing stability (2)	Timber core and Bracing stability (3)	Necessary*
SLS	168.4 mm	26.6 mm	21.9 mm	30 mm

Table 11.4: Deflection from wind load case. *based on H/1000

In SLS the timber core adds a 18% decrease in lateral deflection when comparing a bracing stability system (2) with a timber core and bracing stability system (3) . The amount deflection necessary is based on the design assumption of H/1000 from chapter 10.7. In the model it can be seen that the core does give extra stability in the SLS. Including a timber core in the stability design can thus decrease the amount of material needed in the façade of the building to increase the stiffness.

The change in the maximal axial forces in the bracing is given in table 11.5. The difference a timber core gives to the axial stresses is 33%.

Load case	Bracing only	Timber core and Bracing	Necessary
ULS	1124 kN	748 kN	916 kN

Table 11.5: Axial forces in the bracing

In the case of no timber core (2), the bracings will have to compensate for lateral stability. As can be seen in the ULS Unity checks, the bracing connection is not sufficient in this case (see 11.6. To get a connection that will be sufficient more dowels need to be added to the connection. The new arrangement will be 3 x 23 dowels instead of 3 x 16 dowels. For the cross section, the bracing is still capable to take up the tension.

Failure mechanism	Element	Loads	UC
Slotted in steel connection	bracing	1123.75 kN	1.38
Tension	bracing	1133.83 kN	0.67

Table 11.6: No core failure mechanism

ULS

In the ultimate limit state, the unity checks are all sufficient for the normal situation with 10 floors and a timber core.

Failure mechanism	Element	Location	Loads	UC
Compression strength	Column	1st floor, middle column	1063,45 kN	0,43
Elastic buckling load	Column	1st floor, middle column	1063,45 kN	0,44
Bending moment	Beam	1st floor, middle beam	44,73 kNm	0,61
Shear	Beam	1st floor, middle beam	50,84 kN	0,79
Moment 0	CLT	1st panel, parallel to the load	1,18 N/mm^2	0,05
Moment 90	CLT	1st panel, parallel to the load	0,04 N/mm^2	0,00
Tension/Compression 0	CLT	1st panel, parallel to the load	9,81 N/mm^2	0,47
Tension/Compression 90	CLT	1st panel, parallel to the load	0,17 N/mm^2	0,43
σb + Tension/Compression 0	CLT	1st panel, parallel to the load	-7,74 N/mm^2	0,47
σb + Tension/Compression 90	CLT	1st panel, parallel to the load	0,17 N/mm^2	0,44
Shear in plane vertical	CLT	1st panel, parallel to the load	1,28 N/mm^2	0,64
Shear in plane horizontal	CLT	1st panel, parallel to the load	0,25 N/mm^2	0,13
Slotted in steel connection	Bracing	4th floor, parallel to the load	-766 kN	0,94
Horizontal line hing y direction	CLT	1st panel, perpendicular to the load	0 N/mm^2	0,00
Horizontal line hinge x direction	CLT	1st panel, parallel to the load	54 N/mm^2	0,09
Vertical line hinge x direction	CLT	1st panel, corner.	49,2 N/mm^2	0,31

Table 11.7: Loads and unity check ULS

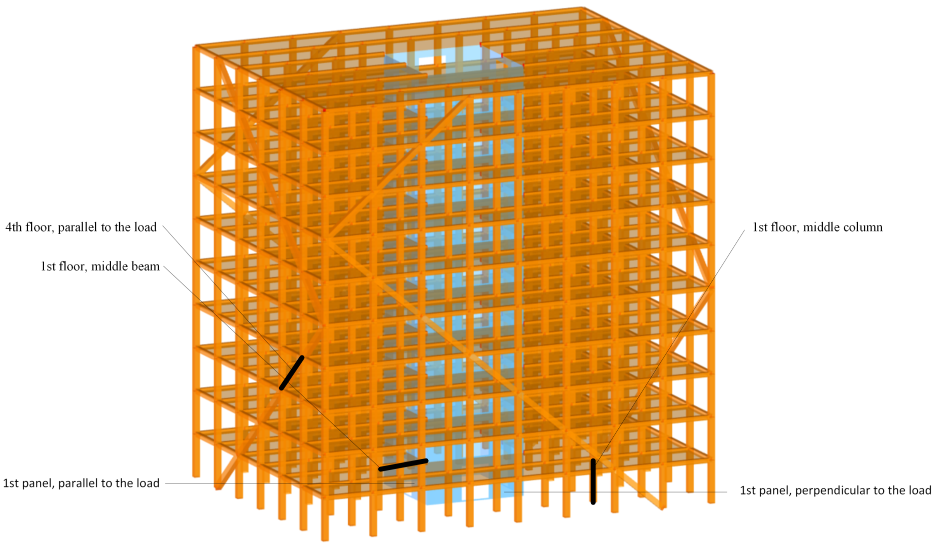

Figure 11.3: Overview unity checks

SLS

Like the ULS, in the SLS the unity checks are sufficient in case of a core and bracing system.

Failure mechanism	Element	Loads	UC
Top lateral deflection	building	22.9 mm	0.76
Top lateral acceleration	building	0.08 m/s^2	0.66

Table 11.8: SLS checks, bracing and timber core

To reach the limit of the unity check the bracing could be adapted by decreasing the cross section, or to decrease the amount of dowels in the connection that give stiffness to the bracing. For the decrease in material, there can be opt for a 210x400 timber cross section for the bracing, instead of a 400x400. The amount of dowels that can be decreased is limited by the strength of the connection in the ULS. The arrangement of dowels that is still capable of maintaining its strength is 3X13 dowels instead of 3x16.

Even if no core was added to the building the lateral stability will suffice in the SLS. With the connection that was proposed for the ULS, the cross section of the bracing can be decrease from 400x400 to 300x400 mm.

Failure mechanism	Element	Loads	UC
Top lateral deflection	building	27.8 mm	0.93
Top lateral acceleration	building	0.08 m/s^2	0.68

Table 11.9: SLS checks, bracing, no timber core

11.1.1. Support loads

If the core is contributing to the lateral stability, the foundation can expect a increase in load for which it needs to be designed. In the load case that includes the wind load, the line support is 210 kN/m higher than the one without the wind load.

Load case	maximum line support kN/m
$1.2 \cdot permanent + 1.5 \cdot wind + 0.6 \cdot variable$	510.18
$1.2 \cdot permanent + 1.5 \cdot variable$	300.76

12

Sensitivity analysis

12.1. Line hinge stiffness

The relation between the core horizontal line hinge stiffness and the decrease in lateral deflection by using a timber core is given in graph 12.1. The vertical axis shows how much the core contributes to the reduction of the global deflection. Each scenario with a specific stiffness in the core's connection is compared to the scenario without a core.

In the graph the stiffness of the vertical line hinge and the stiffness of the bracing are fixed as in table 11.2 and 11.2.

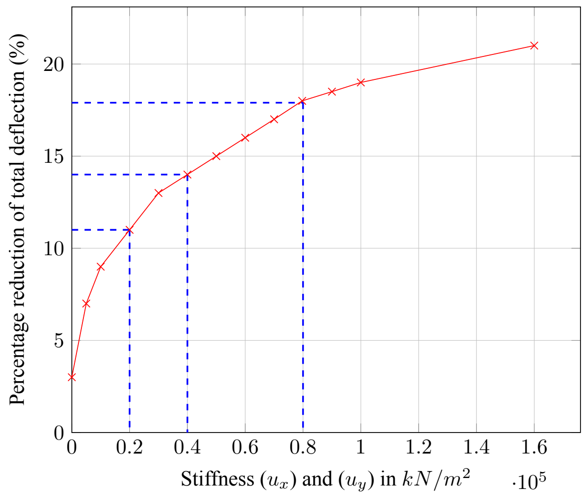

Figure 12.1: Relationship between stiffness horizontal line hinge core (u_x and u_y) and reduction in deflection

As can been seen, the graph has a stagnating course as the stiffness increases the persentage reduction increases less. This indicates that while the stiffness of the connections is an important factor initially, over time, other variables (such as the material) start to become the limiting factors for the deflection. The stiffness are based on the amount of dowels per meter. For the three stiffness given in blue the connections have the following dowel set up:

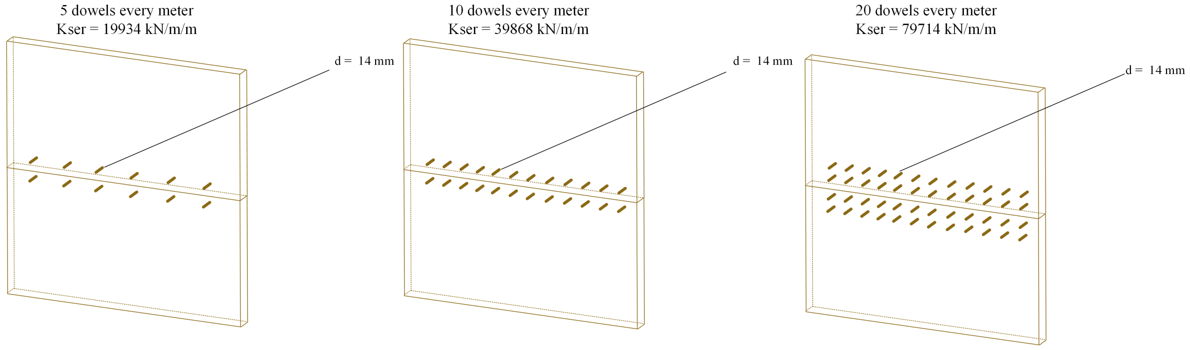

Figure 12.2: Different horizontal line connections core

The relation between the total deflection and the stiffness of the vertical line hinge in the core is given in graph 12.3 Here the stiffness of the horizontal line hinge in the core and the stiffness of the bracing are fixed as in table 11.2 and 11.2.

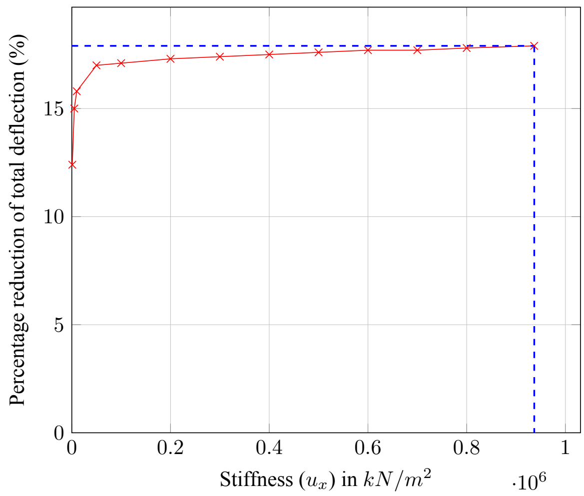

Figure 12.3: Relationship between stiffness vertical line hinge core (u_x) and reduction in deflection

The stiffness can be significant reduced from the original determined stiffness 11.2, before the percentage reduction of the deflection will be affected.

12.1.1. Longer CLT elements

With the introduction of longer CLT elements that span over more than two stories, less connections are needed which make the core stiffer. In graph 13.29, the relationship between the stiffness of the line hinges and the deflection is given for the 3 meter high panels and the 6 high panels. The longer panels give a 7 % reduction in deflection for the given stiffness. This makes that the contribution of the core to the total stability also increases with 6 % to 7%. The 6 m panels show the same stagnating behaviour as the 3 m panels which is described in last section.

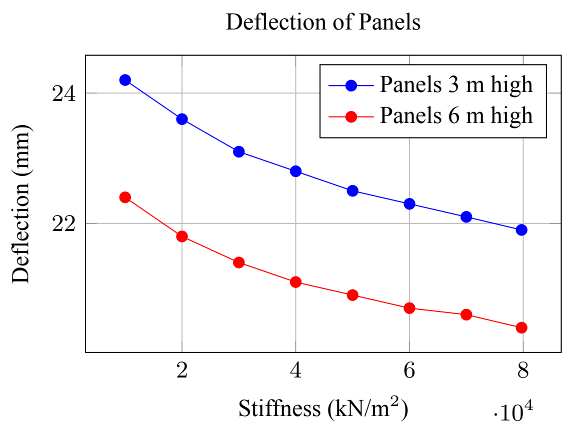

(a) Deflection vs. Stiffness core panel connection

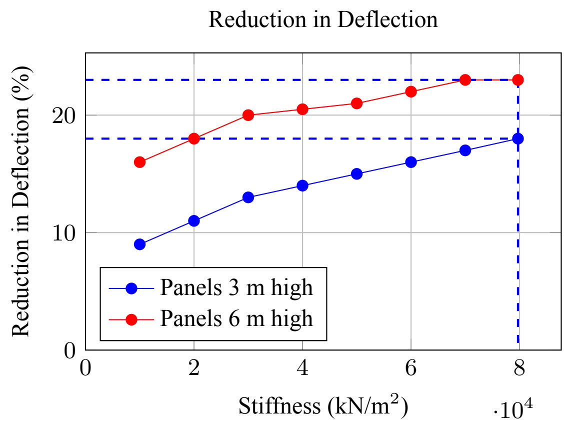

(b) Reduction in Deflection vs. Stiffness core panel connection

Figure 12.4: Deflection (a) and Reduction in Deflection (b) for Panels of Different Heights

12.2. cut-out

The cut-out represents the openings in the core that are necessary for accessing the core. In graph 12.5, the relationship between the percentage of cut-out and the reduction in deflection provided by the core is illustrated.

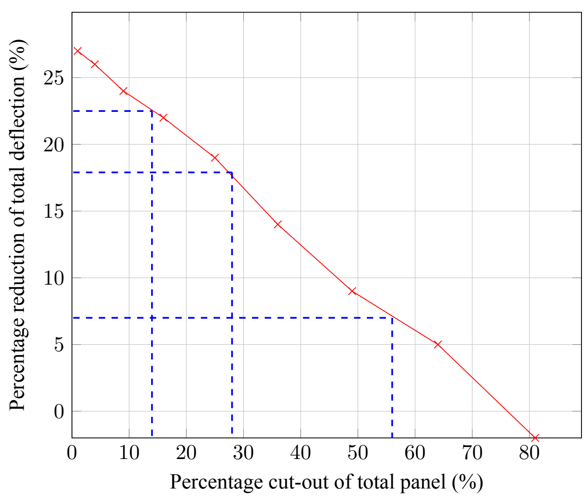

Figure 12.5: Relationship between percentage cut-out and reduction in deflection

The blue lines representing the following openings:

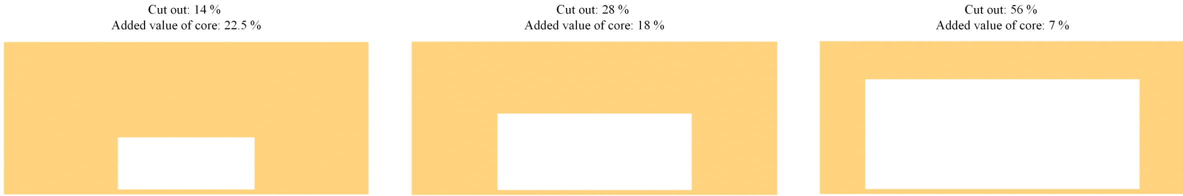

Figure 12.6: Different cut-out examples

The graph showing the cut-out percentage in relation to the reduction in total deflection of the core, indicates a gradual decrease.

With less material in the core and also the lintels getting narrower, the capacity of the CLT gets reached rapidly. With a cut-out of 65% of the total area, the maximum UC of 1 is exceeded. In graph 12.7, the unity check of $\sigma_{c/t.0}$ put against the cut-out of the core panels.

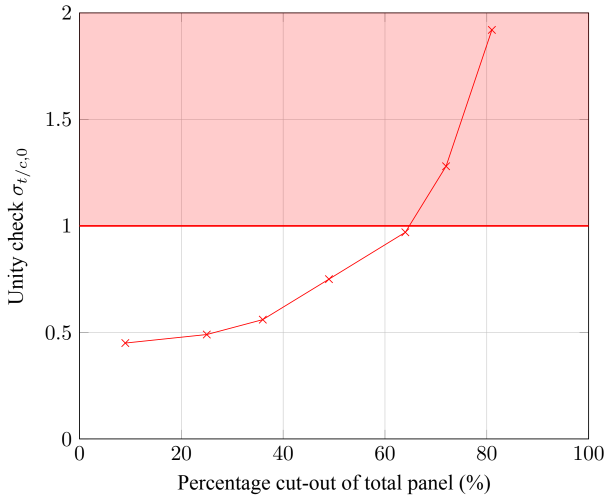

Figure 12.7: Relationship between percentage cut-out and the unity check of the CLT panels $\sigma_{t/c,0}$

12.3. Plot dimensions

The contribution of the core depends on the plot in which the building is situated. A larger plot makes that the bracings are further apart increasing Steiners law and thus increasing the moment of inertia compared to the core. In graph 12.8 the plot is put up against the contribution of the core. A building with the parameters of table 11.3 was used.

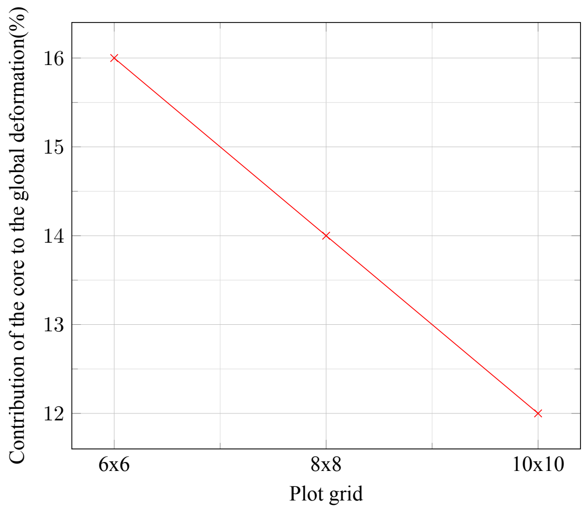

Figure 12.8: Relationship between plot layout and reduction in deflection

he graph shows a linear relationship. As the plot increases in size, the bracing becomes more effective, while the contribution of the core remains constant. Consequently, the core's contribution to the total deflection decreases.

12.4. Amount of floors

For lower buildings a timber core can add more value to the global deformation. In graph 12.9, the number of floors are reduced together with the stiffness of the bracing. So that with each height the deformation in SLS is H/1000. With the reduction in height, there is also a decrease in deflection. As a result, the stiffness in the bracing connections can be reduced while maintaining the same deflection limit. This is indicated by the red line in the graph 12.9. The blue line represents the contribution of the core to the deflection, where, for each height, the building's deflection with a core is compared to the building's deflection without a core.

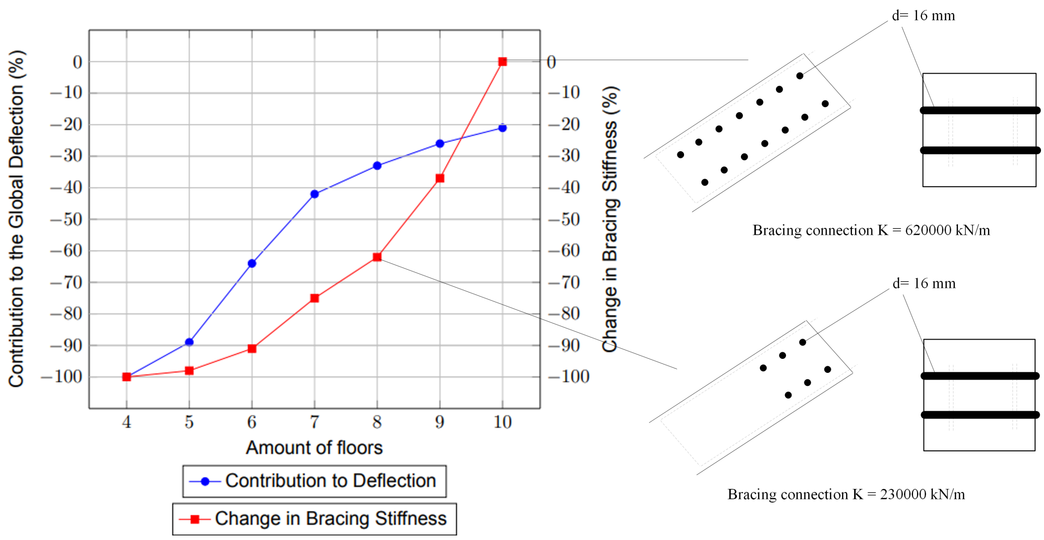

Figure 12.9: Contribution to Global Deflection and Change in bracings Stiffness vs. Amount of floors

As the height of the building increases, the required bracing stiffness must increase rapidly. The contribution of the timber core to overall stability diminishes as the building height grows. For a 4-story building, the timber core provides 100% of the stability, meaning that in the SLS, no additional bracing is needed to meet the deflection criteria.

12.5. Conclusion

Introducing a timber core increases the stiffness of the structure, thus reducing the global deflection. However, line hinges and cut-outs are applied within the core of the model, which reduce the stiffness of the core and, consequently, its contribution to minimizing the global deflection 12.10.

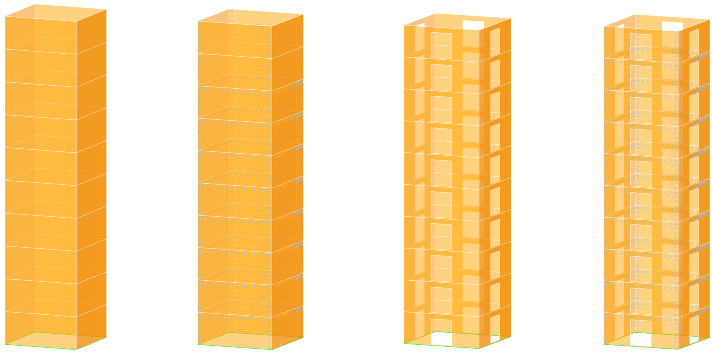

	14.1 mm	19.4 mm	19.7 mm	21.9 mm
	47 %	27 %	26 %	18 %
Horizontal line hinges	-	79713 kN/m/m	-	79713 kN/m/m
Vertical line hinges	-	936760 kN/m/m	-	936760 kN/m/m
Persentage opening	0 %	0 %	28 %	28 %

Figure 12.10: Introducing a timber core in a timber construction

13

Fire situation/Removal scenarios

13.1. Approach

The construction has to be designed to maintain its capacity during exposure to fire [42]. The model is like the Urban Woods designed for a exposure time of 120 minutes. In the model, there are no fire compartments for a clear representation. The bracing diagonals and the columns are affected on all sides, while the surfaces will be affected on one side and the beams supporting the floors will be affected from three sides. The fire situation gives a reduced cross section for all the elements following the equations from chapter 8.

Member	Original	Reduced	Affected
Columns	400x400 mm	218x218 mm	4 sides
Bracing	400x400 mm	218x218 mm	4 sides
Beams	280x320 mm	98x229 mm	3 sides
CLT Core	200 mm	120 mm	1 side

Table 13.1: Cross section reduction members

In the accidental scenario, the force from the wind will be reduced by a factor of 0.2. The following scenarios will be discussed 13.1.

Scenario 1, 1 element from the bracing removed
Scenario 2, 2 elements from the bracing removed
Scenario 3, no core, 1 element from the bracing removed

The different scenarios will be analysed for internal forces and connection forces. Scenario 1 and 2 will also be tested in a extreme variant where the whole bracing(s) are removed.

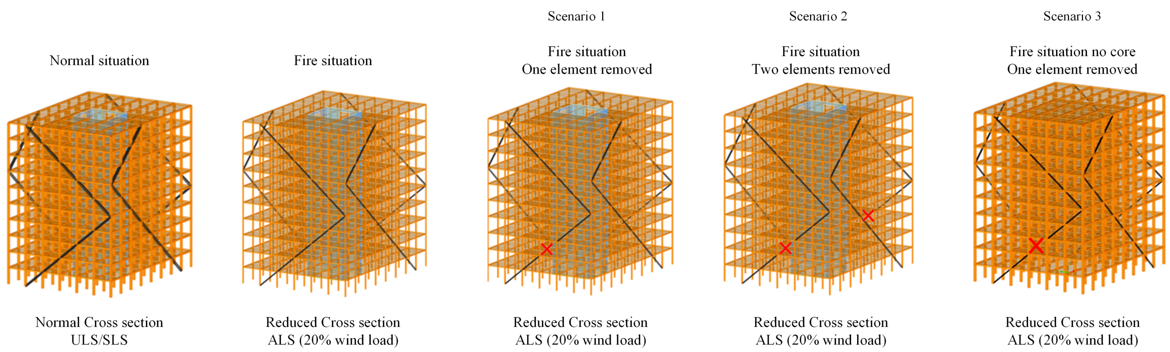

Figure 13.1: Removal scenarios with their cross section and limit state

13.2. Removing 1 element (scenario 1)

From the fire situation with the reduced cross section and the accidental limit state. One element from the bracing gets removed. Three removal situations of 1 diagonal were investigated and the one with the most impact on the CLT is explained further. For the results of the diagonal tests see Appendix D.3. The diagonal that will be removed can be seen in figure 13.4 and figure 13.3. From the deflection, it can be seen that the building with the wind from the left, tends to rotate anti-clockwise 13.2, and clockwise if the wind is coming from the other side. In the accidental limit state, the maximum global deflection goes from 10.1 mm to 12.1 mm after the removal of a single element. While global deflection is not critical in the accidental limit state, analyzing the deflection helps to explain the force flow within the structure.

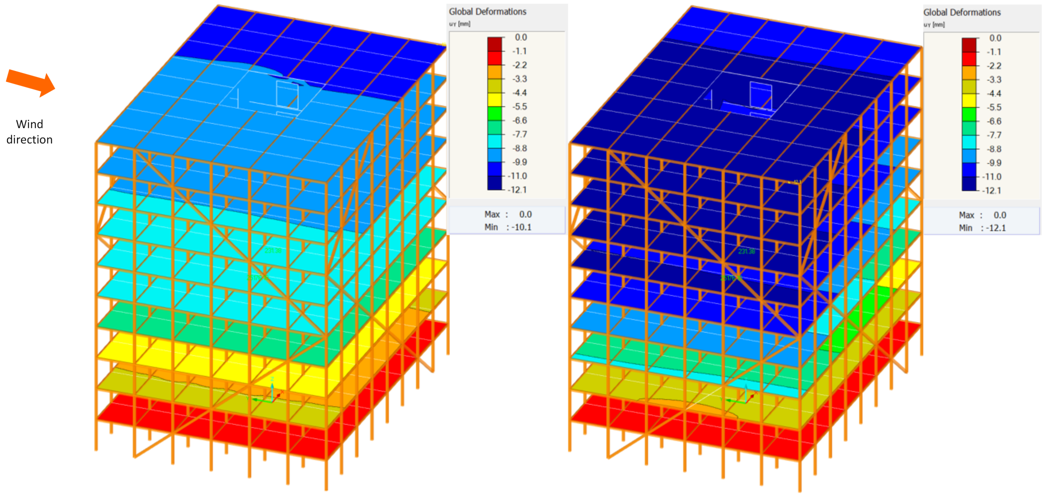

Figure 13.2: Global deformation u_Y before and after removal of element.

What happens is that the beams next to the diagonal that is removed will take up more axial force. While the beams in the bracing that is affected will take up less normal force, see figure 13.4.

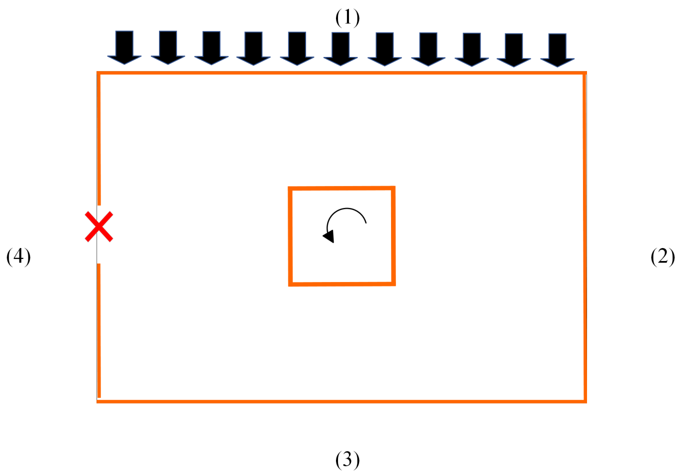

Figure 13.3: Top view, removing element.

(4) (4)

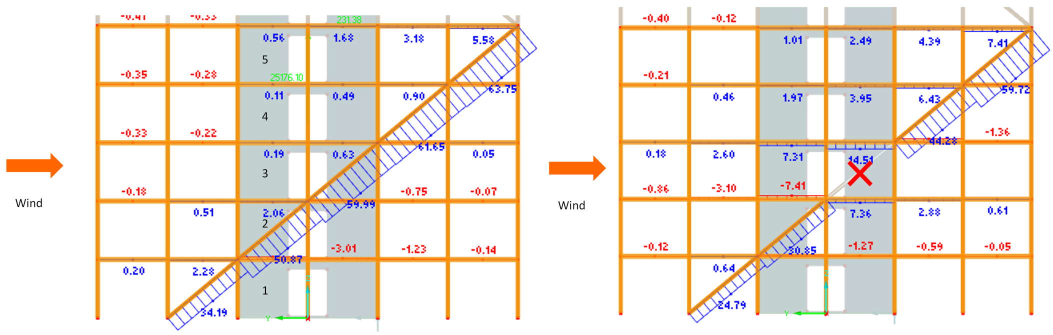

Figure 13.4: One bracing element removal before and after, normal load.

The beam directly above the removed bracing increases in tension from 0.63 kN to 14.51 kN. And the beam on the lower left side of the removed bracing goes from tension to compression from 2.06 kN to -7.41. This is because, the forces of the bracing have to be redirected to the beams.

The bracing perpendicular to the bracing that is affected will experience more axial force than in the original situation.

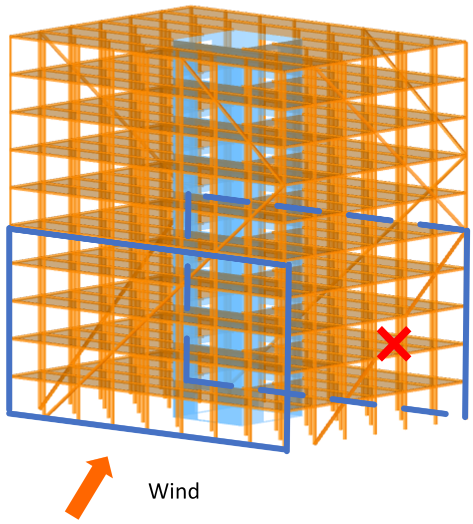

Figure 13.5: Overview of the sides perpendicular to the removed diagonal.

With one side experiencing more tension (left side) with an increase from -28.44 kN to -1.92 kN, while the other side (right side) experiences more compression from -30.68 kN to -57.29 kN figure 13.6. The bracing on the opposite side of the affected bracing is also experiencing some minor force shifts. This is also caused by the redirection of bracing forces, combined with the uneven distribution of forces resulting from the removal of an element on only one side.

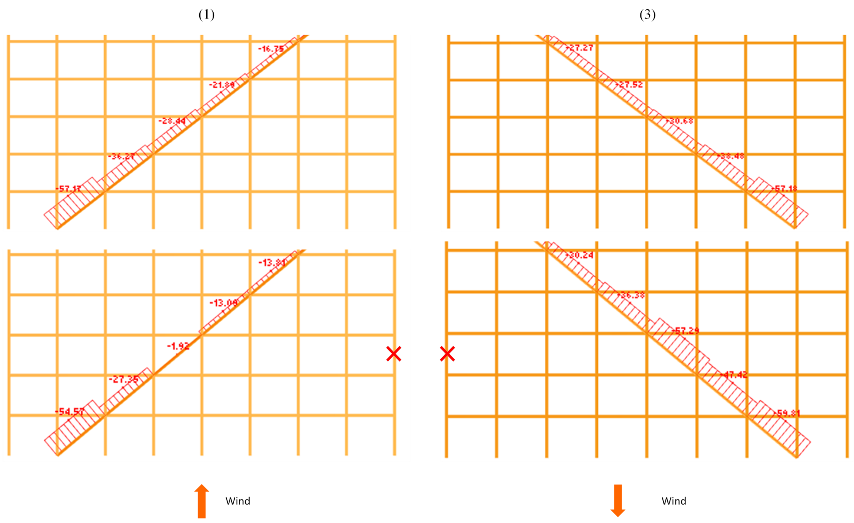

Figure 13.6: Force distribution bracing perpendicular to affected bracing before and after (left and right side).

The internal design forces n_x and n_y for the third floor before and after removal are given in figures: 13.8 13.7. The panel-to-panel connection is free for the u_x and ϕ_x direction and rigid in the u_y and u_z. It can be seen that the internal forces shifts trough the CLT floor panels. This means that the floor is able to transfer forces in the case of a diagonal removal to the core. When all the diagonals are still in tact, most of the lateral forces are taken by the façade. The floor show tension forces at one side after the removal of the bracing element.

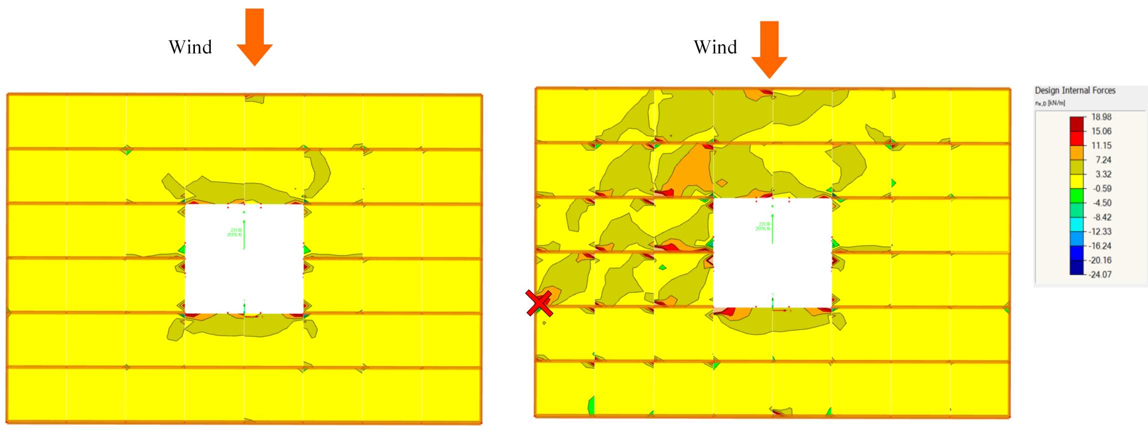

Figure 13.7: Floor 3 $n_{x,D}$ before and after 1 element removal.

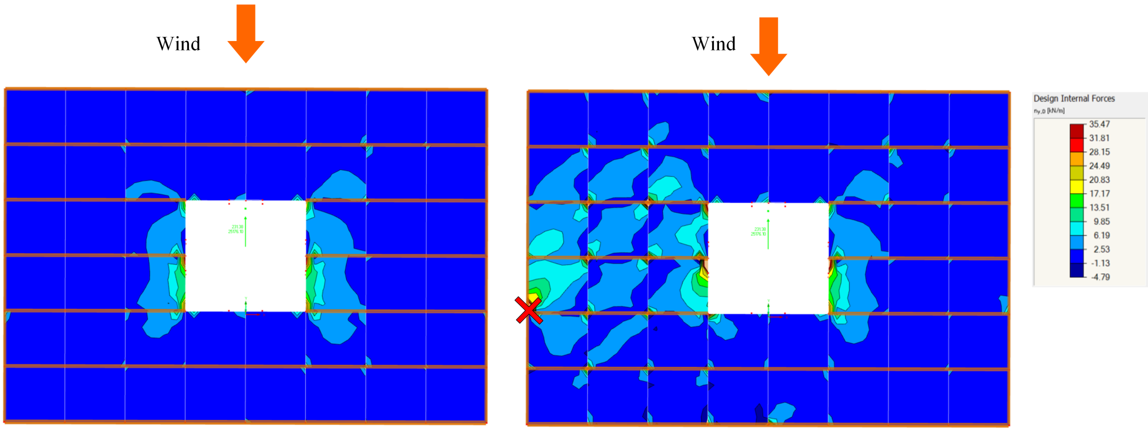

Figure 13.8: Floor 3 $n_{y,D}$ before and after 1 element removal.

The connections in the floor panels will experience a force increase because of the lateral load transfer to the core. As can be seen in figure 13.9 where the 4^{th} floor is displayed. The shear forces on the side of the removed element increase more than 10 times.

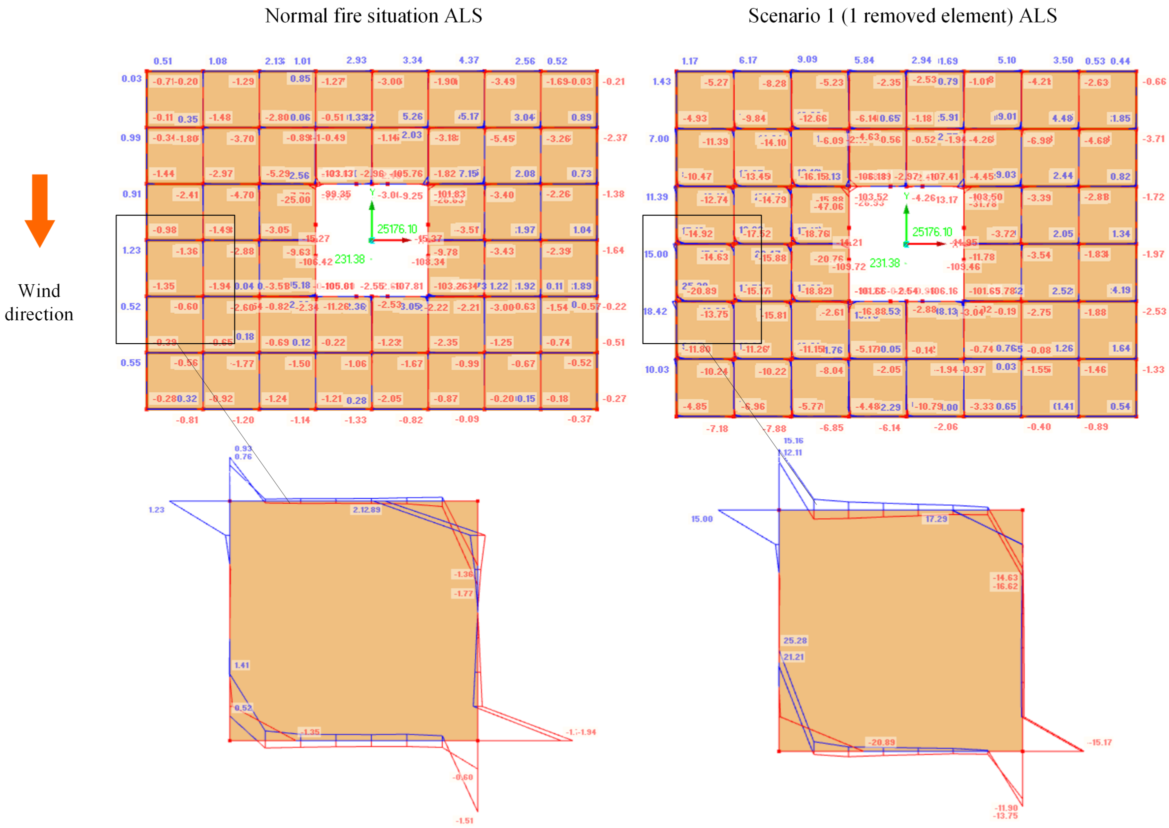

Figure 13.9: Line connections 4^{th} floor before (left) and after (right) removal of one element v_y

The unity checks of the normative CLT panel (panel 1 in figure 13.10) in the fire situation will experience some minor increases (see table 13.2). The unity check for the int($\sigma_{t/c,90} + \tau_{y'z'}$ is above one. This is caused by peak forces in the corner that need to be distributed evenly. However for the comparison the raw data from RFEM will be used.

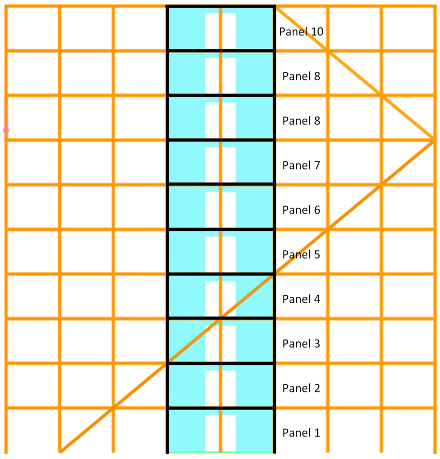

Figure 13.10: Overview panels

Failure mechanism	UC normal situation ALS	UC one element removed ALS	% increased
$\sigma_{b,0}$	0.34	0.35	0%
$\sigma_{b,90}$	0.01	0.01	0%
$\sigma_{t/c,0}$	0.37	0.37	0%
$\sigma_{t/c,90}$	0.89	0.90	1%
$\sigma_{b+t/c,0}$	0.61	0.61	0%
$\sigma_{b+t/c,90}$	0.91	0.91	0%
$\tau_{y'z'}$	0.11	0.11	0%
$\tau_{x'z'}$	0.42	0.42	0%
$\tau_{x'y'}$	0.42	0.42	0%
$int(\tau_{x'z'} + \tau_{x'y'})$	0.19	0.19	0%
$int(\sigma_{t/c,90} + \tau_{y'z'})$	1.07	1.08	1%

Table 13.2: Percentage of the UC in panel 1, after removing bracing element (see D.2 for description).

The most change of forces appeared to be in panel 3 (see figure 13.10). In table 13.3, it can be seen that the shear in the xy plane increases with 36 %. However, the highest Unity Checks are in panel 1.

Failure mechanism	UC normal situation ALS	UC one element removed ALS	% increased
$\sigma_{b,0}$	0.02	0.03	50%
$\sigma_{b,90}$	0.0	0.0	0%
$\sigma_{t/c,0}$	0.28	0.31	11%
$\sigma_{t/c,90}$	0.23	0.29	26%
$\sigma_{b+t/c,0}$	0.28	0.31	11%
$\sigma_{b+t/c,90}$	0.23	0.29	26%
$\tau_{y'z'}$	0.01	0.01	0%
$\tau_{x'z'}$	0.05	0.05	0%
$\tau_{x'y'}$	0.33	0.38	15%
$int(\tau_{x'z'} + \tau_{x'y'})$	0.11	0.15	36%
$int(\sigma_{t/c,90} + \tau_{y'z'})$	0.23	0.29	26%

Table 13.3: Percentage of the UC in panel 3, after removing bracing element.

The line-support reaction in the core gets a 18 kN/m increase in one corner, while the other corner stays the same compared to the original situation.

To give a clear representation of the forces in the CLT panels, the following figures are obtained from the FEM program. The figures show von Mises stresses.

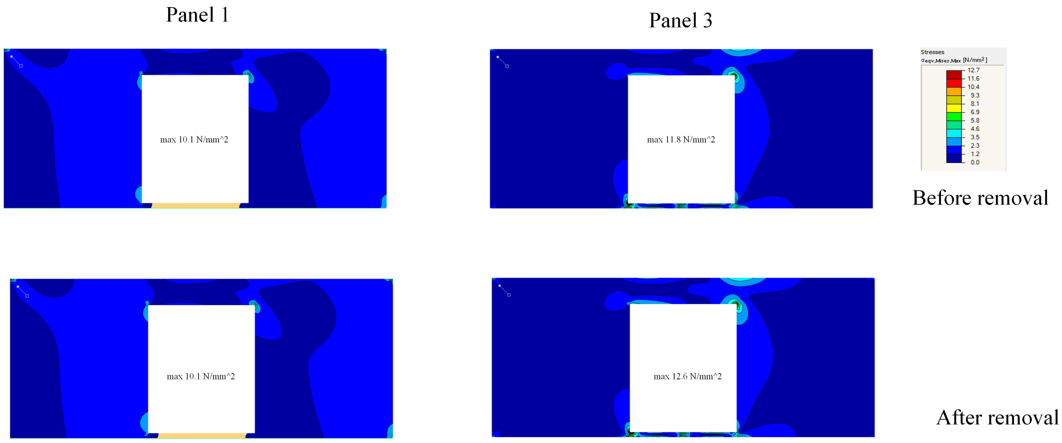

Figure 13.11: Before and after panel 1 and 3 (von Mises stresses), one bracing removal

The von Mises stesses show that in panel 1 higher overall stresses occur, but the peak von Mises stress is higher in panel 3. The stresses increases in panel 3 when removing an element. This can be seen by looking at the maximum stress. This increase is due to the core taking on more forces that were initially carried by the bracing.

13.3. Removing 2 elements (scenario 2)

Two diagonal elements in the bracing will be removed at the same height (see figure 13.13 and figure 13.14). The global deformation will increase from 10.1 to 13.5 mm. The color scale differs from that of the single-element removal, as it is based on the maximum deflection in the removal scenarios.

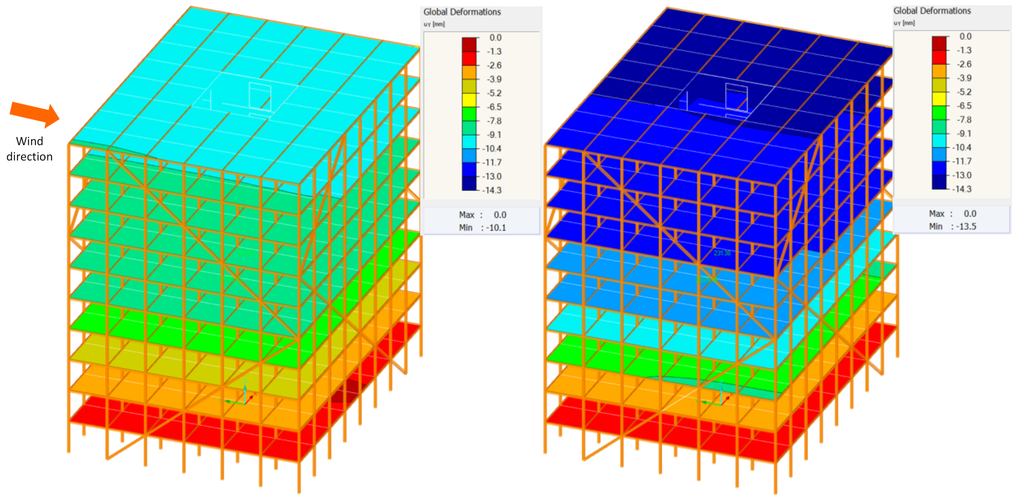

Figure 13.12: Global deformation u_y before and after removal of 2 elements at the same height.

The force distribution in the façade will be like figure 13.14. Compared to the one with only one element removed, the forces increases slightly.

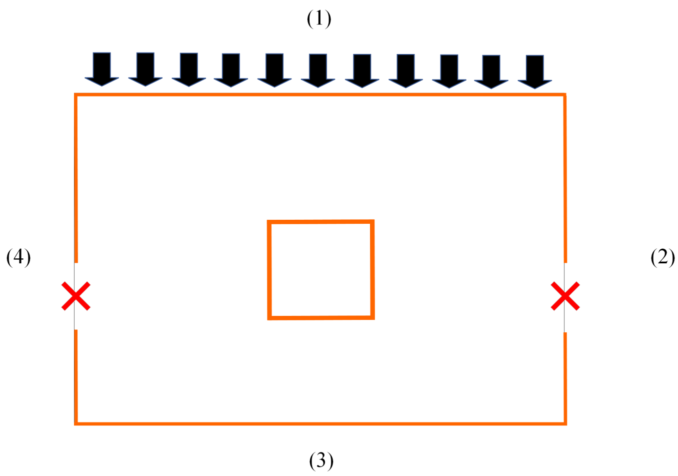

Figure 13.13: Top view, removing 2 elements

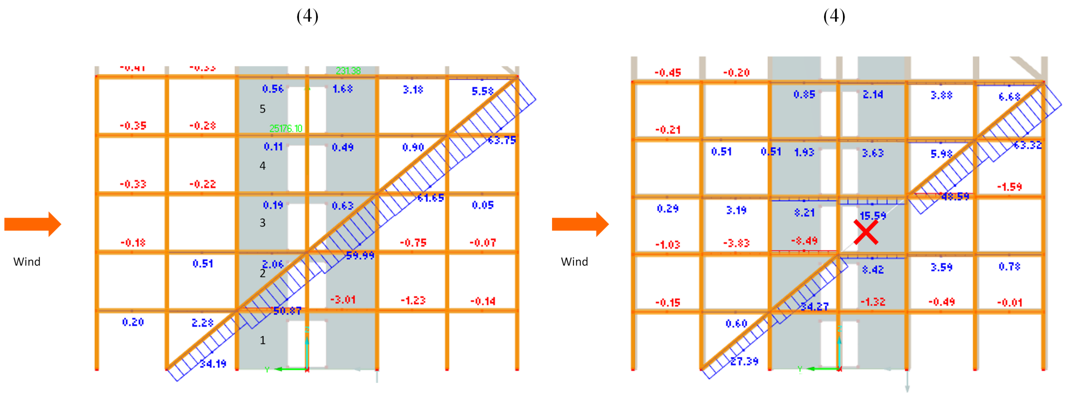

Figure 13.14: Two bracing element removal before and after, normal load

The same effect on the beams in the facade is observed as in the scenario where one bracing element is removed. The force in the beam directly above the removed bracing increases from 0.63 kN to 15.59 kN, while the beam to the lower left changes from a tension of 2.06 kN to a compression of -8.49 kN.

As can be seen in figure 13.15, the bracings perpendicular to the affected bracings are not affected anymore when both sides are removed. No twisting occurs now due to the symmetrical removal of elements.

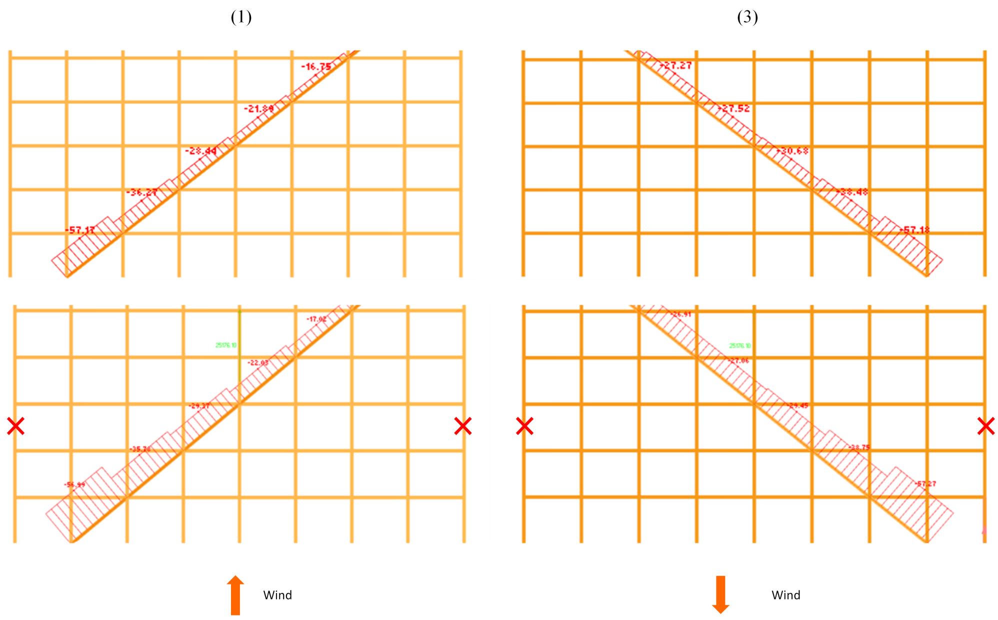

Figure 13.15: Force distribution bracing perpendicular to affected bracings (left and right side)

The line support reactions show that there are no tensile forces in the foundation 13.16.

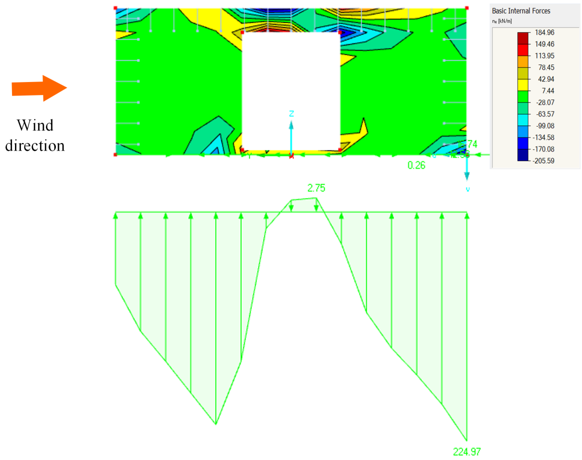

Figure 13.16: Line support reaction, core panel

The internal forces in the third floor, before and after removal of the 2 bracing elements is shown in figure 13.17 and figure 13.18.

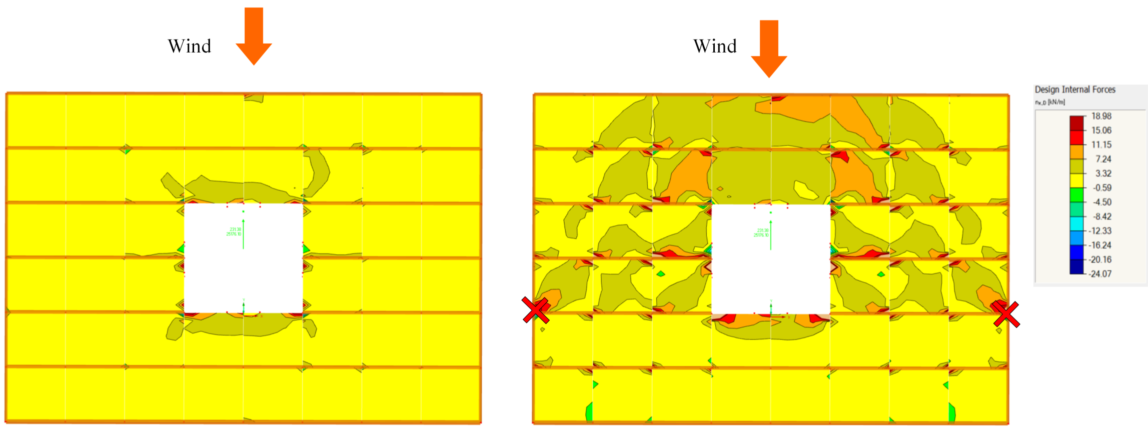

Figure 13.17: Floor 3 $n_{x,D}$ before and after 2 elements removal.

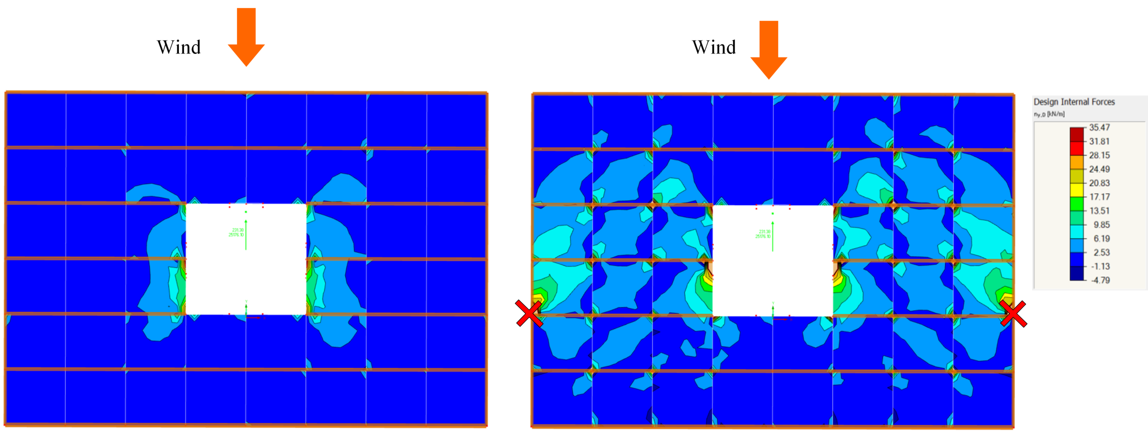

Figure 13.18: Floor 3 $n_{y,D}$ before and after 2 elements removal.

The percentage increase in the CLT panels 1 and panel 3, after the removal of two elements (one on each side) are given in table 13.4 and table 13.5.

Failure mechanism	UC normal situation ALS	UC two elements removed ALS	% increased
$\sigma_{b,0}$	0.34	0.35	3%
$\sigma_{b,90}$	0.01	0.01	0%
$\sigma_{t/c,0}$	0.37	0.37	0%
$\sigma_{t/c,90}$	0.89	0.92	3%
$\sigma_{b+t/c,0}$	0.61	0.62	2%
$\sigma_{b+t/c,90}$	0.91	0.94	3%
$\tau_{y'z'}$	0.11	0.11	0%
$\tau_{x'z'}$	0.42	0.43	2%
$\tau_{x'y'}$	0.42	0.42	0%
$int(\tau_{x'z'} + \tau_{x'y'})$	0.19	0.20	5%
$int(\sigma_{t/c,90} + \tau_{y'z'})$	1.07	1.11	4%

Table 13.4: Percentage of the UC in panel 1, after removing 2 bracing element.

Failure mechanism	UC normal situation ALS	UC one element removed ALS	% increased
$\sigma_{b,0}$	0.02	0.02	0%
$\sigma_{b,90}$	0.0	0.0	0%
$\sigma_{t/c,0}$	0.28	0.32	14%
$\sigma_{t/c,90}$	0.23	0.32	39%
$\sigma_{b+t/c,0}$	0.28	0.32	14%
$\sigma_{b+t/c,90}$	0.22	0.32	39%
$\tau_{y'z'}$	0.01	0.01	0%
$\tau_{x'z'}$	0.05	0.05	0%
$\tau_{x'y'}$	0.33	0.41	24%
$int(\tau_{x'z'} + \tau_{x'y'})$	0.11	0.17	55%
$int(\sigma_{t/c,90} + \tau_{y'z'})$	0.22	0.32	39%

Table 13.5: Percentage of the UC in panel 3, after removing 2 bracing elements.

The line-support reaction gets a 9.5 kN/m increase in both corners compared to the original situation.

To combine the results with all the normative values, the following table gives an overview 13.6.

Fire scenarios	Normal situation ALS	1 side element failure ALS	2 side element failure ALS
Remaining bracing	63.75 kN	59.72 kN	63.32 kN
Beams in façade	5.7 kN	14.51 kN	15.54 kN
Bracing perpendicular	-27.45 kN	5.19 / -57.6 kN	-26.06 kN
Core $\sigma_{t/c,90}$	UC = 0.89	UC = 0.90	UC = 0.92
Core $\sigma_{b+t/c,90}$	UC = 0.91	UC = 0.91	UC = 0.94
Core $int(\sigma_{t/c,90} + \tau_{y'z'})$	UC = 1.07	UC = 1.08	UC = 1.11

Table 13.6: Overview highest value element failure

To provide a clear representation of the forces in the CLT panels, similar to what was done in the one-element removal scenario, the following figures are obtained from the FEM program.

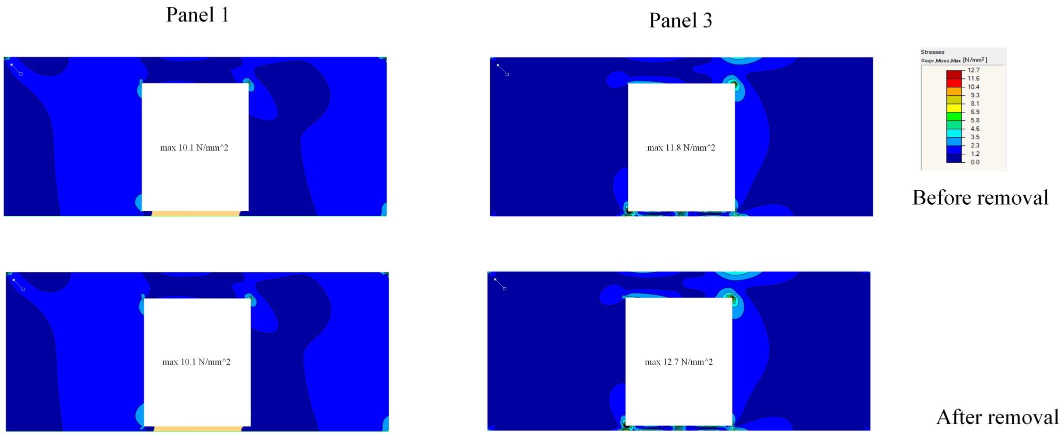

Figure 13.19: Before and after panel 1 and 3, two bracings removal

13.4. No core situation (scenario 3)

In the no core scenario, the robustness for the lateral stability can be examined for when no core is present. Only the scenario in which the bracing on one side is removed is applicable because, if both bracings are removed there will not be any stability system as a second load path. The deflection in the accidental limit state for the fire situation is as expected more than with a core(10.1 mm vs 13.8 mm). After the removal of a single diagonal, the structure tends to rotate even more than in the case of the structure with a core. The deformation goes up to 28.1 mm 13.20. When the whole bracing is removed, the global deformation goes up to 81.4 mm.

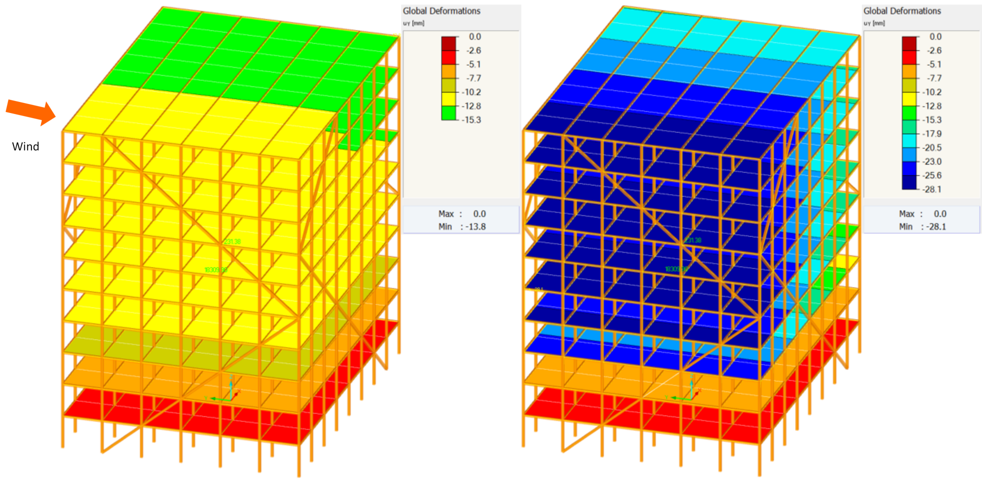

Figure 13.20: Global deformation u_y before and after of 1 element removal (no core).

Figure 13.21: Removing one bracings in the normative direction, no core

The internal forces in the third floor increase when an element is removed, particularly in the area where the connections to the bracings are located 13.22 and 13.23.

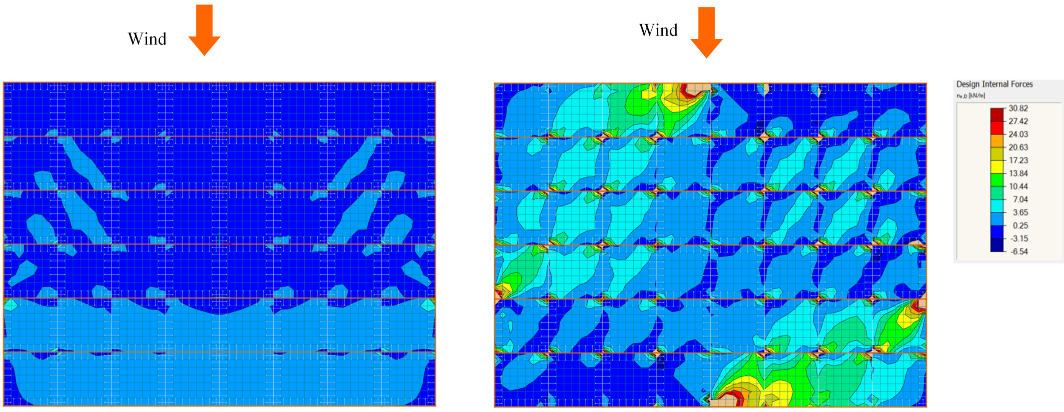

Figure 13.22: Floor 3, $n_{x,D}$ before and after 1 element removal, no core

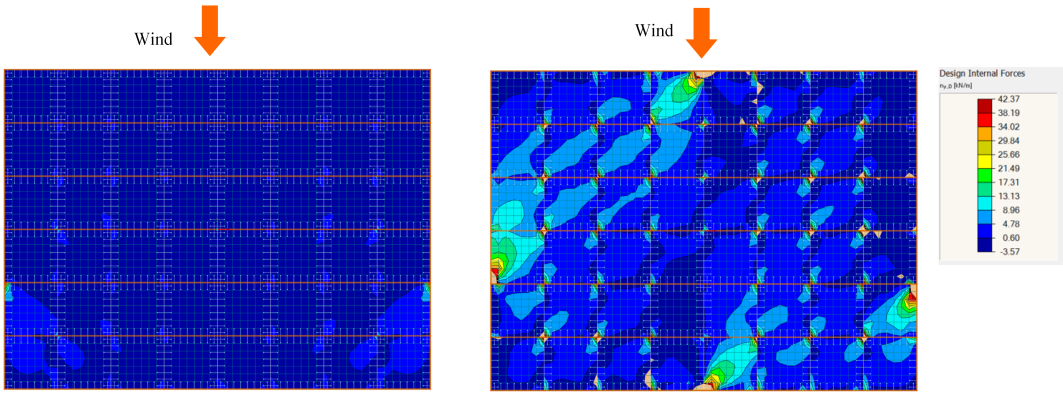

Figure 13.23: Floor 3, $n_{y,D}$ before and after 1 element removal, no core

The internal forces are ten times bigger at the connections with the bracing. These connections are not tested for the amount of force.

Since the connection strength of the bracings are not sufficient enough, the connections are changed to a 3x23 dowels setup. The Unity checks in the normal and in the fire situation would be:

Failure mechanism Removed –>	Element	UC normal	UC fire	UC fire 1 element	UC fire 1 side bracing
$f_{c,0,d}$	Column	0.43	0.87	0.87	0.87
Elastic buckling load	Column	0,44	0.95	0.95	0.95
Bending M_y	Beam	0.18	0.08	0.10	0.10
Shear V_z	Beam	0.26	0.23	0.23	0.23
Tension	Bracing	0.67	0.24	0.38	0.48
Connection	Bracing	0,94	0.28	0.44	0.55
Buckling	Bracing	0.49	0.27	0.44	0.54

In contrast of the scenario with the core, is by an element removal of the scenario without a core, a force increase of 100% at the opposite side of the removed bracing (figure 13.24).

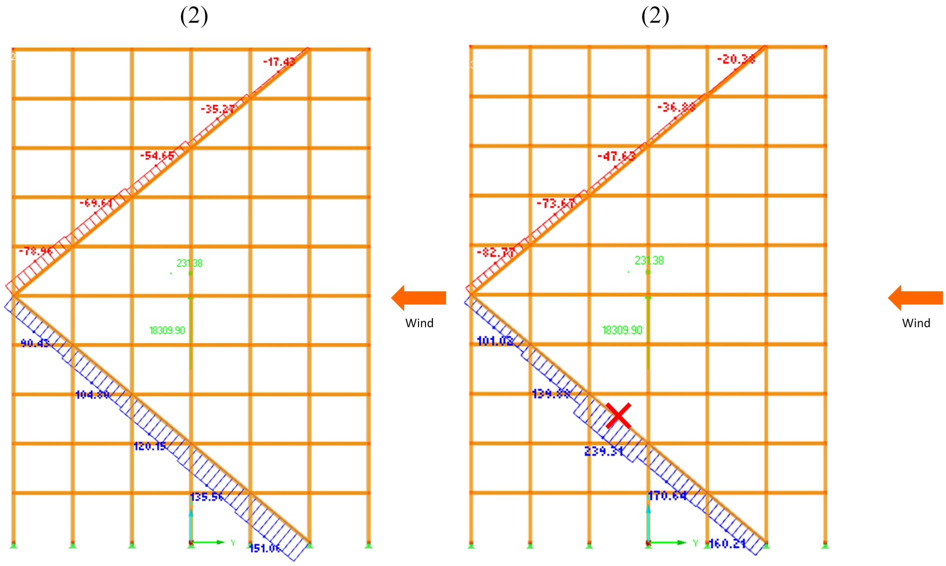

Figure 13.24: Opposite side before and after 1 element removal, no core

The forces in the floor show tension at the height above the removed bracing with the connections to the bracing and compression at the height below the removed bracing also where the bracing connects to the floor.

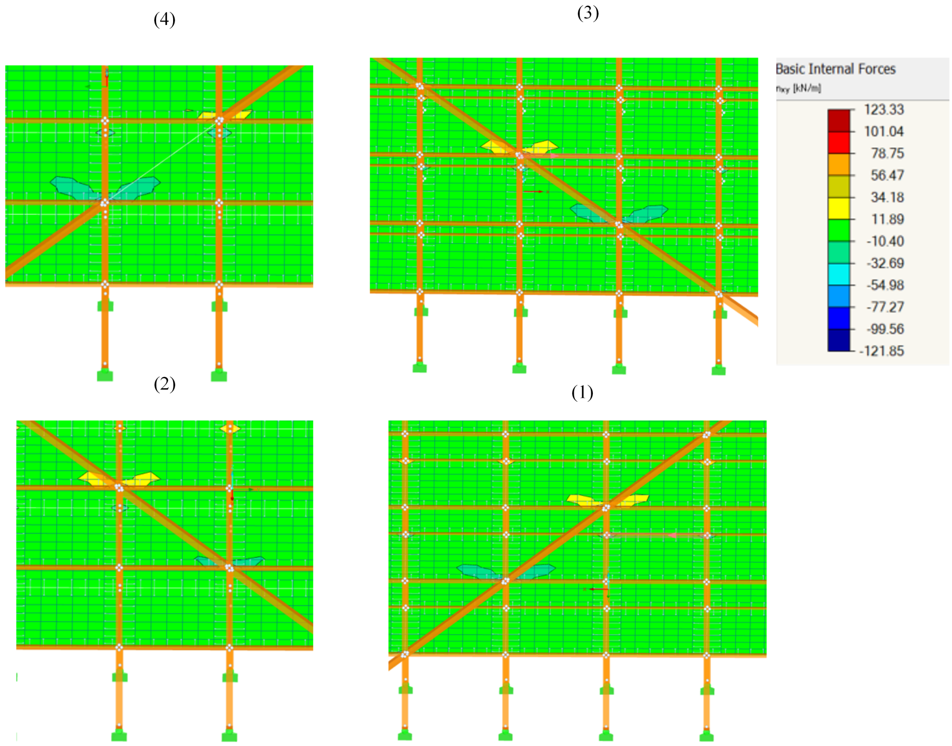

Figure 13.25: Internal forces n_{xy} kN/m floors, no core situation.

13.5. Removing the whole bracing at one side (scenario 1 extreme)

When removing the whole bracing in one side, the beams that were attached to the bracing are experiencing fewer forces (figure 13.26). Also the effect on the bracings perpendicular to the damaged side is bigger (figure 13.27). As well as the effect on the core panels (table 13.7).

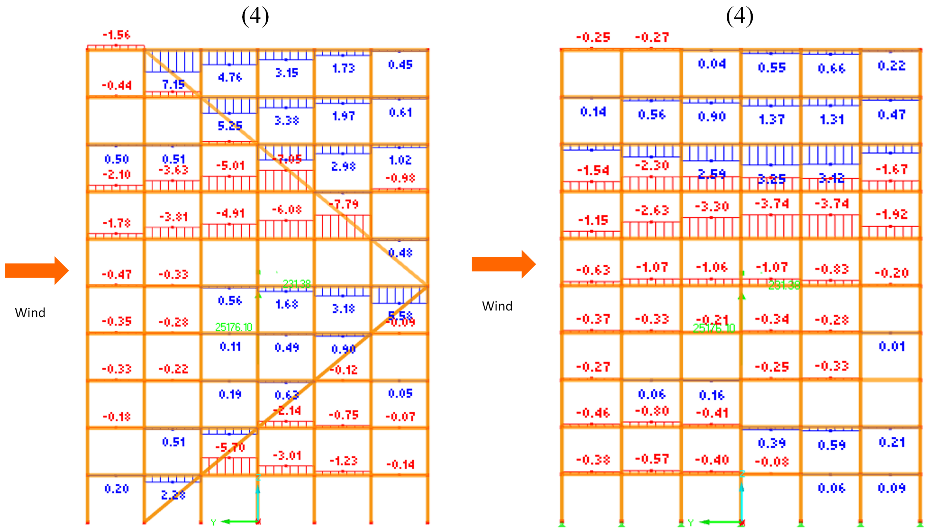

Figure 13.26: Whole bracing removed one side, before and after

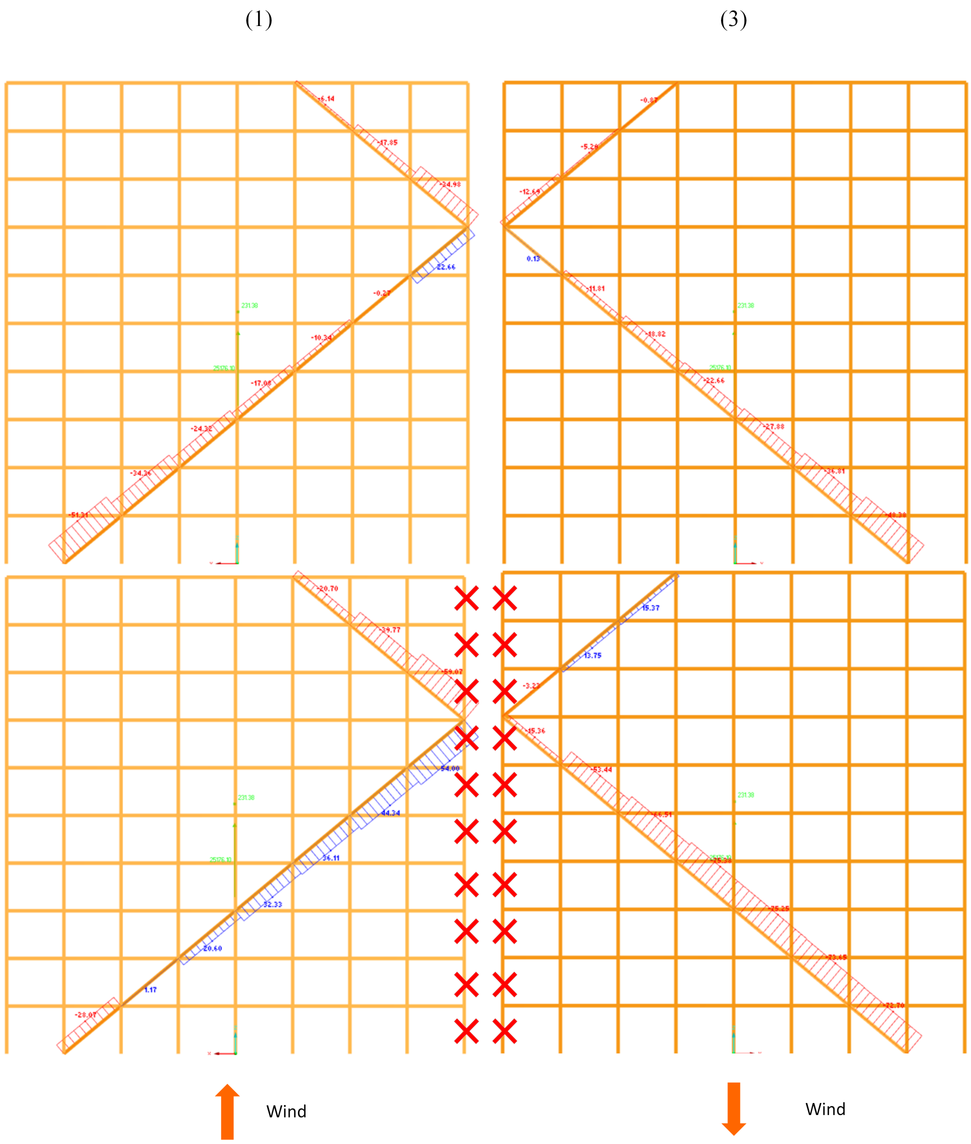

Figure 13.27: Force distribution bracing perpendicular to affected bracing before and after (left and right side)

The left side bracing gets an increase in tension of maximum 44.61 kN. The right side gets an increase in compression of maximum 52.72 kN.

Failure mechanism	UC normal situation ALS	UC whole bracing removed ALS	% increased
$\sigma_{b,0}$	0.34	0.37	9%
$\sigma_{b,90}$	0.01	0.01	0%
$\sigma_{t/c,0}$	0.37	0.39	5%
$\sigma_{t/c,90}$	0.89	0.97	9%
$\sigma_{b+t/c,0}$	0.61	0.65	7%
$\sigma_{b+t/c,90}$	0.91	0.98	8%
$\tau_{y'z'}$	0.11	0.12	9%
$\tau_{x'z'}$	0.42	0.45	7%
$\tau_{x'y'}$	0.42	0.44	5%
$int(\tau_{x'z'} + \tau_{x'y'})$	0.19	0.22	16%
$int(\sigma_{t/c,90} + \tau_{y'z'})$	1.07	1.16	8%

Table 13.7: Percentage of the UC in panel 1, after removing whole bracing on one side

13.6. Removing the whole bracing at two sides (scenario 2 extreme)

Additionally, removing the whole bracing on the opposite side causes the forces in the bracings perpendicular to the affected bracing to revert to their previous state. The forces in lower panel 1 are detailed in Table 13.8.

Failure mechanism	UC normal situation ALS	UC 2 whole bracings removed ALS	% increased
$\sigma_{b,0}$	0.34	0.41	21%
$\sigma_{b,90}$	0.01	0.01	0%
$\sigma_{t/c,0}$	0.37	0.41	11%
$\sigma_{t/c,90}$	0.89	1.10	24%
$\sigma_{b+t/c,0}$	0.61	0.73	20%
$\sigma_{b+t/c,90}$	0.91	1.11	22%
$\tau_{y'z'}$	0.11	0.13	18%
$\tau_{x'z'}$	0.42	0.50	19%
$\tau_{x'y'}$	0.42	0.46	10%
$int(\tau_{x'z'} + \tau_{x'y'})$	0.19	0.28	47%
$int(\sigma_{t/c,90} + \tau_{y'z'})$	1.07	1.31	22%

Table 13.8: Percentage of the UC in panel 1, after removing 2 whole bracings

A overview of the highest forces in the three different situations is given in table 13.9. As can be seen, the UC is above the value one in 1 case for the 1 side failure and in 3 different cases for the 2 sides failure.

Fire scenarios	Normal situation	1 whole side failure	2 whole sides failure
Beams in façade	3.74 kN	14.51 kN	15.54 kN
Bracing perpendicular	50.75 kN	-72 / +53 kN	50.75 kN
Core $\sigma_{t/c,90}$	UC = 0.89	UC = 0.97	UC = 1.10
Core $\sigma_{b+t/c,90}$	UC = 0.91	UC = 0.98	UC = 1.11
Core $int(\sigma_{t/c,90} + \tau_{y'z'})$	UC = 1.07	UC = 1.16	UC = 1.31

Table 13.9: Overview highest value side failure

13.7. Connections

From the equations in chapter 6, the bracing connection strength reduces in the fire situation from:

$$F_{v,Rk} = 816.58kN \tag{13.1}$$

to

$$F_{v,Rk,fi} = 370.73kN \tag{13.2}$$

The maximal force the connections have to endure in the ALS is given in table 13.10.

Removal scenarios	Force in the bracings (kN)	UC
No removal	130.69	0.35
1 element	134.72	0.36
2 elements	120.11	0.32
1 whole side bracing	134.31	0.36
2 whole sides bracings	50.58	0.14

Table 13.10: Forces in the bracing connections, fire situation

For the line hinges in the core, the reduction of the shear capacity that is calculated using the EC will be as described in table 13.11

Line hinge	$F_{v,Rk}$ (kN/m)	$F_{v,Rk,fi}$ kN/m
Horizontal hinge n_y	350	201.43
Horizontal hing n_x	615	403
Vertical hing n_x	160	90

Table 13.11: Reduced force in the line hinges

The forces for the line hinges in the fire situation for different element removals is given in table 13.12.

Removal scenarios	Horizontal ny	Horizontal nx	Vertical nx
No removal	-153	-20.56	-18.03
1 element	-159.85	-26.62	-18.616
2 elements	-163.61	-28.79	-19.76
1 whole side bracing	-171.81	-29.1	-20.76
2 whole sides bracings	-200.33	-38.78	21.468

Table 13.12: Forces in the core panels connection, fire situation

13.7.1. Reduction line hinge connection stiffness

Reducing the horizontal line connection in the core panels for the removal scenarios gives a reduction in the maximal forces for the panels and the line hinges (figure 13.29).The lines representing each removal scenario are parallel to each other, indicating that the behavior is consistent across scenarios, though it start at different release forces.

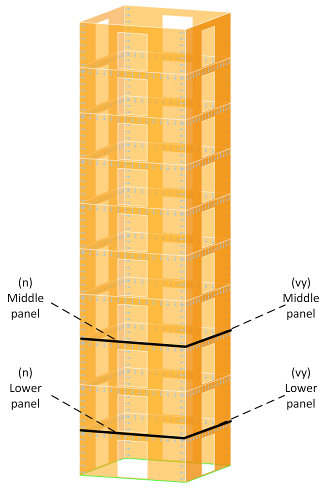

Figure 13.28: Overview line hinges

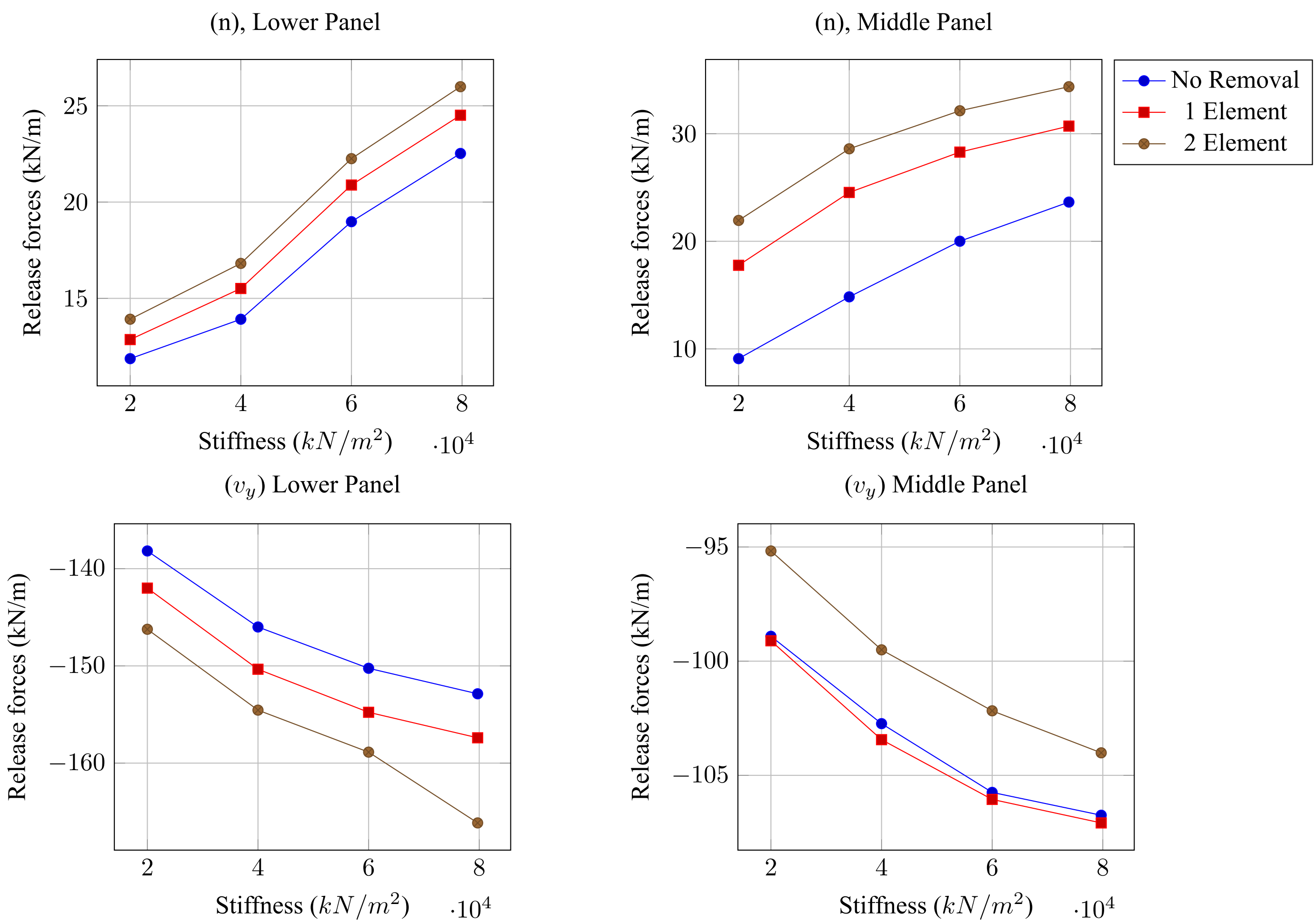

Figure 13.29: Reduction stiffness vs maximum force line hinge

13.8. Unity Checks in the accidental limit state

The comparison of the Unity check in the ULS and the different ALS cases are given in tabel 13.13. For the 2 sides removal of the bracing the unity checks exceed 1 in the ALS because of the horizontal wind force.

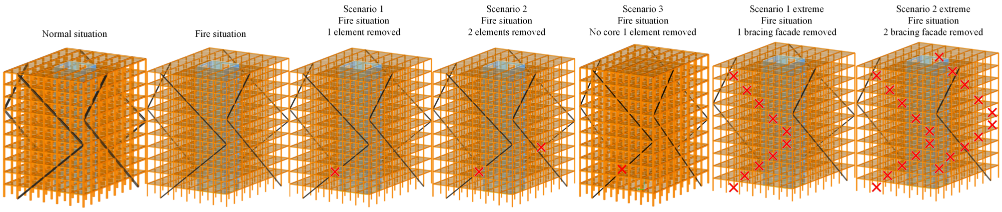

Figure 13.30: Normal situations and fire situations.

Failure mechanism Removed –>	UC ULS	UC ALS	Scenario 1 UC ALS 1 elem	Scenario 2 UC ALS 2 elem	Scenario 3 UC ALS No core 1 elem	Scenario 1 ex UC ALS 1 side	Scenario 2 ex UC ALS 2 sides
$f_{c,0,d}$ column	0.43	0.88	0.89	0.89	0.87	0.89	0.89
Buckling column	0.44	0.96	0.97	0.97	0.95	0.97	0.97
Bending M_y beam	0.19	0.13	0.13	0.13	0.10	0.13	0.13
Shear V_z Beams	0.37	0.27	0.27	0.27	0.23	0.27	0.27
$\sigma_{b,0}$	0.04	0.34	0.34	0.35	-	0.37	0.41
$\sigma_{b,90}$	0.00	0.01	0.01	0.01	-	0.01	0.01
$\sigma_{t/c,0}$	0.43	0.37	0.37	0.37	-	0.39	0.41
$\sigma_{t/c,90}$	0.42	0.89	0.90	0.92	-	0.97	1.10
$\sigma_{b+t/c,0}$	0.43	0.61	0.61	0.62	-	0.65	0.73
$\sigma_{b+t/c,90}$	0.42	0.91	0.91	0.94	-	0.98	1.11
$\tau_{y'z'}$	0.33	0.11	0.11	0.11	-	0.12	0.13
$\tau_{x'z'}$	0.11	0.42	0.42	0.43	-	0.45	0.50
$\tau_{x'y'}$	0.58	0.42	0.42	0.42	-	0.44	0.46
$int(\tau_{x'z'} + \tau_{x'y'})$	0.34	0.19	0.19	0.20	-	0.22	0.28
$int(\sigma_{t/c,90} + \tau_{y'z'})$	0.42	1.07	1.08	1.11	-	1.16	1.31
Bracing connection	0.94	0.35	0.36	0.32	0.44	0.36	0.14
Hor line hinge ny	0.51	0.76	0.79	0.81	-	0.85	0.99
Hor line hinge nx	0.09	0.05	0.07	0.07	-	0.07	0.10
Ver line hinge nx	0.31	0.20	0.20	0.21	-	0.23	0.24

Table 13.13: UC normal situation ULS and UC fire situations ALS

Part III

Research Outcome

14 Discussion

The thesis began with a literature review that explored the principles of timber construction and introduced the design of the Urban Woods project. The review emphasized stability and connection design, while also addressing materials and fire safety considerations. Based on the findings from the literature, a Finite Element Model (FEM) was developed for the case study, simplifying the design of Urban Woods. This model allowed for the alteration of various parameters to examine their dependencies. Additionally, element removal tests were conducted to assess the impact on the structure and its connections. The previous chapter presented these results; this chapter will discuss and interpret them.

14.1. Interpretation of the results

The interpretation of the results is divided into three sections. First, an analysis of the value of the timber core in the model based on the Urban Woods is presented, followed by the results of the sensitivity analysis. Finally, the impact of element removal in the fire situation is discussed.

14.1.1. Timber core

From the results, the timber core showed value in terms of reduction of deflection in the SLS and reduction of axial force in the bracings in ULS. No tension occurred in the support line load at the connection with the core. Some additional compression at the line support of the core occurred because of the horizontal wind force. Tension would occur if the weight of the building is less than the uplift caused by the horizontal wind load acting on the core. This is because a portion of the vertical floor load is applied to the core in the model. In the future, a model could be tested where the vertical load is fully assigned to the columns, and the core is used only for horizontal forces.

14.1.2. Results sensitivity analysis

Three different stability systems where tested on a building with 10 storeys (30 meter). The tests show the superiority of the bracing system compared to the CLT core system. The timber core has 231.4 % more global deformation compared to the bracing system. This depends on the connections and the cross section of the bracing diagonals. The plot of the building is as can be seen in graph 12.8, a parameter that has influence on the contribution of the core to the global deformation.

The connection stiffness for the horizontal line hinge in the core has significant influence on the total deflection of the building. With half the amount of dowels the, reduction of the deflection that is taken by the core goes from 18 % to 14 % 12.1. Which is equal to a cross section reduction of the bracing diagonals of 10 % (from 400 x 400 mm to 380 x 380 mm). Or a bracing stiffness reduction of 20 % (from 2299308 kN/m to 1850000 kN/m).

The stiffness of the vertical line hinge shows considerable tolerance, as the global deflection remains unchanged even when the stiffness is reduced by half. However, if the stiffness is significantly reduced, the total deflection will be affected. A one percent difference in contribution is realised by a reduction of 20 times the stiffness of the vertical connection. This indicates that the stiffness of the vertical line hinge is initially high. Compared to the horizontal core line hinge, its stiffness is ten times greater due to the different screw arrangement.

Another way of increasing the stiffness of the core is by using longer panels. Longer CLT panels reduces the number of hinges, making the core stiffer. Panels spanning two floors instead of one can reduce global deformation by up to 7% for the model. Fewer connections also mean less material usage, providing an additional incentive to use longer CLT panels. However, the transportation and manufacturing of these longer CLT elements can be a bottleneck, as they may increase costs and CO_2 emissions.

Increasing the cutout in the core will decrease the core's contribution to global deformation in a linear manner, while the unity check of the panel will increase rapidly.

As the size of the cut-out in the core increases, there is a proportional reduction in the amount of core material. This reduction leads to a linear decrease in the core's ability to contribute to the overall stiffness and thus the resistance to deformation of the structure. The Unity check rises however rapidly as the cutout size increases. This is because by removing material at the core, it not only reduces stiffness but also concentrates stresses in the remaining material.

In this sensitivity analysis, the core is simplified to a square with one cut-out on each side. In reality, cores come in various sizes and have different placements for doors and elevator shafts. These variations in core design result in different stability outcomes, as the moment of inertia and the placement of the connections vary.

As the number of floors decreases from 10 to 4, the contribution to the global deflection shows a significant increase. With 4 floors no bracing is needed to maintain enough stability in the SLS. The stiffness required in the bracing increases significantly as more floors are added. This is due to the rapidly growing influence of the wind on global deflection, as described in Chapter 7.1. At lower heights, less stiffness is needed in the wind bracings and core to meet the deflection limit (SLS).

14.1.3. Support load

When the core contributes to the global stability of a structure, more load is transferred to the foundation directly beneath the core. In the Ultimate Limit State (ULS), the line load directly under the core of a 10-story building increases by 50 % due to the core's contribution to overall stability. In figure 14.1, on the left is the line support of the normative ULS that does not take in consideration the wind load.

$$1,2 \cdot (Deadload + Permanent - load) + 1.5 \cdot variable - load \tag{14.1}$$

And on the right of the figure, the normative ULS that does take in consideration the wind load.

$$1,2 \cdot (Deadload + Permanent - load) + 1.5 \cdot Wind - load_y + 0.4 \cdot Variable - load \tag{14.2}$$

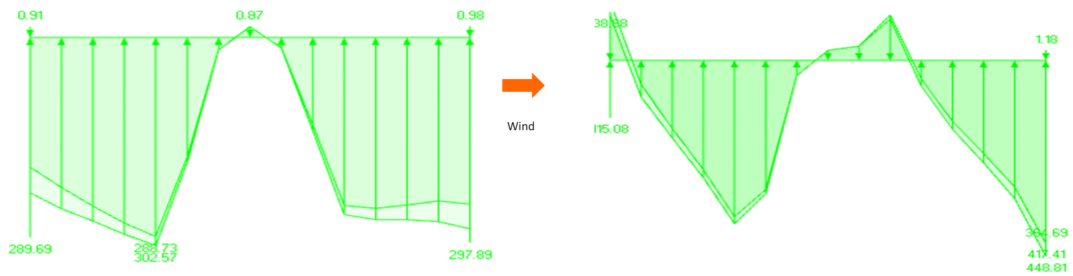

Figure 14.1: Line support, without wind load C04 and with wind load C03.

In the Ultimate Limit State (ULS) that includes wind load, the line support distribution becomes more uneven. Additionally, the ULS with the wind load introduces some tension between the foundation and the core.

14.1.4. Element removal in the fire situation

In the case of the 10-storey building, the construction is able to maintain sufficient capacity to withstand 120 minutes of fire exposure. The building is designed for this exposure by a third party and can be confirmed with the model.

1 element (scenario 1)

Removing one element results in slight rotation of the building. This can be seen in the deformation and in the forces in the bracing perpendicular to the removed diagonal. Due to the presence of the core, the rotation of the construction gets reduced. The maximal global deformation increases with 19.8 %, while with no core presence, the maximal deformation increases with 104 % 13.20.

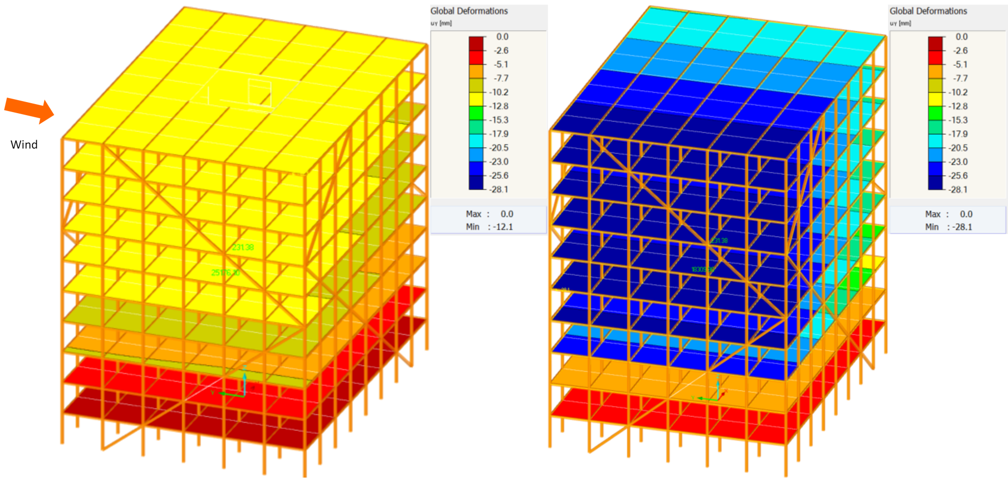

Figure 14.2: Global deformation after element removal, with and without a core.

The increase in unity checks for the first panel is minor compared to the panel at the height where the bracing diagonal was removed. The maximum increase in UC (ALS) for the first panel is 1%, while for the third panel, where the bracing was removed, it is 36%.

At the height of the removed bracing the CLT will take up the lateral force after which the bracing takes it over for the other storeys. The increase in line support shows that a part of the lateral force that normally goes to bracing gets rerouted to the core. The forces that occur in this situation, do not exceed the capacity of the elements.

The connections between the panels will experience an increase in forces due to the missing element in the bracing. This force increase is also greater than the force it experiences during the ULS. This force increase in the floor connection needs to be designed for to make the second load path work.

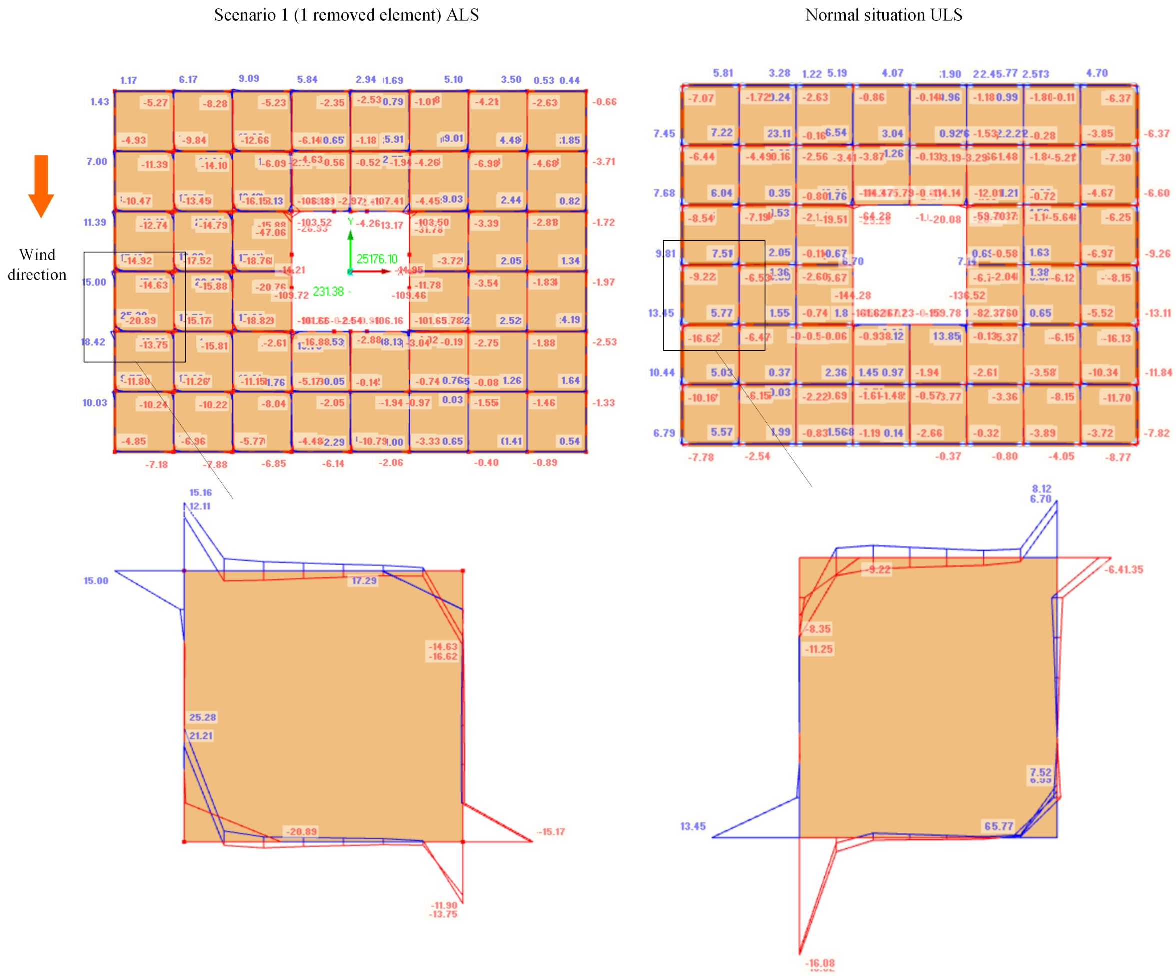

Figure 14.3: Line connections 4^{th} floor Normal ULS situation (right) and 1 element removed situation (right) v_y

2 elements (scenario 2)

With two elements removed, on on each side one, the core is necessary for the lateral stability. The global deflection of the building after removal of the diagonals, is now increased by 34 %. However, the deflection is now equally distributed over the building instead of being rotated. This is also noticeable to the bracings perpendicular to the removed bracings. The core is still capable to take up the extra load after removal of two elements in the ALS. With the Unity checks in panel 1 increasing with a maximum of 5 % and in panel 3 a increase of 55%. For a one or two element(s) removal, the core is able to take up the extra load in the Accidental limit state. The structure demonstrates a high level of robustness with minor increases in internal forces for the core CLT panels.

Influence of the stiffness

When the stiffness of the core decreases, the core takes on less load. The lines representing each removal scenario in the graph of connection stiffness versus release forces are parallel, indicating consistent behavior across scenarios, even though they start from different release forces. The lines exhibit a steady trend.

No core (scenario 3)

The results of the internal forces and the line support of the CLT core indicate that the timber core takes up some of the horizontal forces. However, the results from the no-core test show that the timber building, even without a core, is still capable of withstanding horizontal wind loads in the event of an element removal. Although slightly more deflection is observed, which may be perceived as less safe, it does not violate ALS requirements. The bracing on the opposite side of the removed bracing gets an increase in axial forces of 100%. The connections at the level of the third floor also get an increase in forces. These connections need to be designed for this kind of forces, otherwise the structure would fail at the connections.

Whole bracings façade('s)

From the results with one complete façade removed, the building acted the same as for the one element removed scenario but with more global deflection and more expressed force on the core panels. The global deformation was 33.3 mm which is 200 % more than the deflection in the normal fire situation, and 175 % more than the case with only one element removed. The CLT in the lower panel has a maximum increase in unity check of 16 %. The core is still able to maintain its capacity. Although there needs to be taken a look at the peak forces for the $int(\sigma_{t/c.90} + \tau_{y'z'})$. The case where no core is available, the global deflection is 490 % more than the normal fire situation. Which is 144% more than the case of a core with a bracing removed in one façade.

For the the removal of 2 bracings façades the deflection increases to 45.9 mm, which is a 354% increase from the normal fire situation. Looking at the CLT unity checks the CLT will exceed its capacity for $\sigma_{t/c,90}$, $\sigma_{b+t/c,90}$ and $int(\sigma_{t/c.90} + \tau_{y'z'})$.

Core connections

As the forces in the CLT's core increases with the removal of bracing elements, so does the forces in the line hinges. From the bar plot 14.4, it can be seen that the forces increases in the CLT connections when more bracing elements are removed. However, it will not exceed the remaining capacities of the connections.

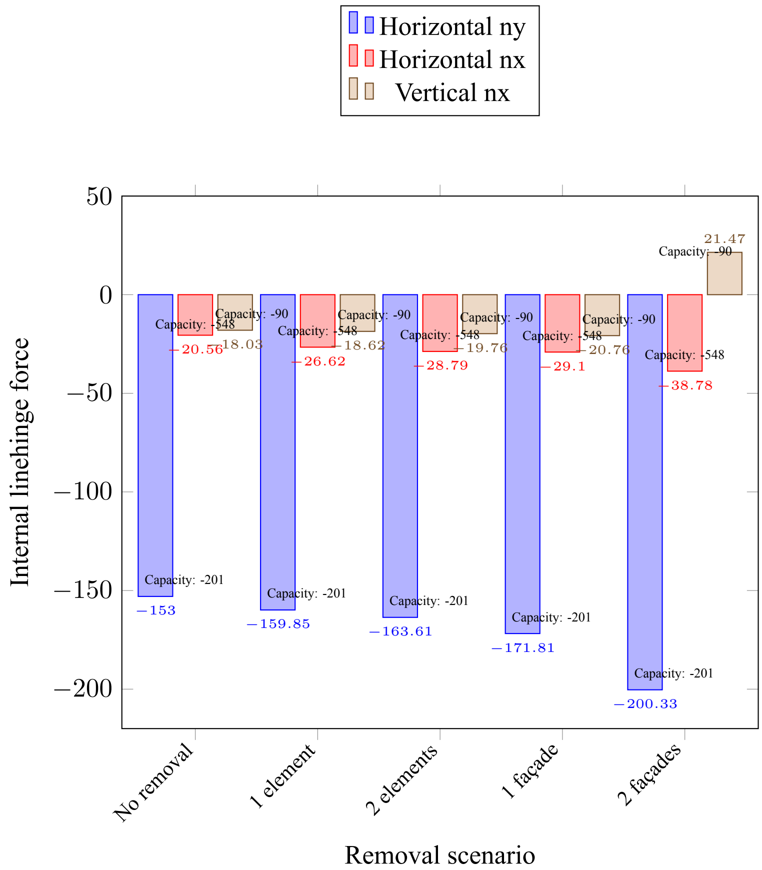

Figure 14.4: Forces in CLT connections, from the removal scenarios (ALS)

15 Conclusion and Recommendations

The aim of this report is to gain insights into the contribution of a CLT core to a stability system, with the main focus on the utilization of the core as a secondary load path.

15.1. Conclusion

Timber is gaining popularity as a construction material, but its use presents new challenges. One significant challenge is the stability of its design, a topic that has been extensively discussed in previous research. The soon-to-be-realized Urban Woods project plans to use a CLT core combined with diagonal bracings in the façade as a stability system. The effectiveness of the CLT core in contributing to the stability design is uncertain. This report aims to provide further insights through the use of a finite element model (FEM).

The FEM model incorporates detailed insights of timber connections and material properties. Additionally, aspects such as stability systems and fire safety considerations are incorporated to address the following sub-question:

What percentage of the lateral force can the core take?

The model with a timber core in the Urban Woods shows an 18% reduction in global deflection compared to the model without a timber core. Additionally to the deflection reduction, the forces in the bracing are reduced by 33% in the model with a timber core. The core parameters that influence these reductions are the connections between the core panels and the cut-outs in the timber core. A core parameter study has been carried out to answer the following question:

How do the core parameters influence the global deflection?

Within the model, various parameters can be altered to evaluate their impact on the building and core design. From these tests, relationships can be derived that illustrate the contribution of the timber core to the stability of a 10-story timber building.

- **Connection stiffness**. The connection stiffness has a considerable amount of influence on the stability of the timber core. In particular the stiffness of the horizontal connections. The relation will stagnate when the stiffness of the connection increases. The connection stiffness can be increased when more dowels or shear plates are added to the connection.
- **Panel length**. Using longer CLT panels in the core reduces the number of connections needed. This increases the stiffness of the core, thereby enhancing its contribution to the overall stability of the structure.
- **Cut-out**. For the use of the core, a cut-out is necessary for the utilization of the inner core space. The cut-out will make the core less stiff. The contribution a CLT core will give to the global deflection is linearly decreasing, as the percentage of the cut-out increases. As the percentage of the cut-out increases, the Unity Check value also rises rapidly.
- **Plot size**. The contribution of the core to the stability is decreasing when the grid layout is increasing in size, with the core dimensions staying the same.

- **Height of the building**. For a building with fewer floors, using a CLT (Cross-Laminated Timber) core is more suitable. As the height increases, deflection and acceleration rise rapidly. Therefore, an additional stability system is required for buildings with five or more floors, as the core's contribution to overall stability diminishes.

Regarding the main question:

Can a timber core sustain lateral load as a secondary load path, in case of failure of the stability bracing?

In a fire scenario, a 10-story timber building with bracing elements and a timber core is tested in the Accidental Limit State (ALS). When bracing elements are removed in this situation, the core is capable of withstanding the additional load. The implications for each removal scenario are as follows:

- **1 element removed** The building experiences a slight rotation, and the bracing perpendicular to the removed element takes on additional internal forces. The CLT in the core at the height of the removed bracing experiences a significantly greater increase in stress compared to other areas of the core. When no CLT core is applied, the building is still able to withstand the extra load. However some extra attention needs to be given to the connection with the floor and the bracing.
- **2 elements removed** When two diagonal bracings are removed (one from each side), deflection increases compared to the single removal scenario, but the building does not rotate.
- **1 whole side bracing removed** The building behaves similarly to the single element removal scenario but with more excessive forces.
- **2 whole sides bracing removed** In this scenario, some of the unity checks in the core's CLT will not suffice anymore. The connections are also reaching its limits but are not exceeding.

Reducing the stiffness in the panel-to-panel connections will reduce the force exhibited in the horizontal line connections. In the event of a fire that results in the removal of an element, the beams do not need to withstand loads for which they were not designed. Specifically, when one element is removed, the bracing perpendicular to the affected bracing will experience an increase of 30.15 kN (from -27.45 kN to -57.6 kN). With a reduced cross-section of 218x218 mm, the Unity Check (UC) will increase from 0.05 to 0.10. This value remains within the acceptable range and is not greater than the maximum UC that a beam experiences in that specific situation. The columns unity checks remain almost the same after a removal of a diagonal. With the columns UC's reaching the value of 1.

15.2. Recommendations

For the structural engineer, using a CLT (Cross-Laminated Timber) core alone in high-rise buildings will not suffice for the stability system. However, a CLT core can still contribute to the overall stability depending on factors such as the stiffness of the CLT-to-CLT connections, the number of cut-outs, and the building's height and width. Additionally, a CLT core enhances the building's robustness by providing a secondary load path for lateral loads in the event of the removal of a bracing element. Therefore it would be recommended to utilise a timber core as a second stability system next to a bracing stability system.

15.3. Recommendations for further research

Another potential alternative for a secondary load path is through the connections between the columns and beams. If these connections are sufficiently stiff, the glulam frame can absorb lateral forces. For the model, it is assumed that the beam-to-column connection is hinged. However, in reality, some stiffness is present in the connections due to their design. In a paper by Maria Felicita [17], a glulam frame with a four-meter span and four different rotational stiffness's is modeled. Depending on the cross sections of the timber elements, buildings can achieve heights ranging from 30 to 130 meters. If the timber frame can withstand Ultimate Limit State (ULS) and Serviceability Limit State (SLS) conditions, it can likely also serve as a secondary load path for the Accidental Limit State (ALS).

For the model, assumptions are made regarding the material properties. These assumptions could be further investigated for implementation into FEM software.

Viscoelastic behaviour

Timber exhibits time-dependent behavior, displaying both elastic and viscous properties. This viscoelastic behavior, which varies over time, can be challenging to model. One specific aspect of timber's viscoelastic behavior is known as creep, where deformation increases under a constant load. To account for creep behavior, it is incorporated as a coefficient in the k_{def} value [55].

Concrete cellar

One case-specific implication is the presence of a concrete cellar. The weight of this cellar ensures that no tension occurs at the foundation. Although the concrete cellar is not included in the model, it is assumed to contribute 50% to the overall lateral deflection. Consequently, the timber construction is also assumed to contribute the remaining 50%. For the SLS, this results in a maximum global deformation given by:

$$L = \frac{H}{1000} \tag{15.1}$$

Modeling of the core

Another case-specific implication involves the modeling of the core. For generalization purposes, the core is represented as a square. In reality, the actual core contains more material but is of a smaller size, resulting in a moment of inertia that is 15% smaller around the x-axis and 61% smaller around the y-axis.

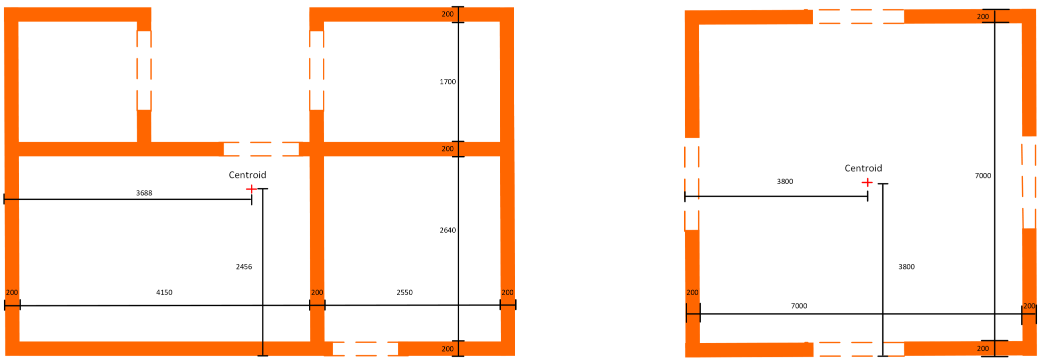

Figure 15.1: Core Urban Woods vs Core RFEM model

Diaphragms action

As been described in chapter 4, some semi-rigid diaphragms action can be expected for the CLT timber floor. The behaviour of the CLT floor depends on the panel-to-panel connections, the amount of floor panels, the relative stiffness of the CLT in the floor to the stiffness of the CLT in the core. In the model it can be seen that the floor is able to transfer the lateral load to the core. However, the connections between the panels are modeled with free rotational release and a free translational release in the x direction, while the translational release in the y and z directions is rigid. The details of the connections to achieve diaphragm action in the floor have not been explored in depth for this thesis.

FEM

The Finite Element Method (FEM) program utilized in this study requires careful consideration. Timber can be a challenging material to model in a finite element program because of its heterogeneity and complexity. Some of the results generated by the model were not directly comparable with hand calculations. Specifically, the interaction between the line hinge and the cut-out produced unexpected results.

This underscores the importance for engineers to exercise caution and not place complete reliance on FEM programs or similar software. Verification through alternative methods, such as hand calculations or additional simulations, is essential to ensure the accuracy and reliability of the outcomes.

References

[1] R. Abrahamsen. “Mjøstårnet - Construction of an 81 m tall timber building”. In: *Internationales Holzbou-Farum* (2017).

[2] Nederlandse technische afspraak. *NTA 4614-3*. 2012.

[3] Sepideh Ashtari. “In-plane Stiffness of Cross-laminated Timber Floors”. In: *The University of British Columbia* (2012).

[4] I. Baltakys. *Berekening Houtconstructie*. Tech. rep. CLT-S, 2021.

[5] D. Barber. “Determination of fire resistance ratings for glulam connectors within US high rise timber buildings”. In: *Fire Safety Journal* (2017).

[6] J.A.J. Huber M. Ekevad U.A. Girhammar S. Berg. “Structural robustness and timber buildings - a review”. In: *Wood Material Science and Engineering* (2018).

[7] M. Audebert M. Taazount A. Bouchair. “Numerical investigations on the thermo-mechanical behavior of steel-to-timber joints exposed to fire”. In: *Engineering Structures* (2011).

[8] Justin R. Brown et al. “Experimental Testing of a Low-Damage Post-Tensioned C-Shaped CLT Core-Wall”. In: *Journal of Structural Engineering* 147.3 (2021), p. 04020357. DOI: `10.1061/(ASCE)ST.1943-541X.0002926`.

[9] J.V. Conlledo. “A computational study on the application of efficient dual structural systems for achieving desirable comfort levels in timber high-rise structures”. In: (2022).

[10] *Cube House*. 2023. URL: `https://www.wiehag.com/en/references/cube-house-amsterdam/` (visited on 09/21/2023).

[11] H. Begrec D. Erdogan. “Tall Timber Architecture: An Opportunity for Green Building as Mjøstårnet”. In: *International Symposium of Architecture* (2021).

[12] D.Boggs. “Acceleration index for human comfort in tall buildings- Peak or RMS?” In: *CTBUH Monograph Chpt. 13: Motion Perception Tolerance and Mitigation* (1997).

[13] *Different types of sawing patterns*.

[14] G.J.P. Ravenshorst E.D. de Munck and A.J.M. Jorissen. *HTO Dictaat Houtconstructies*. Tech. rep. TU Delft, Centrum Hout and TU Eindhoven, 2011.

[15] T. Ehrhart et al. “Rolling Shear Properties of Some European Timber Species with Focus on Cross Laminated Timber”. In: *Inter Proceedings ETH zurich* (2015).

[16] J. Vessby & B. Enquist. “Experimental study of cross-laminated timber wall panels”. In: *European Journal of Wood and Wood Products* (2009).

[17] M. Felicita. “Timber High-Rise Buildings Parametric study of the influence of preliminary design parameters on the wind-induced dynamic response of timber high-rise buildings”. In: (2021).

[18] G. D’Arenzo D. Casagrande A.Polastri M. Fossetti M. Fragiacomo and W. Seim. “CLT Shear Walls Anchored with Shear-Tension Angle Brackets: Experimental Tests and Finite-Element Modeling”. In: *J. Struct. Eng* (2021).

[19] E.F. Hansson. “Analysis of structural failures in timber structures: Typical causes for failure and failure modes”. In: *Engineering Structures* (2011).

[20] *HAUT Amsterdam Residential Building / Team V Architecture*. 2023. URL: `https://www.archdaily.com/989552/haut-amsterdam-residential-building-team-v-architecture` (visited on 09/21/2023).

[21] John Hill. “Tamedia’s Timber Structure”. In: *world architects* (2014).

[22] M. Yurrita J.M. Cabrero B. Iraola. *Failure of timber constructions*. The University of Queensland and Chalmers University of Technology, 2021.

[23] F.F. Janssens. “Influence of a timber outrigger system on cross laminated timber core buildings”. In: *TU-Delft* (2023).

[24] A. Frangi M. Fontana E. Hugi R. Jobstl. “Experimental analysis of cross-laminated timber panels in fire”. In: *Fire Safety Journal 44* (2009).

[25] A. Jorissen. “Double Shear Timber Connections with Dowel Type Fasteners”. PhD thesis. TU Delft, 1998.

[26] M.A. Bjertnaes K.A. Malo. R.B. Abrahamsen. “Some structural desing issues of the 14-storey timber framed building ”Treet” in Norway”. In: *European Journal for Wood Production* (2016).

[27] M. Waller-Novak M. Augustin J. Koppelhuber and K. Pock. “Cross-Laminated Timber Structural Design Volume 2”. In: *pro Holz* (2018).

[28] D. van Loon. *Hoofdberekening, TO-fase Torenlocatie Delft, The Urban Woods Delft*. Tech. rep. Arcadis, 2023.

[29] T. Schauerte M. Johanssen. “Nine storey residential timber construction and the wood building strategy of Växjö municipality”. In: *Internationales Holzbau-Forum IHF* (2015).

[30] K. Flanagan M. Ramage. R. Foster. and R. Bakker. “Super Tall Timber: design research for the next generation of natural structure”. In: *The Journal of Architecture* (2017).

[31] H. Choi G. Ho L. Joseph N. Mathias. *Outrigger Design for High-Rise Buildings, 2nd Edition*. Tech. rep. Council on Tall Buildings and Urban Habitat, 2017.

[32] Mike Mellaard. “Stiffness Moddeling of Large Timber Connections in Stability Trusses”. In: (2023).

[33] J.R. Brown M. Li T. Tannert D. Moroder. “Experimental study on orthogonal joints in cross-laminated timber with self-tapping screws installed with mixed angles”. In: *Engineering Structures* (2020).

[34] R. Nijsse. “High rise buildings structural aspects”. In: 2021.

[35] Nederlandse norm. *NEN-EN 14080*. Tech. rep. Nederlandse Norm, 2013.

[36] Nederlandse norm. *NEN-EN 16351:2011*. Tech. rep. Nederlandse Norm, 2011.

[37] Nederlandse norm. *NEN-EN 16351:2021*. Tech. rep. Nederlandse Norm, 2021.

[38] Nederlandse norm. *NEN-EN 1990+A1+A1/C2*. Tech. rep. Nederlandse Norm, 2019.

[39] Nederlandse norm. *NEN-EN 1991-1-1-draft*. Tech. rep. Nederlandse Norm, 2023.

[40] Nederlandse norm. *NEN-EN 1991-1-4*. Tech. rep. Nederlandse Norm, 2011.

[41] Nederlandse norm. *NEN-EN 1995-1-1+C1+A1*. Tech. rep. Nederlandse Norm, 2011.

[42] Nederlandse norm. *NEN-EN 1995-1-2*. Tech. rep. Nederlandse Norm, 2023.

[43] Nederlandse norm. *NEN-EN 1995-2*. Tech. rep. Nederlandse Norm, 2023.

[44] Nederlandse norm. *NEN-EN 383:2007*. Tech. rep. Nederlandse Norm, 2007.

[45] NOS. “Kabinet komt met nationaal bouwplan, vanaf 2024 100.000 woningen extra”. In: (2022).

[46] G. Fink P. Palma. *Design for robustness, adaptability disassembly and reuse, and repairabiity of taller timber buildings: a state of the art report*. Tech. rep. COST European cooperation in science & technology, 2022.

[47] A.S. Cao A. Frangi P. Palma. “Column removal analyses of timber structures - Framework to assess dynamic amplification factors for simplified structural design methods”. In: *World Conference On Timber Engineering* (2021).

[48] T. Quoc Phong. “Analysis and optimization of the bearing capacity of connecting wooden structures with application of dowel type self-drilling”. In: *Material Science and Engineering* (2020).

[49] United Nations Environment Programme. *2022 Global status report for buildings and construction*. Tech. rep. United Nations, 2022.

[50] A. Sivenkov R. Aseeva B. Serkov. “Fire Behavior and Fire Protection in Timber Buildings”. In: *Springer Series in Wood Science* (2014).

[51] V. Enjily R.Grantham. “Multi-storey timber frame buildings, a design guide”. In: *BRE Centre for Timber Technology and Construction* (2014).

[52] R.M. Foster M.H. Ramage T. Reynolds. “Rethinking CTBUH Height Criteria In the Context of Tall Timber”. In: *CTBUH Special Report* (2017).

[53] V. Salvadori. “Multi-Storey Timber-Based Buildings: An international Survey of Case-Studies with Five or More Storeys Over the last Twenty Years”. In: *Technische Universitat Wien* (2021).

[54] Vittorio Salvadori. “The Development of a Tall Wood Building”. In: *TU Wien* (2017).

[55] H.J. Blaß C. Sandhaas. *Timber Engineering Principles for Design*. KIT Scientific Publishing, 2017.

[56] A. Ringhofer R. Brandner G. Schickhofer. “Withdrawal resistance of self-tapping screws in unidirectional and orthogonal layered timber products”. In: *Materials and Structures* (2013).

[57] G. Flatscher K. Bratulic G. Schickhofer. “Screwed joints in cross-laminated timber structers”. In: *Quebec: World conference of timber engineering* (2014).

[58] R. Brandner T. Bogensperger G. Schikhoffer. “In plane Shear Strength of Cross Laminated Timber Test Configuration, Quantification and influencing Parameters”. In: *Institute of Timber Engineering and Wood Technology* (2013).

[59] M. Popovski I. Gavric J. Schneider. “Performance of two-storey CLT house subjected to lateral laods”. In: *World Conference on Timber Engineering* (2014).

[60] Marco Schuurman. *Building structures 2, Details in concrete (1)*. TU Delft, 2021.

[61] H. Mpidi Bita. & J. Huber. P. Palma. & T. Tannert. “Prevention of Disproportionate Collapse for Multistory Mass Timber Buildings: Review of Current Practices and Recent Research”. In: *American Society of Ciil Engineers* (2022).

[62] *The Urban Woods https://www.theurbanwoods.com/nl/zo-werkt-het/*.

[63] R. Brandner G. Flatscher A. Ringhofer G. Schickhofer A. Tiel. “Cross laminated timber (CLT): overview and develpment”. In: *European Journal of Wood and Wood Productions* (2016).

[64] K.A. Malo H. Stamtopoulos F.M. Massaro S. Tulebekova. “Servicability stiffness of timber connections with dowels and slotted-in steel plates”. In: *World conference on Timber Engineering Oslo* (2023).

[65] J. Konnerth A. Valla W. Gindl U.Mu¨ller. “Measurment of strain distribution in timber finger joints”. In: *Wood Sci Technol* (2006).

[66] *Urban Woods Delft*. 2023. URL: `https://www.theurbanwoods.com` (visited on 09/21/2023).

[67] J. Ehlbeck H. Werner. “Untersuchungen über die Tragfähigkeit von Stabdübelverbindungen”. In: *Holz als Roh- und Werkstoff 46 281-288* (1988).

[68] *Wonen in SAWA*. 2023. URL: `https://woneninsawa.nl/` (visited on 09/21/2023).

[69] T. Tannert X. Zhang M. Popovski. “Experimental Test on Novel Seismic Hold-Downs for Timber Structures”. In: *16th World Conference on Earthquake, 16WCEE* (2017).

[70] T. Znabei. “A Post-tensioned Cross-Laminated Timber core for buildings”. In: *TU-Delft* (2020).

A

Material

A.1. Material used

The following tables shows the materials that were used in the calculations for the case study.
The glulam used for the beams and the columns in the model.

GL24h		unit
minimum bulk density	350	kg/m^3
mean bulk desity	420	kg/m^3
$E_{0,mean}$	11600	N/mm^2
$E_{0,0,05}$	9667	N/mm^2
$E_{90,mean}$	390	N/mm^2
$E_{90,0,05}$	325	N/mm^2
$f_{m,k}$	24	N/mm^2
$f_{t,0,k}$	16,5	N/mm^2
$f_{t,90,k}$	0,5	N/mm^2
$f_{c,0,k}$	24	N/mm^2
$f_{c,90,k}$	2,7	N/mm^2
$f_{v,k}$	2,5	N/mm^2

Table A.1: Glulam beam GL24h

The timber used for the Lamela's in the CLT.

C24		unit
minimum bulk density	350	kg/m^3
mean bulk desity	420	kg/m^3
$E_{0,mean}$	11000	N/mm^2
$E_{0,0,05}$	7400	N/mm^2
$E_{90,mean}$	370	N/mm^2
$E_{90,0,05}$	690	N/mm^2
$f_{m,k}$	24	N/mm^2
$f_{t,0,k}$	14,5	N/mm^2
$f_{t,90,k}$	0,4	N/mm^2
$f_{c,0,k}$	21	N/mm^2
$f_{c,90,k}$	2,5	N/mm^2
$f_{v,k}$	4	N/mm^2

Table A.2: C24 used for CLT

A.2. Material tests

In the model, the Laminate Add-on module is utilized for the core, allowing for the creation and implementation of a Cross-Laminated Timber (CLT) panel. This module provides the capability to modify each layer's parameters, including material, orthotropic direction (grain direction), modulus of elasticity, shear modulus, and Poisson's ratio. In Table A.3, various materials and laminate layups were tested using the same cross-section.

The results indicate that all laminate layups exhibit greater deflection compared to regular Polar and Softwood C24. Among the laminates, the layup with alternating orthotropic directions demonstrates the lowest deflection. This reduced deflection is attributed to the fact that lateral forces must be transferred diagonally to the ground, necessitating stiffness in both orthogonal directions.

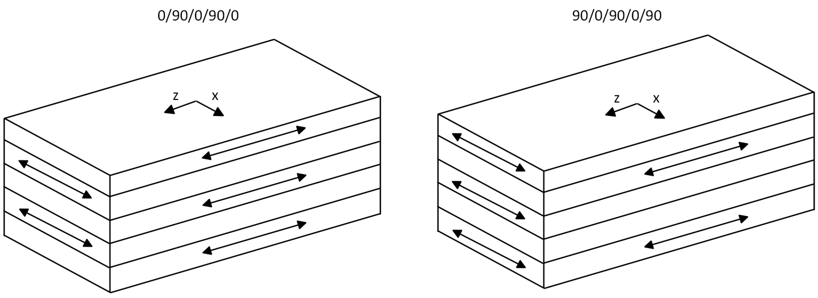

Figure A.1: Lay-up CLT with different directions.

The table highlights the importance of considering both material properties and orthotropic direction in the design of CLT panels for optimizing structural performance under lateral loads. The alternating orthotropic direction scheme proves to be most effective in minimizing deflection, suggesting that strategic orientation of layers can enhance the stiffness and overall stability of the structure.

Material	Deflection LC2
Polar and Softwood timber C24	113.7 mm
Softwood C24 0/90/0/90/0	168.9 mm
Softwood C24 90/0/90/0/90	168.3 mm
Softwood C24 0/0/0/0/0	462.4 mm
Softwood C24 90/90/90/90/90	335.1 mm

Table A.3: Deflection 10 storey core with different materials and orthotropic directions.

The difference in design capacity for the different panel layouts is shown in Table A.4. The thickness of the panels are 40 mm each resulting in a overall thickness of the CLT of 200 mm. The table shows that the 0/90/0/90/0 lay-up has overall the lowest unity checks of the altering schemes. Only the $\sigma_{b,0}$, $\tau_{y'z'}$, $\tau_{x'y'}$ and the $int(\tau_{x'z'} + \tau_{x'y'})$ has a higher UC value for the alterning orthotropic direction scheme. The lay-up with only a 90 degrees orthotropic directions will not suffice since some of the UC's are above 1.

Failure mechanism	0/90/0/90/0	90/0/90/0/90	0/0/0/0/0	90/90/90/90/90
$\sigma_{b,0}$	0.04	0.02	0.00	0.02
$\sigma_{b,90}$	0.00	0.00	0.00	0.00
$\sigma_{t/c,0}$	0.43	0.43	0.25	0.27
$\sigma_{t/c,90}$	0.42	0.50	0.68	2.82
$\sigma_{b+t/c,0}$	0.43	0.43	0.25	0.27
$\sigma_{b+t/c,90}$	0.42	0.50	0.68	2.83
$\tau_{y'z'}$	0.32	0.21	0.13	0.06
$\tau_{x'z'}$	0.10	0.11	0.05	0.22
$\tau_{x'y'}$	0.58	0.56	0.51	0.66
$int(\tau_{x'z'} + \tau_{x'y'})$	0.34	0.32	0.26	0.41
$int(\sigma_{t/c,90} + \tau_{y'z'})$	0.42	0.50	0.74	2.85

Table A.4: Unity check CLT panels different orthotropic direction lay-outs.

B
Formulas

This chapter shows the formulas used for: wind loads, wind acceleration, connection stiffness and connection strength.

B.1. Wind load

The peak velocity pressure can be calculated using Eurocode NEN-EN 1991-1-4. If the factor for terrain orography c_o is equal to 1, the national Annex provides a table for the peak velocity pressure at a certain height for rural, urban and the coast.

For the different zones in figure 10.8 the $c_{pe,1}$ and $c_{pe,10}$ are specified in B.1, following table NB.6-7.1 from the dutch national Annex [40].

Zone	A		B		C		D		E	
h/d	cpe,10	cpe,1	cpe,10	cpe,1	cpe,10	cpe,1	cpe,10	cpe,1	cpe,10	cpe,1
5	-1,2	-1,4	-0,8	-1,1	-0,5		+0,8	+1,0	-0,7	
<=1	-1,2	-1,4	-0,8	-1,1	-0,5		+0,8	+1,0	-0,5	

Table B.1: Wind coefficients for vertical façades with square plot

B.2. Wind acceleration

$$\sigma_{\mathrm{a;x}}(y,z) = c_{\mathrm{f}} \cdot \rho \cdot l_{\mathrm{v}}(z_{\mathrm{s}}) \cdot v_{\mathrm{m}}^2(z_{\mathrm{s}}) \cdot R \cdot \frac{K_{\mathrm{y}} \cdot K_{\mathrm{z}}}{\mu_{\mathrm{ref}}} \cdot \frac{\phi(y,z)}{\phi_{\mathrm{max}}} \tag{B.1}$$

Where:

$\sigma_{\mathrm{a;x}}(y,z)$ is the standard deviation of the characteristic acceleration of a construction point with the coordinates (y,z).
c_{f} is the force coefficient.
ρ is the air density NEN-EN 1994-1-4 .
$l_{\mathrm{v}}(z_{\mathrm{s}})$ is the turbulence intensity at height z_{s}.
$v_{\mathrm{m}}^2(z_{\mathrm{s}})$ is the average wind speed at height z_{s}.
R is the resonant response factor.
K_{y} is the comfort constant by the horizontal y-axis
K_{z} is the comfort constant by the vertical x-axis
μ_{ref} is the mass off the building per unit area.
$\phi(y,z)$ is the vibration.
ϕ_{max} is the value for the vibration shape at the point of maximum amplitude.

The peak acceleration is as follows:

$$\hat{a} = k_p \cdot \sigma_a \tag{B.2}$$

Where:

$\hat{a}$ is the acceleration
k_p is the dimensionless peak factor
σ_a is the standard deviation of the characteristic along wind acceleration

B.3. Wind induced vibrations

The natural frequency can be taken from the RFEM model. The following are from the Urban Woods in the normal situation.

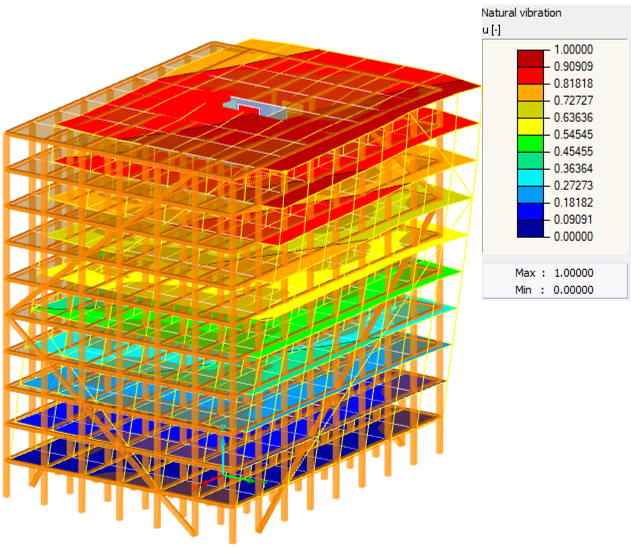

Figure B.1: Natural frequencies, model Urban Woods

Mode No.	Natural frequency f [Hz]	Along wind acceleration m/s^2
1	0.714	0.079
2	0.774	0.077

Figure B.2 shows the along-wind acceleration corresponding to the first mode natural frequency. The results indicate that the limit set by ISO 10137 is reached, whereas the values remain within the permissible limit according to NEN standards.

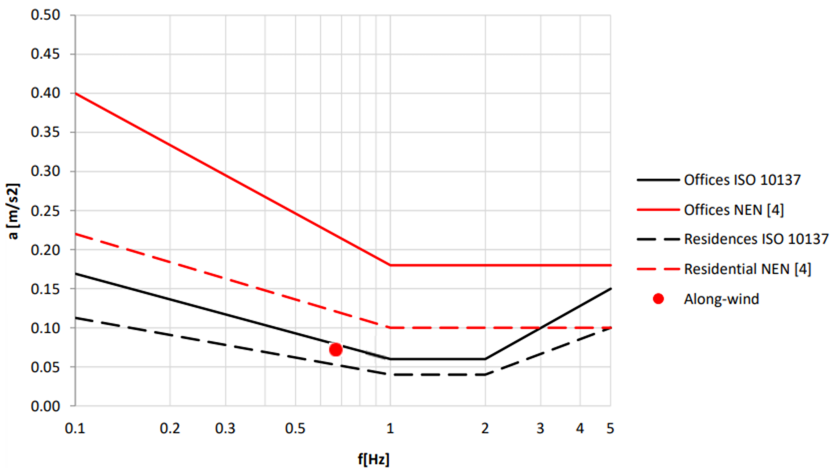

Figure B.2: Evaluation curves for wind-induced vibrations, ISO 10137 and NEN

The results from the Finite element model of the structure with no core are as follows.

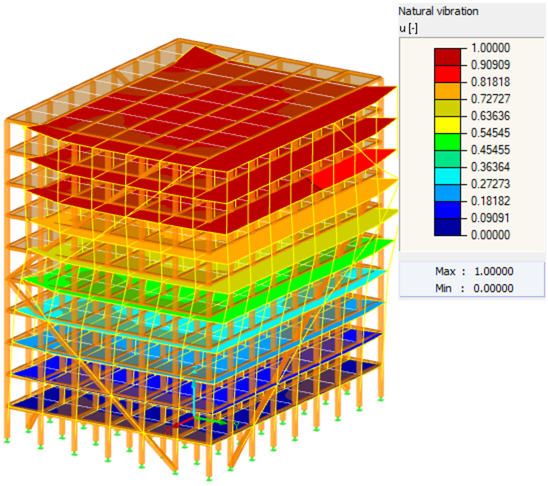

Figure B.3: Natural frequencies, model Urban Woods (no core)

Mode No.	Natural frequency f [Hz]	Along wind acceleration m/s^2
1	0.697	0.079
2	0.778	0.077

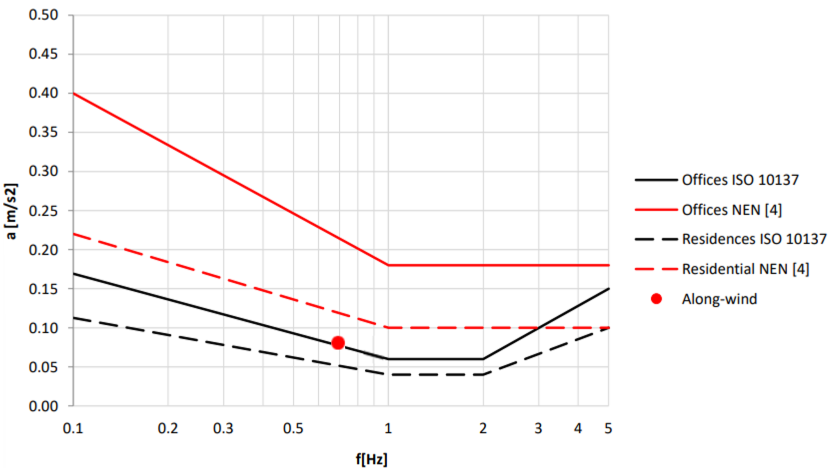

Figure B.4: Evaluation curves for wind-induced vibrations, ISO 10137 and NEN (no core)

B.4. Dowel connection

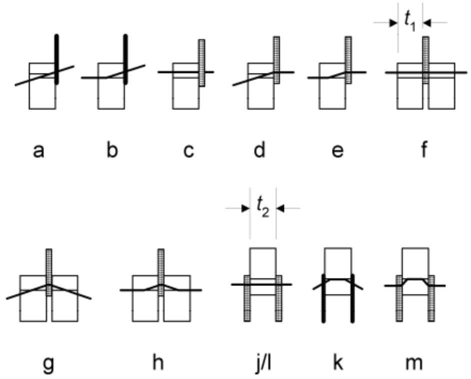

Figure B.5: Types of failures dowel connection

The capacity of the dowels depends on the normative failure mechanism (Figure B.5). For the steel connection with an singular connection equation: B.3 is used for the characteristic strength.

$$F_{v,RK} = min \begin{cases} 0,4 \cdot f_{h,k} t_1 d & (a) \\ 1,15\sqrt{2M_{y,Rk} \cdot f_{h,k} \cdot d} + \frac{F_{ax,Rk}}{4} & (b) \\ f_{h,k} \cdot t_1 \cdot d & (c) \\ f_{h,k} \cdot t_1 \cdot d \left[\sqrt{2 + \frac{4M_{y,Rk}}{f_{h,k} \cdot dt_1^2}} - 1\right] + \frac{F_{ax,Rk}}{4} & (d) \\ 2,3\sqrt{M_{y,Rk} \cdot f_{h,k} \cdot d} + \frac{F_{ax,Rk}}{4} & (e) \\ f_{h,1,k} \cdot t_1 \cdot d & (f) \\ f_{h,1,k} \cdot t_1 \cdot d \left[\sqrt{2 + \frac{4M_{y,Rk}}{f_{h,1,k} \cdot dt_1^2}} - 1\right] + \frac{F_{ax,Rk}}{4} & (g) \\ 2,3\sqrt{M_{y,Rk} \cdot f_{h,1,k} \cdot d} + \frac{F_{ax,Rk}}{4} & (h) \end{cases} \tag{B.3}$$

For a dual connection with thin steel plates on the side, the characteristic strength is as follows:

$$F_{v,RK} = min \begin{cases} 0,5 \cdot f_{h,2,k} \cdot t_2 \cdot d \\ 1,15\sqrt{2 \cdot M_{y,Rk} \cdot f_{h,2,k} \cdot d} + \frac{F_{ax,Rk}}{4} \end{cases} \tag{B.4}$$

And for a dual connection with thick steel plates on the side, the characteristic strength is as follows:

$$F_{v,RK} = min \begin{cases} 0,5 \cdot f_{h,2,k} \cdot t_2 \cdot d \\ 2,3\sqrt{M_{y,Rk} \cdot f_{h,2,k} \cdot d} + \frac{F_{ax,Rk}}{4} \end{cases} \tag{B.5}$$

With:

$F_{v,Rk}$ is the characteristic strength per shear plane.
f_h, k is the characteristic strength.
t_1 is the smallest value of the timber thickness (see Figure B.5).
t_2 is the smallest value of the timber thickness(see Figure B.5).
d is the diameter of the fastener
$M_{y,Rk}$ is the characteristic yield moment.

With connections with multiple slotted in steel plates, the connection consist out of the different failure modes which are described in figure 6.8. These failure modes are in different combinations. For the section between two steel plates only failure mechanism l and m are possible. In figure B.6 the different combinations of failure modes are presented. Eurocode prescribes in clause 8.1.3, that for a connection with multiple shear planes the failure mechanism needs to be compatible with each other to combine the resistance. They can not exist of out of a combination of failure mechanism (a), (b), (g) and (h) or (c), (f) and (j/l) of figure 6.8.

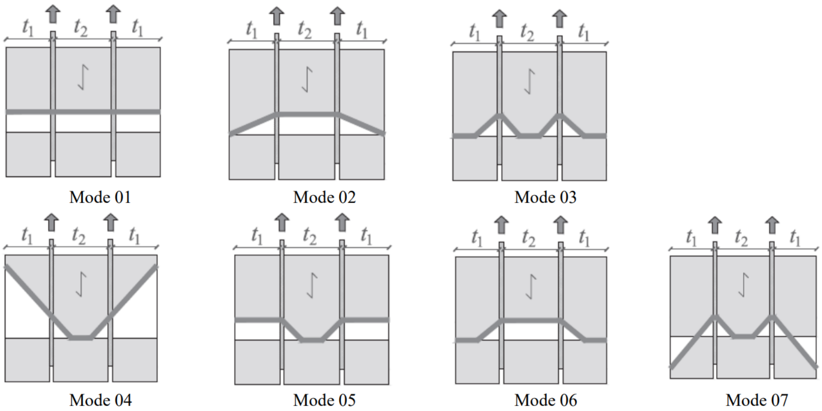

Figure B.6: Combination failure modes two steel plates [48]

For these different Modes Pedersen proposed a method to determine the load capacity for ductile failure F_D.

$$F_D = F_y n_s n_c n_r \tag{B.6}$$

With:

F_y is the load capacity of each shear plane in a single fastener as in B.7 .
n_s is the number of shear planes.

$$F_y = min\begin{cases} \frac{1}{4}(2t_1+t_2)\cdot d\cdot f_{h,0} & (Mode\ 1)\\ (-\frac{1}{2}t_1+\frac{t_2}{4}+\sqrt{\frac{1}{2}t_1^2+\frac{M_y}{d\cdot f_{h,0}}})\cdot d\cdot f_{h,0} & (Mode\ 2)\\ \sqrt{4M_y\cdot d\cdot f_{h,0}} & (Mode\ 3)\\ (\frac{1}{2}t_1+\frac{1}{2}\sqrt{t_1^2+\frac{2M_y}{d\cdot f_{h,0}}})\cdot d\cdot f_{h,0} & (Mode\ 4)\\ (\sqrt{\frac{M_y}{d\cdot f_{h,0}}}+\frac{1}{2}t_1)\cdot d\cdot f_{h,0} & (Mode\ 5)\\ (\sqrt{\frac{M_y}{d\cdot f_{h,0}}}+\frac{1}{4}t_2)\cdot d\cdot f_{h,0} & (Mode\ 6)\\ (-\frac{1}{2}t_1+\frac{1}{2}\sqrt{t_1^2+\frac{2M_y}{d\cdot f_{h,0}}}+\sqrt{\frac{M_y}{d\cdot f_{h,0}}})\cdot d\cdot f_{h,0} & (Mode\ 7) \end{cases} \tag{B.7}$$

B.5. Block shear failure connection

The national annex of the Netherlands states the following about block shear of a steel on timber connection with more than one fastener. The strength of the circumference of the fasteners is considered.

$$F_{bs,Rk} = max\begin{cases} 1,5A_{net,t}f_{t,0,k}\\ 0,7A_{net,v}f_{v,k} \end{cases} \tag{B.8}$$

With:

$A_{net,t}$ is the net intersection perpendicular to the grain.
$A_{net,v}$ is the net shear section parallel to the grain.
$f_{t,0,k}$ is the characteristic tensile strength parallel to the grain.
$f_{v,k}$ is the characteristic shear strength.

With the different failure mechanisms (see figure B.5), the net area is:

$$A_{net,t} = L_{net,t}t_1 \tag{B.9}$$

$$A_{net,v} = \begin{cases} L_{net,v}t_1 & (c,f,j/l,k,m)\\ \frac{L_{net,v}}{2}(L_{net,t}+2t_{ef}) & (a,b,d,e,g,h) \end{cases} \tag{B.10}$$

With:

$L_{net,t}$ is the net width of the intersection perpendicular to the grain.
$L_{net,v}$ is the net length of the shear section at breakage.
t_{eff} is the contributing thickness, which depends on the failure mechanism B.7.

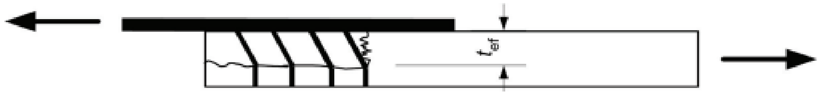

Figure B.7: t_{ef} for disk shear [41]

$$t_{ef} = \begin{cases} 0,4 \cdot t_1 & (a) \\ 1,4\sqrt{\frac{M_{y,Rk}}{f_{h,k} \cdot d}} & (b) \\ 2\sqrt{\frac{M_{y,Rk}}{f_{h,k} \cdot d}} & (e,h) \\ t_1(\sqrt{2 + \frac{M_{y,Rk}}{f_{h,k} \cdot d}} - 1) & (d,g) \end{cases} \tag{B.11}$$

B.6. minimum spacing of the dowels

For the design of the connection, the structural engineer needs to take into account the spacing of the fasteners. The minimum distance of the fasteners depends on the diameter and the angle of the grain. The figure and the table show the minimum distance that the spacing of the dowels needs to be.

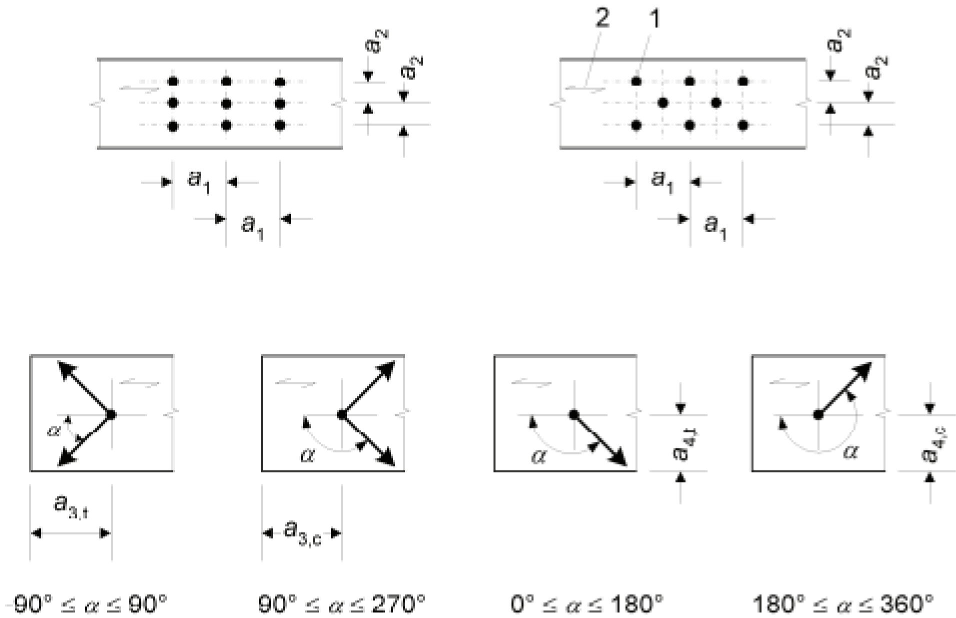

Figure B.8: Distance fasteners [41]

Spacing between/end distance	Angle in degrees	Minimum between/end distance
a_1 (parallel to the grain)	$0 \leq \alpha \leq 360$	$(3 + 2\|cos\alpha\|)d$
a_2 (perpendicular to the grain)	$0 \leq \alpha \leq 360$	$3d$
$a_{3,t}$ (loaded end)	$-90 \leq \alpha \leq 90$	$max(7d; 80mm)$
$a_{3,c}$ (unloaded end)	$90 \leq \alpha \leq 150$ $150 \leq \alpha \leq 210$ $210 \leq \alpha \leq 270$	$max((a_{3,t}\|sin\alpha\|)d; 3d)$ $3d$ $max((a_{3,t}\|sin\alpha\|)d; 3d)$
$a_{4,t}$ (loaded end)	$0 \leq \alpha \leq 180$	$max((2 + 2sin\alpha)d; 3d)$
$a_{4,t}$ (unloaded end)	$180 \leq \alpha \leq 360$	$3d$

B.7. Slip modulus nails and staples

The equation for the slip modulus for nails that are not pre-drilled:

$$K_{ser} = \frac{d^{0.8} \cdot \rho_m^{1.5}}{30} \tag{B.12}$$

And for staples:

$$K_{ser} = \frac{d^{0.8} \cdot \rho_m^{1.5}}{80} \tag{B.13}$$

With:

d is the diameter of the fastener.
ρ_m is the density of the timber member.

B.8. Determination of the stiffness matrix

The following stiffness matrix is based on a CLT panel with the main load-bearing capacity in the x direction [27].

$$\begin{Bmatrix} m_x \\ m_y \\ m_{xy} \\ v_{x,z} \\ v_{y,z} \\ n_x \\ n_y \\ n_{xy} \end{Bmatrix} = \begin{bmatrix} K_x & 0 & 0 & 0 & 0 & 0 & 0 & 0 \\ 0 & K_y & 0 & 0 & 0 & 0 & 0 & 0 \\ 0 & 0 & K_{xy} & 0 & 0 & 0 & 0 & 0 \\ 0 & 0 & 0 & S_x & 0 & 0 & 0 & 0 \\ 0 & 0 & 0 & 0 & S_y & 0 & 0 & 0 \\ 0 & 0 & 0 & 0 & 0 & D_x & 0 & 0 \\ 0 & 0 & 0 & 0 & 0 & 0 & D_y & 0 \\ 0 & 0 & 0 & 0 & 0 & 0 & 0 & D_{xy} \end{bmatrix} \cdot \begin{Bmatrix} \kappa_y \\ \kappa_x \\ \kappa_{xy} \\ \gamma_{xz} \\ \gamma_{yz} \\ \varepsilon_x \\ \varepsilon_y \\ \gamma_{xy} \end{Bmatrix} \tag{B.14}$$

Bending stiffness K_x

$$K_x = EI_0 \tag{B.15}$$

With:

E is the elasticity modulus.
I_0 is the moment of inertial parallel to the grain.

Bending stiffness K_y

$$K_x = EI_{90} \tag{B.16}$$

With:

E is the elasticity modulus.
I_{90} is the moment of inertial perpendicular to the grain.

Torsional stiffness K_{xy}

$$K_{xy} = k_D GI_T = \frac{1}{1 + 6 \cdot \rho_D \left(\frac{d_{max}}{a}\right)^{q_d}} \cdot G_0 \cdot b \cdot \frac{d^3}{12} \tag{B.17}$$

With:

ρ_D and q_d are parameters for torsional stiffness according to a table in ÖNORM B 1995-1-1:2015.
d_{max} is the thickness of the thickest individual layer.
b is the width of the element.
d is the thickness of the whole CLT layer.
a is the mean board width.

Shear stiffness S_x

$$S_x = GA_s = \kappa_0 \cdot \sum G_i \cdot A_i \tag{B.18}$$

With:

κ_0 is the shear correction factor (0.231)
G_i is the shear modulus parallel to the grain
A_i is the area of the CLT panel

Shear stiffness S_y

$$S_y = GA_s = \kappa_{90} \cdot \sum G_i \cdot A_i \tag{B.19}$$

With:

$\kappa_9$0 is the shear correction factor (0.179)
G_i is the shear modulus perpendicular to the grain
A_i is the area of the CLT panel

Extensional stiffness D_x

$$D_x = EA_0 \tag{B.20}$$

With:

E is the elasticity modulus.
A_0 is the area of the panels parallel to the grain.

Extensional stiffness D_y

$$D_y = EA_{90} \tag{B.21}$$

With:

E is the elasticity modulus.
$A_9$0 is the area of the panels perpendicular to the grain.

Shear stiffness in the plate plane D_{xy}

$$D_{xY} = \frac{1}{1 + 6 \cdot \rho_s \left(\frac{d_{max}}{a}\right)^{q_s}} \cdot G_0 \cdot b \cdot d \tag{B.22}$$

With:

ρ_s and q_s are parameters for shear stiffness according to a table in ÖNORM B 1995-1-1:2015.
d_{max} is the thickness of the thickest individual layer.
b is the width of the element.
d is the thickness of the whole CLT layer.
a is the mean board width.

B.9. Load-bearing resistance

Characteristic load-bearing moment $m_{R,x,k}$

$$m_{R,x,k} = W_{0,net} \cdot k_{sys} \cdot f_{m,k} \tag{B.23}$$

With:

$W_{0,net}$ is the moment of resistance in the x direction.
k_{sys} is the coefficient for system strength (1.1).
$f_{m,k}$ is the characteristic bending strength.

Characteristic load-bearing moment $m_{R,y,k}$

$$m_{R,y,k} = W_{90,net} \cdot k_{sys} \cdot f_{m,k} \tag{B.24}$$

With:

$W_{90,net}$ is the moment of resistance in the y direction.
k_{sys} is the coefficient for system strength (1.1).
$f_{m,k}$ is the characteristic bending strength.

Characteristic torsional load-Bearing moment

$$m_{R,T,k} = W_T \cdot f_T \tag{B.25}$$

With:

W_T is the torsional moment resistance.
f_T is the characteristic torsional strength.

Characteristic resistance to lateral force $v_{R,x,k}$

$$v_{R,x,k} = \frac{f_{V,R,k} \cdot I_0 \cdot b}{S_{R,0}} \tag{B.26}$$

With:

$f_{V,R,k}$ is the characteristic shear strength.
I_0 is the moment of inertia in the x direction.
b is the width of the panel.
$S_{R,0}$ is the maximum rolling shear stress in the x direction.

Characteristic resistance to lateral force $v_{R,y,k}$

$$v_{R,y,k} = \frac{f_{V,R,k} \cdot I_{90} \cdot b}{S_{R,90}} \tag{B.27}$$

With:

$f_{V,R,k}$ is the characteristic shear strength.
I_{90} is the moment of inertia in the y direction.
b is the width of the panel.
$S_{R,90}$ is the maximum rolling shear stress in the y direction.

Characteristic axial resistance tension in x and y direction

$$n_{R,x,t,k} = A_{0,net} \cdot f_{t,0,k} n_{R,y,t.k} = A_{90,net} \cdot f_{t,0,k} \tag{B.28}$$

With:

$A_{0,net}$ is the area of the panels parallel to the grain.
$A_{90,net}$ is the area of the panels perpendicular to the grain.
$f_{c,0,k}$ is the characteristic tension strength

Characteristic axial resistance compression in x and y direction

$$n_{R,x,c,k} = A_{0,net} \cdot f_{c,0,k} n_{R,y,c.k} = A_{90,net} \cdot f_{c,0,k} \tag{B.29}$$

With:

$A_{0,net}$ is the area of the panels parallel to the grain.
$A_{90,net}$ is the area of the panels perpendicular to the grain.
$f_{c,0,k}$ is the characteristic compression strength

Characteristic shear resistance in the panel plane

$$n_{R,xy,k} = \begin{cases} f_{V,S,k} \cdot min(A_{0,net}, A_{90,net}) \\ f_{V,T,k} \cdot \frac{min(A_{0,net}, A_{90,net}) \cdot a}{3 \cdot d_{i,max}} \\ f_{V,k} \cdot A_{Gross} \end{cases} \tag{B.30}$$

With:

$f_{V,S,k}$ is the characteristic shear resistance of the individual lamellas.
$f_{V,T,k}$ is the characteristic shear torsional resistance.
$f_{V,k}$ is the characteristic shear resistance.
$A_{0,net}$ is the area of the panels parallel to the grain.
$A_{90,net}$ is the area of the panels perpendicular to the grain.
$d_{i,max}$ is the maximal lamella thickness.

B.10. CLT verification

The simplified method of the calculation of the wall design racking resistance is:

$$F_{v,Rd} = \sum F_{i,v,Rd} \tag{B.31}$$

With:

$F_{i,v,Rd}$ is the design value of the strength in the plane.

$$F_{i,v,Rd} = \frac{F_{t,Rd} b_i c_i}{s} \tag{B.32}$$

With:

$F_{t,Rd}$ is the design value of the strength of a individual connection loaded in shear.
b_i is the width of the wall panel.
s is the fastener spacing.

$$c_i = \begin{cases} 1 \quad for \quad b_i \geq b_0 \\ \frac{b_i}{b_0} \quad for \quad b_i < b_0 \end{cases} \tag{B.33}$$

B.11. Load-combinations

B.11.1. ULS

$$1,35 \cdot (Deadload + Permanent - load) + 0.6 \cdot Variable - load \tag{B.34}$$

$$1,2 \cdot (Deadload + Permanent - load) + 1.5 \cdot Wind - load_x + 0.4 \cdot Variable - load \tag{B.35}$$

$$1,2 \cdot (Deadload + Permanent - load) + 1.5 \cdot Wind - load_y + 0.4 \cdot Variable - load \tag{B.36}$$

$$1,2 \cdot (Deadload + Permanent - load) + 1.5 \cdot variable - load \tag{B.37}$$

B.11.2. SLS

$$1 \cdot (Deadload + Permanent - load) + 1 \cdot Wind - load_x + 0.4 \cdot Variable - load \tag{B.38}$$

$$1 \cdot (Deadload + Permanent - load) + 1 \cdot Wind - load_y + 0.4 \cdot Variable - load \tag{B.39}$$

$$1 \cdot (Deadload + Permanent - load) + 1 \cdot Variable - load \tag{B.40}$$

B.11.3. Accidental Limit State

$$1 \cdot (Deadload + Permanent - load) + 0.2 \cdot Wind - load_x + 0.3 \cdot Variable - load \tag{B.41}$$

$$1 \cdot (Deadload + Permanent - load) + 0.2 \cdot Wind - load_y + 0.3 \cdot Variable - load \tag{B.42}$$

$$1 \cdot (Deadload + Permanent - load) + 1 \cdot Variable - load \tag{B.43}$$

B.12. Member verification

Compression perpendicular to the grain

For the wind bracing the compression forces need to be considered on the beams[55].

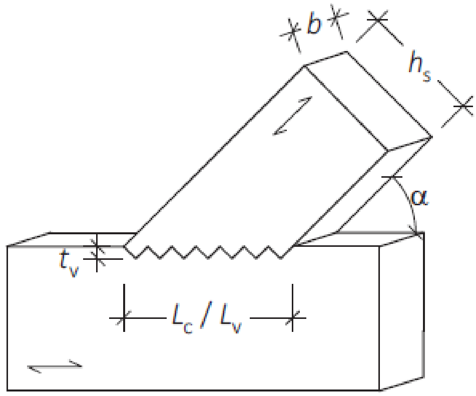

Figure B.9: Compression capacity perpendicular to the grain

Verification of the compression capacity with a angle perpendicular to the grain B.9.

$$F_{c,90,R} = \frac{A_c \cdot f_{c,90} \cdot k_{c,90}}{sin\alpha} \tag{B.44}$$

With:

$$L_c = \frac{h_s}{sin\alpha} \tag{B.45}$$

and:

$$A_c = b \cdot (L_c + 2 \cdot 30mm) \tag{B.46}$$

Verification of the shear capacity:

$$F_{v,R} = A_v \cdot f_v \tag{B.47}$$

With:

$$L_v = \frac{h_s}{sin\alpha} \tag{B.48}$$

And:

$$A_v = b \cdot L_v \tag{B.49}$$

Bending

Bending moment of a beam without risk of buckling are:

$$\sigma = \frac{M_y \cdot z}{I_y} \tag{B.50}$$

With:

M_y is the bending moment about the y-axis
I_y Moment of inertia about the y-axis
z Distance from the neutral axis

σ stress at distance z from neutral axis

The verification for a bending moment around one axis is then:

$$\sigma_{m,d} \leq f_{m,d} \tag{B.51}$$

The combination of tension and bending moment has the following verification:

$$\frac{\sigma_{t,0,d}}{f_{t,0,d}} + \frac{\sigma_{m,y,d}}{f_{m,y,d}} + k_m \cdot \frac{\sigma_{m,z,d}}{f_{m,z,d}} \leq 1 \tag{B.52}$$

$$\frac{\sigma_{t,0,d}}{f_{t,0,d}} + k_m \cdot \frac{\sigma_{m,y,d}}{f_{m,y,d}} + \frac{\sigma_{m,z,d}}{f_{m,z,d}} \leq 1 \tag{B.53}$$

With:

k_m is a capacity coefficient, assumed to be 0.7 for a timber rectangular cross-section.

The combination of axial compression and bending moment has the following verification:

$$(\frac{\sigma_{c,0,d}}{f_{c,0,d}})^2 + \frac{\sigma_{m,y,d}}{f_{m,y,d}} + k_m \cdot \frac{\sigma_{m,z,d}}{f_{m,z,d}} \leq 1 \tag{B.54}$$

$$(\frac{\sigma_{c,0,d}}{f_{c,0,d}})^2 + k_m \cdot \frac{\sigma_{m,y,d}}{f_{m,y,d}} + \frac{\sigma_{m,z,d}}{f_{m,z,d}} \leq 1 \tag{B.55}$$

Shear

The shear force can be calculated using the following for a rectangular cross section:

$$\tau = \frac{3}{2} \cdot \frac{V}{A} \tag{B.56}$$

Verification is for shear:

$$(\frac{\tau_{y,d}}{f_{v,d}})^2 + (\frac{\tau_{z,d}}{f_{v,d}})^2 \leq 1 \tag{B.57}$$

Torsion

The stress caused by torsion will be calculated as follows:

$$\tau_{tor} = \frac{M_T}{\alpha \cdot h \cdot b^2} \tag{B.58}$$

With

α is a factor depending on the ratio h/b.

For the verification the following condition should be met:

$$\tau_{tor,d} \leq k_{shape} \cdot f_{v,d} \tag{B.59}$$

With:

$f_{v,d}$ is the design shear strength

The Eurocode does not require a combination verification from stresses from shear and torsion.

Buckling

From the Timber Engineering principles [55], the elastic buckling load can be determined by the following equation:

$$N_{crit} = \frac{1}{\frac{4 \cdot l^2}{\pi^2 \cdot E \cdot I} + \frac{l}{K_r}} \tag{B.60}$$

For lateral torsional buckling of a beam, the critical stress can be calculated as follows:

$$\sigma_{m,crit} = \frac{\pi \cdot \sqrt{E_{0.05} \cdot I_z \cdot G_{0.05} \cdot I_{tor}}}{l_{ef} \cdot W_y} \tag{B.61}$$

The verification for the buckling strength will be:

$$\sigma_{m,d} \leq k_{crit} \cdot f_{m,d} \tag{B.62}$$

With:

k_{crit} coefficient depending on the relative slenderness $\lambda_{rel,m}$ (see B.10).

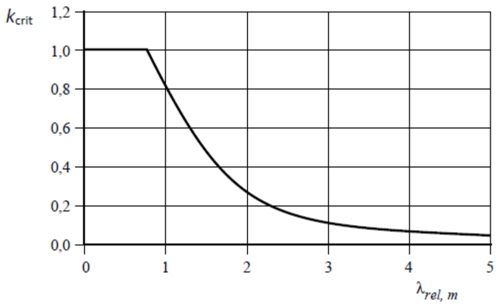

Figure B.10: k_{crit} coefficient depending on the relative slenderness [55]

C
FEM model check

To verify the accuracy of the FEM program results, they are compared with hand calculations in this section.

C.1. Small models

In the initial tests of the FEM model, the core alone and the core within the building were tested to determine if the global deflection would be the same in both cases under the same horizontal load. This was not the case for the first design, where the line hinge intersected with the cut-out. This is illustrated in Figure C.1. When the cut-out is not intersecting with the line hinge then the problem does not occur.

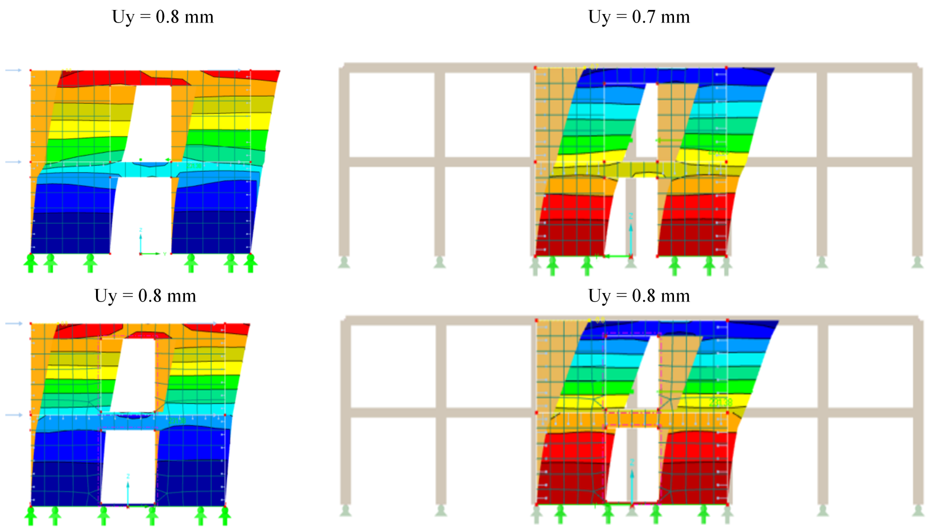

Figure C.1: Difference in wall design core, top two are with line hinge intersected by the cut-out, bottom two without an intersection.

C.2. Moment of inertia

To compare the stability of the two systems, the moment of inertia plays an important role. For an example of a clamped beam with a wind load q and a homogeneous elasticity modulus E, the deflection u is as follows:

$$u = \frac{ql^4}{8EI} \tag{C.1}$$

The Urban woods has a core with a dimension of 7300 x 4940 (see figure C.2). The moment of inertia is for the I_{yy} : $4,25 \cdot 10^{13} mm^4$ and for the I_{xx}: $1,93 \cdot 10^{13} mm^4$. For a C24 timber profile with the modulus of elasticity of $E = 1100kN/cm^2$, a length of $l = 32m$ and a q load of $q = 42.3kN/m$ the u would be:

$$u = \frac{42.3 * 7300 \cdot (32 \cdot 10^3)^4}{8 * 1.1 \cdot 10^4 \cdot 1.93 \cdot 10^{13}} = 26.115mm \tag{C.2}$$

The deflection in reality is much higher. This is because of the openings in the core that are needed for the doors. Also, because of the connections in the panels, that will lead to a less stiff core. With the bracings, the material is placed at the location of the façades. The distance to the centroid has an exponential influence on the moment of inertia due to Steiners law. With a I_{yy} of $5.63 \cdot 10^{14}$ and a I_{xx} of $3.05 \cdot 10^{14}$

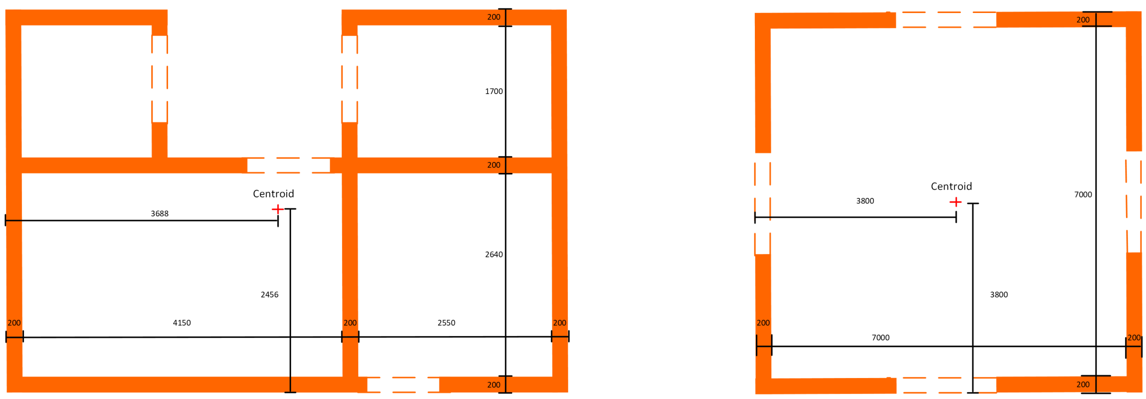

Figure C.2: Core layout of the Urban Woods and core layout model

As shown in Figure C.2, the core model has been simplified to facilitate easier parameterization. The new moment of inertia for the I_{yy} and I_{xx} : $4.98 \cdot 10^{13} mm^4$

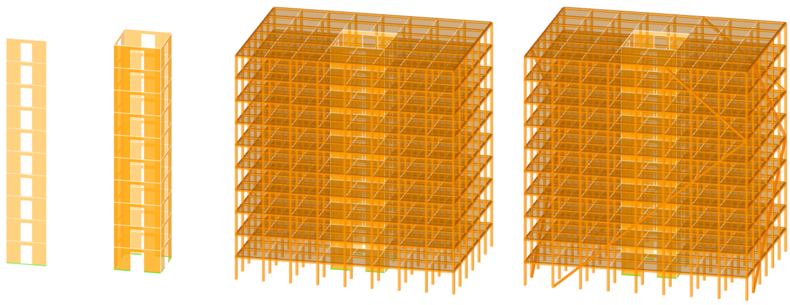

Figure C.3: Parametric design of core in 2D, Core in 3D, building in 3D and building with wind bracing in 3D

For a 30 meter stiff core with no cut-outs, the 2D and the 3D models was calculated in the RFEM software and verified by hand calculations. The 3D core has a heart to heart distance of 7200 mm, and a thickness of 200 mm (see figure C.2). The 2D model is one slab of 7180 mm. The following results were present.

- The 2D core had a 25.4 mm maximum deflection.
- The hand calculation for the 2D model is 22.1 mm.
- The 3D core had a 9.6 mm maximum deflection.
- The hand calculation for the 3D core is 7.5 mm.

With walls that are less than 2 times taller than they are long, the deflection is a combination of the flexural deformation and the shear deformation. For a clamped beam with a single point load F, the deformation calculation is as follows:

$$d = \frac{F \cdot h^3}{3 \cdot EI} + \frac{F \cdot h}{A_v \cdot G} \tag{C.3}$$

The stiffness in this situation will then be:

$$k = \frac{F}{d} = \frac{3 \cdot EI \cdot A_v}{h^3 \cdot A_v + 7.5 \cdot I \cdot h} \tag{C.4}$$

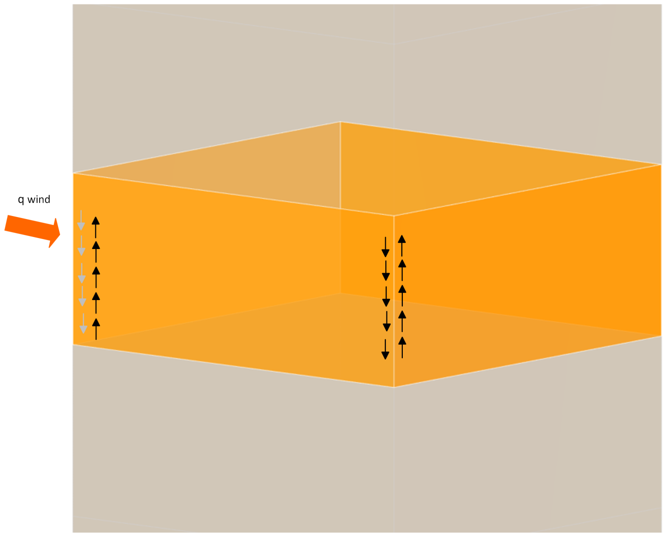

Figure C.4: Overview of force distribution in the corners of the core

Because of the connections in the corner of the core in the 3D model, the support in the u_z direction gets a stiffness depending on the kind of corner connections 6. The connections of the panels perpendicular to the force can prevent the uplifting. For the 2D model, the stiffness in the nodal supports are 0 in the z direction. Increasing the stiffness of the nodal supports will result in a lower deflection in the lateral direction. From both models the lintels are the spots where there is the most internal forces in y direction as-well as in x direction. Also the corner points at the foundation show high forces. The reason that the internal forces are less in the 3D model is that some of the external force is transmitted trough the panels perpendicular to the force. The maximum support reaction for the 2D model is higher than that of the 3D model. This is as expected since the panel perpendicular to the force is able to have a support reaction.

To check the assumption that all the lateral force from the wind load is taken by the core, the building with the core needs to have the same deflection as the core on his own for the same wind load. The building surrounding the core has dimension of 28.8 meter by 21.6 meter. The following result was present:

- The Whole building had a maximum deflection of also 9.6 mm.

The deflection of the whole model is the same than the deflection of only the core when point loads are applied. This means that all the lateral force is taken by the core.

The hand calculations are based on the bending stiffness with the moment of inertia considering a fully monolith core made of timber. In practise this is not the case that is why the effective bending stiffness can be considered. The effective bending stiffness takes into consideration the interaction factor γ. For γ = 0, no interaction is considered between the two composites, and for γ = 1, full interaction is considered. The γ factor decreases the steiner part of the moment of inertia as follows from the Eurocode [41]:

$$(EI_{eff}) = \sum(E_i I_i + \gamma_i E_i A_i a_i^2) \tag{C.5}$$

The γ interaction factor is calculated as follows:

$$\gamma_i = \frac{1}{1 + \frac{\pi^2 E_i A_i s_i}{K_i l^2}} \tag{C.6}$$

With:

s_i is the between distance.
K_i is the slip modulus K_{ser} for SLS and K_u for ULS.
l is the length between two hinges.

The γ_i for a corner connection with a slip modulus of 45 kN/mm and a elasticity modulus of 6600 N/mm^2 is 0.91. With the interaction factor, the moment of inertia of the core is $4.18 \cdot e^{13}$. The deflection for the core becomes 12.14 mm. In the RFEM model with the same modulus of elasticity and slip modulus, the deflection is 19.2 mm.

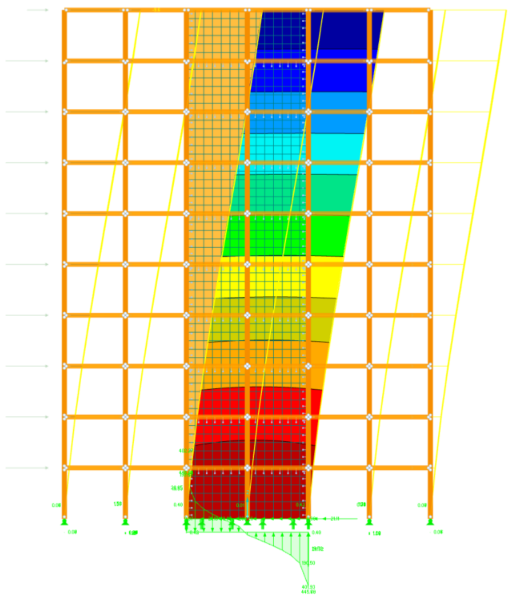

Figure C.5: Support reactions whole building with stiff core

D

Model tests

D.1. Deflection different directions

In table D.1, the top lateral deflection is given for every wind direction in SLS for a 10 storey timber building.

Direction wind	Deflection core + bracing (mm)	Deflection bracing (mm)	Deflection core (mm)
x	15.1	17.8	127.7
y	22.9	27.8	168.4
$-x$	15.6	18.5	127.7
$-y$	21.9	26.6	168.4

Table D.1: Deflection 10 storey building in every direction

D.2. RFEM laminate output

The laminate add-on in RFEM has the following output for the Unity check, which are described as follows:

Failure mechanism	Description
$\sigma_{b,0}$	Moment parallel to the grain
$\sigma_{b,90}$	Moment perpendicular to the grain
$\sigma_{t/c,0}$	Tension/Compression parallel to the grain
$\sigma_{t/c,90}$	Tension/Compression perpendicular to the grain
$\sigma_{b+t/c,0}$	Moment plus Tension/Compression parallel to the grain
$\sigma_{b+t/c,90}$	Moment plus Tension/Compression perpendicular to the grain
$\tau_{y'z'}$	Shear stress in the y axis in the direction of the z axis
$\tau_{x'z'}$	Shear stress in the x axis in the direction of the z axis
$\tau_{x'y'}$	Shear stress in the x axis in the direction of the y axis
$int(\tau_{x'z'} + \tau_{x'y'})$	Combination of $\tau_{x'z'}$ and $\tau_{x'y'}$
$int(\sigma_{t/c,90} + \tau_{y'z'})$	Combination of $\sigma_{t/c,90}$ and $\tau_{y'z'}$

Table D.2: Removal of three different diagonals, 1) first floor, 2) third floor and 3) fifth floor

D.3. Diagonal removal tests

For the removal of a single diagonal element, 3 different elements where removed to find out which removal had the most impact on the CLT.

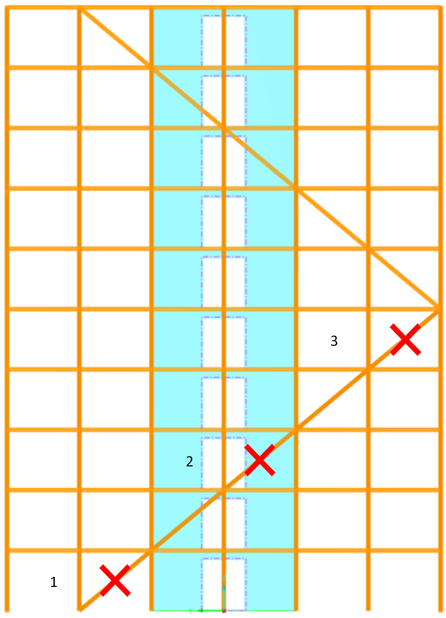

Figure D.1: The three different element removals, 1) first floor, 2) third floor and 3) fifth floor

Failure mechanism	UC normal ALS	UC first floor removed	UC third floor removed	UC fifth floor removed
$\sigma_{b,0}$	0.34	0.35	0.35	0.34
$\sigma_{b,90}$	0.01	0.01	0.01	0.01
$\sigma_{t/c,0}$	0.37	0.39	0.37	0.37
$\sigma_{t/c,90}$	0.89	0.91	0.92	0.91
$\sigma_{b+t/c,0}$	0.61	0.63	0.62	0.62
$\sigma_{b+t/c,90}$	0.91	0.92	0.94	0.92
$\tau_{y'z'}$	0.11	0.11	0.11	0.11
$\tau_{x'z'}$	0.42	0.42	0.43	0.42
$\tau_{x'y'}$	0.42	0.44	0.42	0.42
$int(\tau_{x'z'} + \tau_{x'y'})$	0.19	0.20	0.20	0.19
$int(\sigma_{t/c,90} + \tau_{y'z'})$	1.07	1.09	1.11	1.09

Table D.3: Removal of three different diagonals, 1) first floor, 2) third floor and 3) fifth floor

D.4. Calculation Stiffness/Strength hinges for model

In this section, the calculation of the line hinges and member hinges are given for the core and the bracing.

D.4.1. Horizontal line hinge

The horizontal connection will have 2 rows of dowels every 100 mm (see figure D.2).

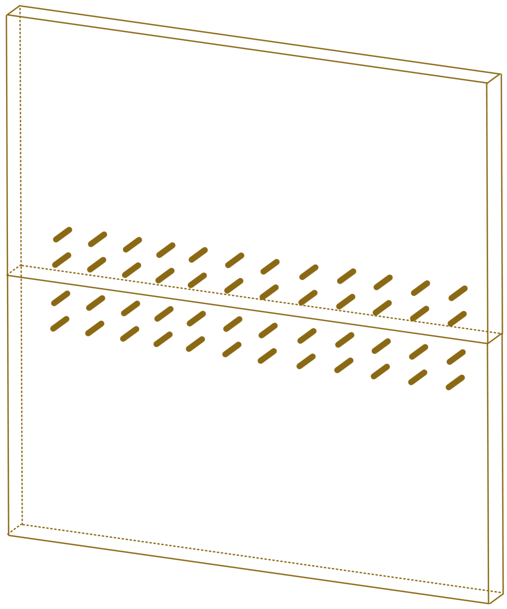

Figure D.2: Horizontal line hinge

Stiffness

Stiffness is in the x and y direction the same for the line hinge

$$K_{ser} = \frac{\rho_m^{1.5} \cdot d_{ef} \cdot 2}{23} \tag{D.1}$$

$$Kser = \frac{350(kg/m^3)^{1.5} \cdot 14(mm) \cdot 2 \cdot 2}{23} = 15942.71kN/m \tag{D.2}$$

$$15942.71 \cdot \frac{1000mm}{100mm} \cdot \frac{1}{2} = 79713.57kN/m^2 \tag{D.3}$$

Capacity

The capacity of the line hinge is not the same for the x and y direction. Because of the effective amount of dowels decreases when more dowels are put in a row.

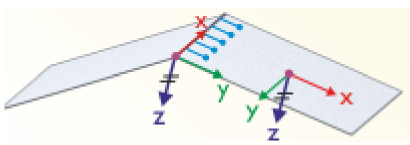

Figure D.3: Caption

From the failure modes B.3, failure mode (e) is the normative one.

$$M_{y,Rk} = 0.3 \cdot f_{u,k} \cdot d^{2.6} \tag{D.4}$$

$$M_{y,Rk} = 0.3 \cdot 720N/mm^2 \cdot 14^{2.6} = 206246.53Nmm \tag{D.5}$$

$$F_{v,Rk} = 2.3 \cdot \sqrt{M_{y,Rk} \cdot f_{h,k} \cdot d} + \frac{F_{ax,Rk}}{4} \tag{D.6}$$

$$F_{v,Rk} = 2.3 \cdot \sqrt{206246.53(Nmm) \cdot 29.6184 \cdot 14} + \frac{0}{4} = 21.27kN \tag{D.7}$$

$$n_{eff} = n_x^{0.9} \cdot \frac{a_1}{13 \cdot d}^{0.25} \tag{D.8}$$

capacity in the x direction

$$n_{eff,x} = 10^{0.9} \cdot {\frac{100(mm)}{13 \cdot 14(mm)}}^{0.25} = 6.84 \tag{D.9}$$

$$F_{v,Rk,d,y} = n_{eff} \cdot F_{v,Rk} \cdot \frac{k_{mod}}{\gamma_m} \cdot 2(dowels/m) = 350kN/m \tag{D.10}$$

capacity in the y direction

$$n_{eff,y} = 2^{0.9} \cdot {\frac{100(mm)}{13 \cdot 14(mm)}}^{0.25} = 2.4 \tag{D.11}$$

$$F_{v,Rk,d,x} = n_{eff} \cdot F_{v,Rk} \cdot \frac{k_{mod}}{\gamma_m} \cdot 10(dowels/m) = 615kN/m \tag{D.12}$$

D.4.2. Vertical line hinge

For the vertical line hinge, self-tapping screws are used which will have a angle of 45 degrees.

$$d_{ef} = d - 2 = 13 - 2 = 11 \tag{D.13}$$

Stiffness

$$f_{h,\varphi} = \frac{0.082\rho_k(1 - 0.01d)}{(2.5\cos^2\varphi + \sin^2\varphi)(k_{90}\sin^2\theta + cos^2\theta)} \tag{D.14}$$

$$f_{h,\varphi} = \frac{0.082 \cdot 350(kg/m^3)(1 - 0.01 \cdot 13(mm))}{(2.5\cos^2 45 + \sin^2 45)(1.155\sin^2 45 + cos^2 45)} = 13.24 \tag{D.15}$$

$$x_i = f_{h,\varphi} \cdot d_{ef} \cdot tan\varphi \tag{D.16}$$

$$x_i = 13.24 \cdot 11 \cdot tan45 = 72.83 \tag{D.17}$$

$$l_{ef} = 1200(mm) - 72.83(mm) = 1127.17(mm) \tag{D.18}$$

$$k_{\perp} = \frac{\rho_m^{1.5} \cdot d}{23} \tag{D.19}$$

$$k_{\perp} = \frac{380^{1.5} \cdot 8}{23} = 8373.8 \tag{D.20}$$

$$k_{ax} = 25 \cdot d \cdot l_{ef} \tag{D.21}$$

$$k_{ax} = 25 \cdot 13 \cdot 1127.17 = 366330.3 \tag{D.22}$$

$$k_{\parallel} = \frac{1}{\frac{1}{k_{ax,1}} \frac{1}{k_{ax,2}}} \tag{D.23}$$

$$k_{\parallel} = \frac{1}{\frac{1}{366330.3} \frac{1}{366330.3}} = 183165.2 \tag{D.24}$$

$$K_{A,STS} = k_{\perp}\sin^2(\phi) + k_{\parallel}\cos^2(\phi) \tag{D.25}$$

$$K_{A,STS} = 8373.8\sin^2(45) + 183165.2\cos^2(45) = 93.68kN/mm \tag{D.26}$$

Capacity

$$f_{ax,k} = 0.52d^{-0.5} \cdot l_{ef}^{-0.1} \cdot \rho_k^{0.8} \tag{D.27}$$

$$f_{ax,k} = 0.52 \cdot 13(mm)^{-0.5} \cdot 1107.45(mm)^{-0.1} \cdot 7850(kg/m^3)^{0.8} = 93.43N/mm^2 \tag{D.28}$$

$$f_{h,0,k} = 0.082(1 - 0.01d)\rho_k \tag{D.29}$$

$$f_{h,0,k} = 0.082(1 - 0.01 \cdot 13)420 = 29.96 \tag{D.30}$$

$$f_{h,\alpha,k} = \frac{f_{h,0,k}}{k_{90}\sin^2\alpha + \cos^2\alpha} \tag{D.31}$$

$$f_{h,\alpha,k} = \frac{29.96}{1.59\sin^2 45 + \cos^2 45} = 23.14 \tag{D.32}$$

$$F_{ax,k,Rk} = \frac{n_{eff} \cdot f_{ax,k} \cdot l_{ef} \cdot k_d}{1.2\cos^2\alpha \cdot \sin^2\alpha} \tag{D.33}$$

$$F_{ax,k,Rk} = \frac{1 \cdot 93.43 \cdot 1107 \cdot 1}{1.2\cos^2 45 \cdot \sin^2 45} = 359736N \tag{D.34}$$

$$F_{v,Rk} = 0.4 \cdot f_{h,\alpha,k} \cdot t_1 \cdot d \tag{D.35}$$

$$F_{v,Rk} = 0.4 \cdot 23.1373 \cdot 200 \cdot 13 = 24.06kN \tag{D.36}$$

$$F_{v,Rk,d} = F_{v,Rk} \cdot spacing \cdot \frac{k_{mod}}{\gamma_m} \tag{D.37}$$

$$F_{v,Rk,d} = 24.06(kN) \cdot 10(pc/m) \cdot \frac{0.8}{1.25} = 160kN/m \tag{D.38}$$

Bracing hinge
Stiffness

$$M_{y,k} = 0.3 \cdot f_{u,k} \cdot d^{2.6} \tag{D.39}$$

$$M_{y,k} = 0.3 \cdot 720 \cdot 16^{2.6} = 291854Nmm \tag{D.40}$$

Stiffness per fastener.

$$K_{ser} = \frac{\rho_m^{1.5} \cdot d}{23} \cdot 2 \tag{D.41}$$

$$K_{ser} = \frac{420^{1.5} \cdot 16}{23} \cdot 2 = 11975.57 \tag{D.42}$$

With two steel plates slotted in, four shear planes are in place. This makes the total stiffness per fastener.

$$K_{ser} = 11975.57 \cdot 4 = 47902.27 \tag{D.43}$$

Total stiffness per connection:

$$K_{ser,total} = 3 \cdot 16 \cdot 47902.27 = 2299308.83N/mm \tag{D.44}$$

Strength

$$f_{h,0,k} = 0.082(1 - 0.01d)\rho_k \tag{D.45}$$

$$f_{h,0,k} = 0.082 \cdot (1 - 0.01 \cdot 16) = 28.93 \tag{D.46}$$

$$M_{y,k} = 0.3 f_{u,k} d^{2.6} \tag{D.47}$$

$$M_{y,k} = 0.3 \cdot 720 \cdot 16^{2.6} = 291854Nmm \tag{D.48}$$

Failure mode 7

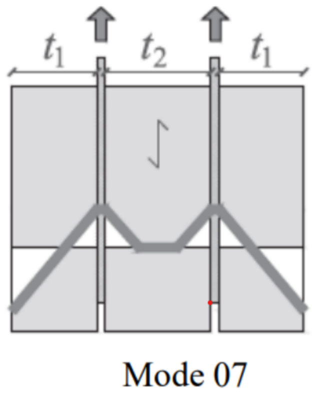

Figure D.4: Failure mode 7

$$F_y = (-\frac{1}{2}t_1 + \frac{1}{2}\sqrt{t_1^2 + \frac{2M_y}{d \cdot f_{h,0}}} + \sqrt{\frac{M_y}{d \cdot f_{h,0}}} \cdot d \cdot f_{h,0} \tag{D.49}$$

$$F_y = (-\frac{1}{2}t_1 + \frac{1}{2}\sqrt{126^2 + \frac{2 \cdot 291854}{16 \cdot 28.93}} + \sqrt{\frac{291854}{16 \cdot 28.93}} \cdot 16 \cdot 291854 = 12.76kN \tag{D.50}$$

$$n_{eff} = n^{0.9} * \frac{a_1}{13 \cdot d}^{0.25} \tag{D.51}$$

Effective amount of dowels in a row.

$$n_{eff} = 16^{0.9} * \frac{60}{13 \cdot 16}^{0.25} = 8.89 \tag{D.52}$$

$$F_{y,total,d} = n_{eff} \cdot n_{collumns} \cdot F_y \frac{k_{mod}}{\gamma_m} \tag{D.53}$$

$$F_{y,total,d} = 8.89 \cdot 3 \cdot 12.76 \frac{0.8}{1.25} = 870.77kN \tag{D.54}$$